

**Radiometric Studies to Understand Disequilibrium of Uranium across a  
few Exploratory blocks of Mahadek basin, Meghalaya and its  
Implication on Uranium Exploration.**

*By*

**BHARAT MOHAN KUKRETI**

**Enrolment No. PHYS 01201304046**

**BHABHA ATOMIC REASERCH CENTRE**

*A thesis submitted to the*

*Board of Studies in Physical Sciences*

*In partial fulfilment of requirements*

*for the Degree of*

**DOCTOR OF PHILOSOPHY**

*of*

**HOMI BHABHA NATIONAL INSTITUTE**

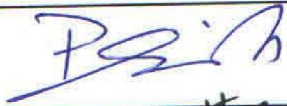
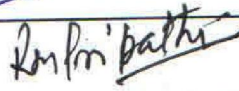
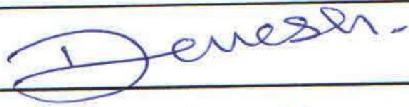
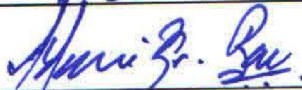


**October, 2015**

# Homi Bhabha National Institute

## Recommendations of the Viva Voce Committee

As members of the Viva Voce Committee, we certify that we have read the dissertation prepared by **Bharat Mohan Kukreti** entitled "**Radiometric Studies to Understand Disequilibrium of Uranium across a few Exploratory blocks of Mahadek basin, Meghalaya and its Implication on Uranium Exploration**" and recommend that it may be accepted as fulfilling the thesis requirement for the award of Degree of Doctor of Philosophy.

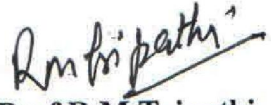
Chairman: Prof. P.Singh		24/02/2016
Guide/Convener : Prof. R.M.Tripathi		24/02/2016
Examiner : Prof. D. Walia		24/02/2016
Member1: Prof . G.G. Pandit		24/02/2016
Member2: Dr A. K. Rai		24/02/2016
Technical Adviser: Dr B. K. Bhaumik		24/02/2016

Final approval and acceptance of this thesis is contingent upon the candidate's submission of the final copies of the thesis to HBNI.

I hereby certify that I have read this thesis prepared under my direction and recommend that it may be accepted as fulfilling the thesis requirement.

Date: 24 /02/ 2016

Place: Mumbai

  
Guide: Prof R.M Tripathi

## **STATEMENT BY AUTHOR**

This dissertation has been submitted in partial fulfilment of requirements for an advanced degree at Homi Bhabha National Institute (HBNI) and is deposited in the Library to be made available to borrowers under rules of the HBNI.

Brief quotations from this dissertation are allowable without special permission, provided that accurate acknowledgement of source is made. Requests for permission for extended quotation from or reproduction of this manuscript in whole or in part may be granted by the Competent Authority of HBNI when in his or her judgment the proposed use of the material is in the interests of scholarship. In all other instances, however, permission must be obtained from the author.



(Bharat Mohan Kukreti)

## **DECLARATION**

I, hereby declare that the investigation presented in the thesis has been carried out by me. The work is original and has not been submitted earlier as a whole or in part for a degree / diploma at this or any other Institution / University.

A handwritten signature in blue ink, appearing to read 'Bharat Mohan Kukreti', is centered on the page.

(Bharat Mohan Kukreti)

## List of Publications arising from the thesis

### Journals

1. Interpolation study on ambient gamma levels in parts of Khasi Hills, Meghalaya (India): Preliminary findings for U exploration. **B.M.Kukreti**, G.K. Sharma, Pramod Kumar, Sandeep Hamilton. *Journal of Earth System Science*. Accepted (2016).
2. Development of experimental approach to examine U occurrence continuity over the extended area Reconnoitry Boreholes: Lostoin Block, West Khasi Hills district, Meghalaya (India). **B.M.Kukreti**, Pramod Kumar, G.K.Sharma. *Applied Radiation and Isotopes*.**104**,167-174 (2015).
3. Developing a correlation index and U disequilibrium factor for the exploratory boreholes in Wahkut block of West Khasi Hills district, Meghalaya (India). **B.M. Kukreti**, Pramod Kumar. *Applied Radiation and Isotopes*.**72**,6-10 (2013).
4. Multivariate Analysis of Subsurface Radiometric Data in Rongsohkham area, East Khasi Hills district, Meghalaya (India) : Implication on Uranium Exploration.**B.M Kukreti**., Pradeep Pandey, R.V. Singh. *Applied Radiation and Isotopes*.**70**,1644-1648 (2012).
5. Performance analysis of gamma ray spectrometric parameters on digital signal and analog signal processing based MCA systems using NaI(Tl) detector. **B.M. Kukreti**, G.K Sharma. *Applied Radiation and Isotopes*.**70**,901-905 (2012).

### Conferences

1. Distribution characteristics of natural gamma background levels around the capital city Shillong , Meghalaya (India). **B.M. Kukreti**, G.K. Sharma, M.S Rao, T. Ramabhadraih, Arjun Bhaskar Rao, A. Bhuphang. NSRP-19, Kalpakkam, TN (Dec 2012).

2. Assessment of ambient gamma radiation levels in the sedimentary environment of Khasi Hills, Meghalaya (India). **B.M.Kukreti**, Sandeep Hamilton, G.K. Sharma, Pramod Kumar. NSE-19, Kottayam, Kerala (Dec 2014).



(Bharat Mohan Kukreti)

*Dedicated to...*

*My wife Rashmi Kukreti and loving daughters Ishita and Aditi*

## ACKNOWLEDGEMENT

The motivation behind this work goes to number of persons to whom, I would like to thank on a more personal level. My sincere thanks to Prof P. Singh, my mentor & former Head, IADD, BARC, for his kind support at every level. His vast work experience, problem solving approach and generosity all have been constant source of inspiration and energy to me.

I would also like to express my deep sense of gratitude to Dr(s) S.Kailas and S.L. Chaplot former Director(s), Physics Group, BARC, for all their kind support and encouragements.

I wish to record my deep sense of gratitude and sincere thanks to my guide Prof R.M.Tripathi, Head, HPD, BARC, for his constant support, research guidance and valuable suggestions to the research methodology of this work.

I would also like to express my sincere thanks to Prof G.G. Pandit, Head EMAS, and BARC for her valuable suggestions during the course of discussion on this research work.

My sincere thanks to Dr B.S. Tomar, Head RCD, BARC, for constant motivation, affection and moral support to me, in this endeavour.

It's great privilege to acknowledge then support received from all the contemporary higher-ups of AMD especially then Director (s) Shri P.B. Maithani and Shri P.S. Parihar, Shri K. Umamaheshwar (Addl Director) and Dr S.S. Raghuvanshi (Head Physics group).

It's my pleasure to thank Dr A.K. Rai, Director AMD and member HBNI doctoral committee, for his critical observations and valuable suggestions on improving the quality of this work.

I would also wish to express my reverence and sense of deep gratitude to then Regional Director(s) at NER namely Dr R.Mohanty and Shri G. B. Joshi for all their support, encouragements and help rendered to me throughout this work.

It gives me immense pleasure to acknowledge a great mind Dr. B.K.Bhaumik, VECC and my technical adviser to HBNI doctoral committee for his critical inputs to this work. I am grateful to him for sparing the time for technical discussion and thorough review of this work with vital suggestions to this research work that helped me a lot to bring this work in present form. It was both a privilege and an honour to work with him. His passion for excellence in scientific task, generosity and ready to help attitude will always remain source of inspiration and motivation to me.

At Physics lab, NER, I wish to thank all my former colleagues for their collective efforts and cooperation. I would like to give special thanks to all my co-authors and especially G. Jeganathan, G.K. Sharma and Arjun Bhaskar for providing valuable feedback on the technical work undertaken in the region. The wholehearted laboratory support rendered by the technical staff in the lab especially H.M.Swer and N.Deb is wishfully being acknowledged.

During my working tenure at NER, I am extremely thankful to my wife Rashmi for her understanding, support and single handed handling of family responsibilities including towards two school going kids, then back home at New Delhi.

At the divisional level, I would like to express my sincere thanks to Head IADD, Shri P.V. Bhagwat and Head FOTIA Shri S. Gupta for all their cooperation and support.

Last but not the least my special thanks to Dr A.K. Gupta, NPD, BARC, my batch mate and friend, for all the useful technical discussion and motivational support in this endeavour.

# CONTENTS

	<b>Page No</b>
<b>LIST OF ABBREVIATION USED</b>	<b>v-vi</b>
<b>SYNOPSIS</b>	<b>vii-xiii</b>
<b>LIST OF FIGURES</b>	<b>xv-xvi</b>
<b>LIST OF TABLES</b>	<b>xvii-xviii</b>
<b>CHAPTER 1: Introduction</b>	<b>1-15</b>
1.1 About Uranium Exploration	2
1.1.1 Decay Series	3
1.1.2 Prospecting Method	4
1.1.3 Environmental Behaviour	4
1.1.4 Hosting Environments	6
1.1.5 Geographical Distribution	7
1.2 Overview of Indian Uranium Resources	8
1.2.1 Bhima Basin	9
1.2.2 Cuduppa Basin	10
1.2.3 Mahadek Basin	10
1.2.4 Singhbhum Sear Zone	11
1.3 About Mahadek Basin	11
1.3.1 Geological Setting	11
1.3.2 Uranium Equilibrium Conditions	13
<b>CHAPTER 2: Analytical Setup and Measurements</b>	<b>17-33</b>
2.1 Natural Gamma Ray Spectrum	18
2.2 Gross Gamma Measurement	19
2.2.1 Equivalent Assembly	20

2.2.2 Core Assay Assembly	21
2.3 Beta Gamma Assembly	22
2.3.1 Radiometric $U_3O_8$ Benchmark Study	23
2.4 Gamma Ray Spectrometry	24
2.4.1 Working Principle	25
2.4.2 Sample Thickness Optimization	27
2.5 Gamma Ray Borehole Logging	32
<b>CHAPTER 3: Ambient Gamma Radiation Measurements</b>	<b>35-48</b>
3.1 Material	37
3.2 Field Measurements	37
3.3 Working Approach	38
3.4 Data Analysis	39
3.4.1 Gamma Profiling of Litho Units	39
3.4.2 Analytical Model of Sample Variogram	40
3.5 Sample Variogram Compatibility Check	42
3.6 Interpolation of Sample Data Points	44
3.7 Preliminary Findings	46
3.7.1 Analytical Model of Sample Variogram	46
3.7.2 Interpolation of Sample Data points	47
<b>CHAPTER 4: Uranium Hosting Environment Investigation</b>	<b>49-66</b>
4.1 About Rangsohkham Exploratory block	50
4.2 Borehole $\gamma$ -ray Logging Status	52
4.3 Uranium Mineralisation Discontinuity Study	52
4.3.1 Sample Generation and Classification	52
4.3.2 Radiometric Analysis	54

4.3.3	Experimental Approach	56
4.3.3.1	Hypothesis Building	56
4.3.3.2	Multivariate Analysis	56
4.4	Data Analysis	57
4.4.1	Hypothesis Testing	57
4.4.2	Uranium Equivalent Activity	58
4.4.3	Radioelemental Correlation Matrix	58
4.5	Rangsohkhham Exploratory block Findings	59
4.6	Validation of Experimental Findings	60
4.6.1	Lostoin Exploratory block	60
4.6.1.1	Data Acquisition	60
4.6.1.2	Uranium Behaviour in the System	63
4.6.2	Key Findings-Lostoin Exploratory block	65
4.7	Uranium Disequilibrium Status	65
	<b>CHAPTER 5: Exploratory Blocks: Disequilibrium Investigation</b>	<b>67-88</b>
5.1	About Wahkut Exploratory block	68
5.2	Uranium-Surface Equilibrium Condition	70
5.3	Boreholes $\gamma$ -ray Logging Status	70
5.4	Uranium Mineralization Exploratory Aspect	71
5.4.1	Confirmation of $\gamma$ -ray Logs	71
5.4.2	Uranium Disequilibrium Investigation	73
5.4.3	Uranium Disequilibrium-Vertical Distribution	75
5.5	Wahkut Exploratory block Findings	76
5.5.1	Confirmation of $\gamma$ -ray Logs	76
5.5.2	Uranium Disequilibrium Pattern	77

5.6 Validation of Wahkut Exploratory block Findings	78
5.6.1 About Lostoin Exploratory block	79
5.6.1.1 Boreholes $\gamma$ -ray Logging Status	79
5.6.1.2 Confirmation of $\gamma$ - ray Logs	80
5.6.1.3 Uranium Disequilibrium Status-Coring boreholes	82
5.6.1.4 Uranium Disequilibrium Status-Non coring boreholes	82
5.6.1.5 Uranium Disequilibrium-Vertical distribution	85
5.7 Lostoin Exploratory block Findings	86
5.7.1 Confirmation of Subsurface Uranium Mineralization	86
5.7.2 Uranium Disequilibrium Status	87
<b>CHAPTER 6: Summary and Conclusion</b>	<b>89-93</b>
<b>REFERENCES</b>	<b>95-99</b>
<b>APPENDIX-A</b>	<b>101-106</b>
<b>APPENDIX-B</b>	<b>107-110</b>

## LIST OF ABBREVIATION USED

ANOVA	:	Analysis of Variance
$\beta/\gamma$	:	Beta Gamma (radiometric uranium estimation method)
BH	:	Boreholes
BM	:	Basement(Geological environment)
d	:	Disequilibrium factor for uranium series
dMCA	:	Digital signal processing based MCA
DSP	:	Digital Signal Processing
DTH	:	Down The Hole drill
$eU_3O_8$	:	Equivalent uranium oxide (measured by gamma activities)
GT	:	Grade Thickness
GM	:	Geiger Mueller radiation detector
GPS	:	Global Positioning System
IAEA	:	International Atomic Energy Agency
K	:	Potassium and represents radioactive K-40
KMP	:	Kylleng-Mawthabah-Pyndensohiong (best known as Domiasiat)
LM	:	Lower Mahadek (type of sandstone from Mahadek formation)
MCA	:	Multi Channel Analyzer
MDL	:	Minimum Detection Limit
PPM	:	Part Per Million
PPB	:	Part Per Billion
Ra	:	Radium
Ra(eq)	:	Radium equivalent
RMD	:	Relative Mean Difference
Rn	:	Radon and represents Rn-222

ROI	:	Region of Interest
SSZ	:	Singhbum Sheer Zone
Th	:	Thorium
ThO <sub>2</sub>	:	Thorium oxide
U	:	Uranium
UM	:	Upper Mahadek (type of sandstone from Mahadek formation)
U <sub>3</sub> O <sub>8</sub>	:	Uranium oxide

## SYNOPSIS

Mahadek basin of Meghalaya, host one of the largest and richest grade proven sandstone-type uranium deposits in the country. Together with main deposits viz Domiasiat (now KMP) and Wahkyn the basin readily contains more than 21,000 tones of proven ore reserves. Uranium mineralization is hosted by the Lower Mahadek sandstone of upper Cretaceous age and direct geological evidence in the basin offers large uranium reserves potential of medium to small ore pocket size, grade  $<0.10\%$   $U_3O_8$ , disposed at shallow depth.

Departmental (AMD) exploration experience of over four decades in the basin, shows challenging conditions of working environment such as inaccessibility, typical prevailing tropical to subtropical climate (heavy rain falls), thick forest and poor logistics (roads and communication) etc. Further, oxidizing tendency and high mobility of uranium in the sedimentary environment such as Mahadek basin, makes  $\gamma$ - ray logs measured in the boreholes by gross gamma measurements, vulnerable to the uranium migration conditions in the geological system.

Uranium, being pure alpha emitter, field exploration mostly relies on indirect  $\gamma$ - ray measurements techniques with daughter products (Ra group) contributing  $\approx 98\%$ . Disequilibrium in uranium series have varied causes led by the environmental redox conditions, long lived decay products to different physical and chemical properties of decay products. Under normal condition, uranium in  $U^{+4}$  state remains insoluble but on getting oxidised, converts to  $U^{+6}$  state called uranyl ion. Uranyl ion being soluble in water, get transported over a long distance particularly under the sedimentary environment. And thus selectively leaving behind trail of  $\gamma$ - emitting daughter products (deficient in uranium) creates disequilibrium in U series. On getting reducing environment, transported uranyl ion reduced to  $U^{+4}$  state with uranium getting precipitated. Similarly, other major disequilibrium cause is decay product radon ( $Rn^{222}$ ) in Ra

group. Radon being inert gas with 3.8 days half lives, travels considerable distance in the soil/rock matrix before getting escaped from the geological system through fault/ fractures etc and thus creating disequilibrium in uranium series.

Radiometric assay on grab samples across a few exploratory blocks of Mahadek basin, shows varying degree of surface mineralization uranium conditions measured in terms of disequilibrium factor ( $d$ ). Drawn and analysed surface samples ( $n=47$ ) for Rangsohkham exploratory block indicates mostly equilibrium conditions ( $d=1.1$ ), whereas Lostoin exploratory block grab samples ( $n=33$ ) indicates severe departure of equilibrium conditions ( $d<1$ ) and Wahkut exploratory block grab samples ( $n=21$ ) indicating parent favoring ( $d>1$ ) equilibrium condition ( $d=1.56$ ). Thus varying degree of uranium disequilibrium need to be assessed as it affects bulk uranium ore tonnage, measured by gross  $\gamma$ - measurements, in the exploratory block boreholes.

During exploration phase, abrupt discontinuity has been readily observed between the surface uranium mineralization and its subsurface extension, in one of the exploratory block of basin. Similarly, there are instances of measured  $\gamma$ -ray logs in reconnoitory boreholes, though showing good subsurface uranium mineralization but lacks good core recovery ( $\geq 90\%$ ) to affirm the  $\gamma$ -ray logs free from radon contamination with high degree of confidence.

To examines some of the behavior aspect of uranium disequilibrium conditions seen over the sedimentary environments of Mahadek basin and confirmations of  $\gamma$ -ray logs across the exploratory blocks, a systemic radiometric studies have been undertaken in parts of basin covering Rangsohkham exploratory block (East Khasi Hills district), Wahkut and Lostoin exploratory blocks (West Khasi Hills district). Apart from characterization of these study blocks being undertaken, study work also have implication in decision making and assessment of the inferred category of uranium ore often found amid environmental constrains and inaccessibility in the area.

The work reported in the thesis is presented under the 6 chapters. In **Chapter 1** it is stated, brief introduction about migratory behaviour of uranium in the natural environment, uranium occurrence and its distribution over different geological environments, major uranium deposits in the country and salient geological features of Mahadek basin.

In **Chapter 2**, it is stated, detailed analytical setup and optimised channel sensitivities etc for radiometric analysis of drawn grab samples (surface), subsurface samples (borehole sludge) and core samples. Radiometric studies being undertaken includes gross gamma activity ( $eU_3O_8$ ) analysis,  $U_3O_8(\beta/\gamma)$  analysis, gamma ray spectrometric analysis of primordial radio elements (both at ppm and % levels) and radiometric core assay of drilled core.

For ppm level analysis under the prevailing background and limited counting time, gamma spectrometric parameters have been especially optimized on 5"x4" NaI(Tl) detector and dMCA system in the lab. Similarly for radiometric  $\beta/\gamma$  analysis, used for the estimation of  $U_3O_8(\beta/\gamma)$  in geological samples and study of uranium disequilibrium, have been benchmarked to the chemical analysis and experimental findings shows good consistency between the two set of analytical results at high degree of confidence(>90%).

In **Chapter 3** it is stated, spatial variation of ambient gamma dose levels in relation to the major litho units of Mahadek basin for identification and delineation of potential uranium exploration targets using environmental radiometric survey in the basin.

Study comprises georeference based measurements of ambient gamma levels over 320 sample data points covering 673 line km of Khasi Hills. Acquired sample data points were first clustered and represented by box plots for the major litho units of Mahadek basin and then processed on geo-statistical software (Surfer<sup>TM</sup>) to develop analytical model of sample variogram in order to interpolate sample data points using kriging technique. Study findings show encouraging surface indicators with mostly elevated gamma dose levels in parts of West Khasi Hills area. The delineated gamma anomalous zones are lithologically well correlated to

the existing uranium occurrences in the basin. With the closure spatial resolution (~1km), the approach demonstrated under this study holds promising application in locating the potential uranium occurrences over the inaccessible and similar geologically extended area in the basin.

In **Chapter 4** it is stated, abrupt discontinuity observed for the surface uranium mineralization and its subsurface extension, in one of the study block Rangsohkham of Mahadek basin. Located under the East Khasi Hills district, this block lies about 30 km east of the said uranium mineralized cluster of Domiasiat and Wahkyn exploratory blocks and have gross geological similarity to it. Radiometric analysis of Rangsohkham exploratory block surface grab shows good surface uranium mineralization average  $U_3O_8 = 0.17\%$  (n=47), range (0.010-1.81%) with U series almost in equilibrium status (d=1.1).

However, despite such favorable surface indicators,  $\gamma$ -ray logs of logged boreholes failed to intercept the expected subsurface uranium mineralisation. The problem was then studied using systematic representative sampling of 11 boreholes reconnaissance boreholes, selected on random basis, across the three geological environmental conditions in the block. Subsequently, the status of uranium index have been studied across the three distinct geological formations of this block namely Upper Mahadek (UM), Lower Mahadek (LM) and Basement (BM).

To confirm uranium status over the hosting environment (Lower Mahadek), bivariate correlation matrix (3x3) has been developed using analysed primordial radioelements (K, Ra and Th) data of study block. Had there been no uranium enrichment U and Th being geochemically coherent, should give high coefficient of correlation. However, poor U-Th correlation index 0.268 reflected on the hosting environment (LM) shows that U enrichment has taken place in the system (Th concentration has been found to be low). Study results thus confirms continuation of three distinct geological formations (including hosting environment) of Mahadek basin and affirms uranium bearing potential to the eastern part of Mahadek basin

This proposition of uranium exploration model developed across the study block Rangsohkham's hosting environment has been further investigated over the similar geological formation in Lostoin exploratory block having good subsurface uranium mineralization (intercepted by the logged boreholes). Representative samples drawn from the uranium hosting environment (LM) from 24 non-coring boreholes of Lostoin exploratory block (located under West Khasi Hills district) that is about 15 km west of Domiasiat uranium deposit, shows matching U-Th index for the hosting environment. This confirms uranium enrichment continuity for Lower Mahadek I formation, over an aerial extent of 60 km in Mahadek basin.

In **Chapter 5** it is stated, comprehensive study of uranium disequilibrium status and its exploratory implications, covering Wahkut and Lostoin exploratory blocks both located under the West Khasi Hills district. Exploratory block Wahkut lies about 20 km west-south to the Domiasiat uranium deposit, as well adjoining (east) to the Wahkyn uranium deposit.

Wahkut exploratory block have special significance to this study work, as it contributes good data base on coring boreholes (33 out of 72) with high quality core recovery (>90%). Statistically, this block drives significant data base on the mineralised ore zone grade thickness (GT) for the coring boreholes of this study work. In view of the observed varying degree of uranium disequilibrium on surface samples across the three study block, higher degree of core recovery is much required to study detailed uranium disequilibrium status (both at micro and macro levels). Uranium mineralisation grade (G) and thickness (T) being analysed using radiometric core assay of drilled borehole, have been used to map uranium ore mineralisation envelopes in the  $\gamma$ -ray logs as well to negate the suspected radon interference in the exploratory boreholes.

Using pre-defined experimental criteria of 1.0 m zone thickness (T) at 0.010%  $eU_3O_8$  cut off grade (G), a population of 18 such simultaneous qualifying zones (borehole log and core assay) of 15 coring borehole, shows uranium mineralization grade thickness continuity

index 0.92 between the two set of variables with high confidence (81.5%). Developed continuity index 0.92 has now been used as predictor to the  $\gamma$ -ray logs mineralized zone (GT) data base for exploratory block Lostoin coring boreholes (n=7). The predicted results on the core assay grade thickness (GT) continuity for 6 qualifying mineralised zones of Lostoin exploratory block vis à vis that are experimentally observed in this block, shows good agreement. Lostoin exploratory block had some inherent environmental and administrative constraints leading to limited coring boreholes and poor core recovery. These experimental results, not only validates measured *insitu*  $\gamma$ -ray logs in the field but also confirms logged boreholes free from suspected radon contamination (indicated by the varying degree of surface disequilibrium conditions).

As an environmental indicator to the uranium mobility in the geological system, uranium disequilibrium status for the coring boreholes (mineralised) of Wahkut exploratory block (19 B.H) and Lostoin exploratory block (5 B.H) have been studied in the detail (both at micro and macro levels). Study findings indicate similar nature of parent favouring disequilibrium factor across the two exploratory blocks, in the basin.

In view of poor coring boreholes data base coupled with poor core recovery in Lostoin exploratory block, the concept of representative sampling approach, used to validate uranium hosting environment U-Th geo-coherence continuity over Lostoin exploratory block, was used independently to investigate status of uranium disequilibrium in Lostoin exploratory block. In the process, investigated uranium disequilibrium status on 22 non-coring (mineralised) boreholes of Lostoin exploratory block gave disequilibrium factors 1.48 much similar to that of Wahkut exploratory block, in the basin.

Thus after validating uranium exploratory index parameters both for the hosting environment and mineralised zone experimentally in Lostoin bock, for all practical purpose status of uranium disequilibrium across the Lostoin exploratory block is conservatively estimated

as 1.46. The examined exploratory block shows parent favouring subsurface uranium mineralization with skewed distribution of disequilibrium. Now bulk uranium ore tonnage measured by gross  $\gamma$ - ray logs can be factored by the estimated disequilibrium factor (1.46) for actual ore tonnage.

The estimated disequilibrium factor 1.46, hold good over reasonably aerial extent (~16 km) across the two blocks in the basin. The confidence parameters generated under this study work have implication not only to assess inferred category uranium ore in the block but also in setting up a road map for the systematic exploration of large uranium potential occurring over extended areas in the basin amid prevailing environmental and exploratory impediments. Summary, conclusions and further scope of study work in the basin are presented in **chapter 6**.

**Deliberately left blank**

## LIST OF FIGURES

FIGURE	Page No
1.1: U-238 series and decay products	3
1.2: Global Major Uranium Occurrence	6
1.3: Distribution of global Uranium Resources	7
1.4: Distribution of Uranium resources in India	8
1.5: Major Uranium province in the country	10
1.6: Mahadek basin with geological map	12
1.7: U disequilibrium status on Rangsohkham exploratory block grab samples. Dotted line shows equilibrium line (m:indicates disequilibrium factor)	13
1.8: U disequilibrium status on Lostoin exploratory block grab samples. Dotted line shows equilibrium line (m:indicates disequilibrium factor)	14
1.9: U disequilibrium status on Wahkut exploratory block grab samples. Dotted line shows equilibrium line (m:indicates disequilibrium factor)	14
2.1: Typical natural gamma ray spectrum in geological sample	19
2.2: Core assay assembly using circular array of GM detectors	21
2.3: Beta/gamma ( $\beta/\gamma$ ) assembly	23
2.4: Radiometrically analysed $U_3O_8(\beta/\gamma)$ vs chemically analysed $U_3O_8$	24
2.5: dMCA based Gamma ray spectrometer using 5"x4" NaI(Tl) detector	25
2.6: Compton contribution to $\gamma$ - ray spectrometry	26
2.7: Old Sample geometry: 4" dia 200 gms	28
2.8: Channel Sensitivity vs Sample thickness(expressed in terms of weight).	29
2.9: New Sample geometry: 5" dia 400 gms	30
2.10: Acquired $\gamma$ -ray spectrum on optimized dMCA system	31
2.11: Gamma Ray logging system for exploratory boreholes	32
3.1: Georeference based ambient gamma measurements in part of Khasi Hills	37

<b>3.2:</b> Gamma Profiling of major litho units in Mahadek basin	39
<b>3.3:</b> Sample variogram-Analytical model developed on sample data points. Numbers in the plot indicates total number of observations pairs associated with each bin	42
<b>3.4:</b> Ambient gamma levels - Predicted vs Measured	44
<b>3.5:</b> Interpolation of ambient gamma levels in Parts of Khasi Hills, showing delineated hot spots	45
<b>3.6:</b> Standard error associated to the interpolated gamma levels in parts of Khasi Hills	45
<b>4.1:</b> Rangsohkham exploratory block with drilled boreholes. Typical vertical cross section of borehole is shown by line section A-B	51
<b>4.2:</b> Uranium Index across the three Geological environments of Rangsohkham exploratory block	55
<b>4.3:</b> Lostoin exploratory block with drilled boreholes scheme	61
<b>5.1:</b> Wahkut exploratory block- Drilled borehole scheme with 'WC' as coring boreholes	69
<b>5.2:</b> Wahkut exploratory block-Developed grade thickness (GT) continuity index for uranium mineralization	73
<b>5.3:</b> Uranium disequilibrium distribution-Wahkut exploratory block	78
<b>5.4:</b> Lostoin exploratory block Grade Thickness (GT) behavior-Predicted vs Observed	80
<b>5.5:</b> Lostoin exploratory block: U disequilibrium status using representative sampling	84
<b>5.6:</b> Lostoin exploratory block: Conservative estimates of U disequilibrium	84

## LIST OF TABLES

TABLE	Page No
2.1: Optimised equivalent assembly parameters on 3"x3" NaI(Tl) detector setup	20
2.2 : Optimised core assay assembly for typical 52 mm drilled borehole core	22
2.3: $\beta/\gamma$ assembly setup with optimised parameters	23
2.4: Channel sensitivities on optimised sample geometry: Predicted vs Measured	30
2.5: Optimised Spectral parameters: 5"x4" NaI(Tl) detector based dMCA system	31
3.1: Acquired sample data points in parts of Khasi Hills: Statistical summary	40
3.2: Sample variogram grid geometry parameters	41
3.3: Developed sample variogram model parameters	42
3.4: Developed sample variogram model: Compatibility check	43
3.5: Variance analysis on predictability of sample data points	44
4.1: Representative sampling of major Geological environments in Rangsohkham exploratory block	53
4.2: Analytical Summary on representative samples from major Geological environments	54
4.3: Rangsohkham exploratory block, drawn representative samples: ANOVA Test	57
4.4: Analysed uranium equivalent activity-Regression Model for Rangsohkham exploratory block	58
4.5: Radio elemental Correlation Matrix-Rangsohkham exploratory block	59
4.6: Representative sampling of U hosting environment-Lostoin exploratory block	62
4.7: Analytical summary-Lostoin exploratory block representative samples	63
4.8: Uranium hosting environment- Benchmark study using multivariate analysis of study blocks	64
4.9: Uranium hosting environment- Benchmark study on radio elemental correlation matrix of study blocks	64
5.1: Wahkut exploratory block qualifying boreholes: $\gamma$ - ray logs and core assay	72

<b>5.2:</b> U disequilibrium status- Wahkut exploratory block qualifying boreholes	74
<b>5.3:</b> Vertical nature of U disequilibrium-Wahkut exploratory block	76
<b>5.4:</b> Lostoin exploratory block coring boreholes: $\gamma$ - ray logs and core assay	81
<b>5.5:</b> Uranium disequilibrium status- Lostoin exploratory block coring boreholes	82
<b>5.6:</b> Analytical summary-Lostoin exploratory block mineralised group samples	83
<b>5.7:</b> Vertical nature of Uranium disequilibrium-Lostoin exploratory block	85
<b>5.8:</b> Investigated disequilibrium status-Lostoin exploratory block	87

# **CHAPTER 1**

## **Introduction**

Radiometric studies on Mahadek basin exploratory blocks comprising Rangsohkham (East Khasi Hills district), Wahkut and Lostoin (West Khasi Hills district) in Meghalaya, have shown varying equilibrium conditions of surface uranium mineralization. At present, the basin hosts one of the largest and richest grade sandstone-type uranium deposits in the country with more than 21,000 tones of proven uranium resources. Uranium being pure alpha emitter, exploration work rather relies on indirect measurements of  $\gamma$ -radiation predominantly coming from Ra-group. However, oxidizing tendency of uranium in a open geological system makes prospecting work, based on gamma measurements, vulnerable to the prevailing environmental conditions.

Geological evidence in Mahadek basin indicates occurrence of large uranium potential with medium to small ore pocket size (grade  $<0.10\% U_3O_8$ ) disposed at shallow depth. But the high uranium mobility under the sedimentary environment together with logistics and exploratory impediments in the basin, makes exploration task extremely challenging and resources intensive.

Environmental conditions leading to disequilibrium in uranium series, depends on numbers of factors such as environmental redox conditions, long lived decay products (of uranium) to different physical and chemical properties of decay products. This Chapter discuss these relevant details on uranium prospecting in the subsequent section, together with uranium behaviour in natural environment & distribution over different geological environments and major uranium occurrences in the country.

**1.1 About Uranium Exploration:** Uranium is one of the abundantly found elements in the earth crust (rock/soil) with average concentration 2-3 ppm and sea water about 3 ppb. Natural uranium contains  $^{238}\text{U}$  and  $^{235}\text{U}$  the two major isotopes of uranium with relative abundance 99.28% and 0.72% respectively. These isotopes being high Z elements, are unstable in nature

and undergo radioactive disintegration with half-lives of several million years ( $^{238}\text{U}:4.5 \times 10^9 \text{ y}$  &  $^{235}\text{U}: 7.0 \times 10^8 \text{ y}$ ).

**1.1.1 Decay Series** Uranium is pure alpha emitter and disintegrate by a series of alpha and beta decays to form intermediate unstable decay products (also known as daughter products). U-238 decay series shown in Fig.1.1, contains 14 decay products in total with Pb-208 being stable one. Based on these decay products, U-238 decay series is divided into two major groups commonly known as U-group also called parent group (containing 4 decay product with 2  $\beta$  emitter) and Ra group (containing 10 decay product with 4  $\beta$  emitter). Since U-group is deficient in  $\gamma$ -emitters (most  $\beta$  emitters are also  $\gamma$  emitters), it contributes only about 2% of total gamma activities measured in the decay series. On the other hand Ra- group, having comparatively lower half-lives daughter products, contains several  $\beta$  emitters that nearly contributes 98% of the total gamma activity in the series.

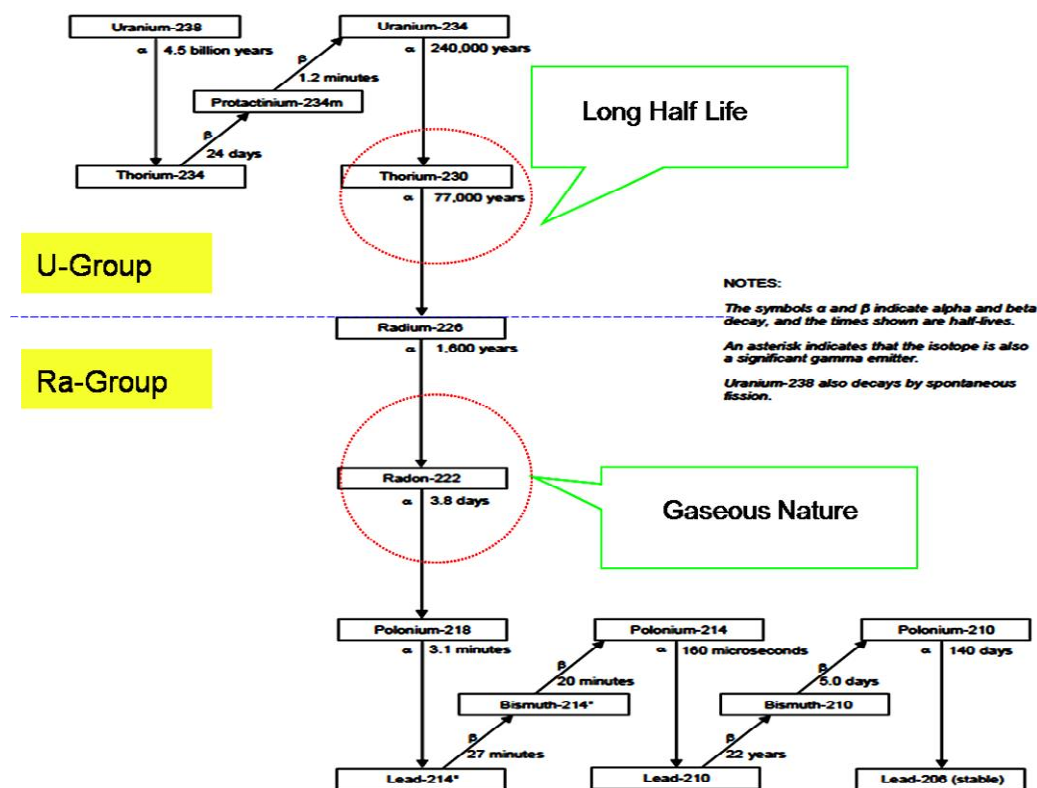


**Fig.1.1:** U-238 series and decay products.

**1.1.2 Prospecting Method:** There are several methods [1,2,3] for uranium prospecting but  $\gamma$ -radioactivity measurements, though an indirect method, is the most popular among them. Gamma detection method offers inherent advantage under field conditions, in comparison to alpha and beta measurements. Since  $\gamma$ -ray is having zero rest mass, can travel considerable distance in soil/rock matrix and effectively providing greater depth resolution for uranium prospecting in field. Due to these inherent advantages, high yield gamma activity ( $\approx 98\%$ ) from Ra-group has been widely used in uranium prospecting such as radiometric ground survey and aerial survey etc.

U-238 decay series, contains one of the long lived decay product Th-230 in U-group with half life 77,000 years (Fig.1.1) . Thus series nearly requires about half million years to attain equilibrium condition (also known secular equilibrium). Accordingly, uranium deposit formed about million year back in a closed geological system,  $\gamma$  activity based measurement gives quick and direct estimate of uranium occurrence in the system. Nevertheless, gamma activity based measurement is indirect in nature as measured signal emanates mostly from Ra-group decay products rather than parent uranium.

**1.1.3 Environmental Behavior:** The basic assumption of existence of equilibrium conditions, in uranium decay series, is much dependent on the prevailing environmental conditions. In real word, there are several uncontrollable variables in the surrounding geological environment [3] leading to deviation of equilibrium conditions in uranium series, commonly known as disequilibrium. There are varied cause of disequilibrium [4] in uranium series and the most important of them are environmental redox conditions, long half lives of decay products, different physical and chemical properties of decay products.

Unlike most metallic elements, uranium does not occur in free state and easily get oxidised containing mixture of  $\text{UO}_2$  and  $\text{UO}_3$ . Under non oxidising conditions, uranium in

tetravalent state  $U^{+4}$  is insoluble in water, however in presence of oxidising conditions  $U^{+4}$  state get converted to  $U^{+6}$  state known as uranyl ion  $(UO_2)^{+2}$ . Uranyl ion is soluble in water and easily gets transported over long distances particularly under the sedimentary environment [5] such as of Mahadek basin. Migrated uranium from the system leaves behind a trail of  $\gamma$ -emitting decay products depleted in uranium and thus giving rise to disequilibrium in uranium series. On getting reducing environment (carbonaceous matter, sulphides etc) transported uranyl ion, reduces back to  $U^{+4}$  state with uranium getting precipitated. Therefore, depending upon surrounding environmental conditions, prevailing topography and water movements, uranium can migrate over several kilometre from the source rocks before getting precipitated to form uranium mineral (high concentration uranium). Since U-group (Fig.1.1) contributes lower  $\gamma$ -activity ( $\approx 2\%$ ) of total gamma activity in the series,  $\gamma$ -detection method, if used for this younger type uranium deposit, underestimates uranium concentration depending upon geological time scale of its evolution.

In a similar way, other major disequilibrium cause in uranium series arises due to decay product radon (Fig.1.1) .  $Rn^{222}$  being inert gas with 3.8 days half lives, travels considerable distance in the soil/fractured rock matrix and gets easily escaped through fault/ fractures etc in the geological system and effectively creating disequilibrium in uranium series. Although this kind of disequilibrium is short lived, as disturbed equilibrium in uranium series is restored within a much shorter time scale of one month. But it has serious implications in open geological system namely sedimentary environment, adversely affecting *insitu* gamma measurements under field conditions.

Thus, with varying geological and environmental uncertainties, apparent uranium concentration measured by  $\gamma$ -ray measurements, no longer represents direct uranium

concentration. And hence understanding of uranium's environmental behaviour needs to be examined carefully during prospecting work in field.

**1.1.4 Hosting Environments:** Geologically, uranium occurrence is defined as naturally occurring with anomalous concentration. Occurrences that are economically recoverable (in terms of ore bulk tonnage) under the prevailing geological environment are called deposits. Depending upon varying geological settings, IAEA [6] have classified uranium deposits under 15 major categories.

As on defined cut-off date 01 Jan 2013, Uranium Red Book [7] has reported 7.64 million tonnes of proven global uranium resources. Distribution of this reported global uranium resources, across the major IAEA classified uranium hosting environments is summarised below on Fig.1.2.

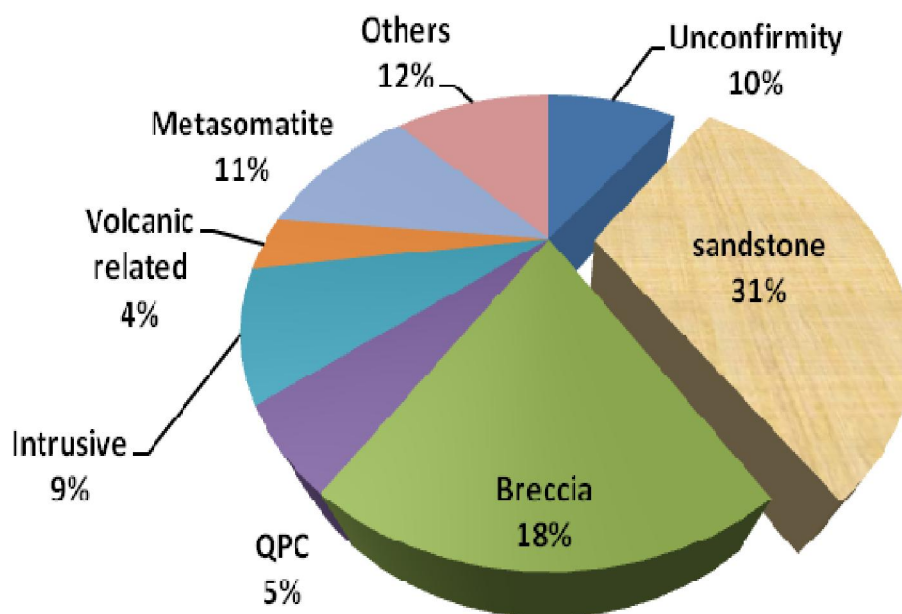


**Fig.1.2:** Global Major Uranium Occurrence [Red Book 2014].

These identified global uranium resources are economically recoverable with cost criteria < US\$260/kg of uranium (Red Book-2014). Summarised distribution in Fig.1.2, clearly shows Sandstone, Breccia, and Unconformity types uranium deposits contributing more than 50% of

global proven uranium resources. In today's global scenario, sandstone-type deposit alone contributes nearly one third of its proven uranium resources. In this context, Mahadek basin of Meghalaya, containing largest sandstone type deposit in the country, holds greater potential for further augmentation of uranium resources in the country.

**1.1.5 Geographical Distribution:** Distribution of 7.64 million tonnes of global proven uranium resources [7] is not uniform. On the said cut-off date (01.01.2013) global distribution status for the reported uranium resources is shown in Fig.1.3. Plotted distribution clearly shows Australia, Kazakhstan, Canada and Russia are the leading contributing nations with together accounting more than 50% of global proven uranium resources. Further, to the largest contributory nation, Australia alone contributes as much as one fourth of the proven global resources. Indian contribution of 1,19,900 tones on the said cut-off date stands merely 2% of global resources. Countries having varying contribution <2% are grouped together and listed under 'Others' category.

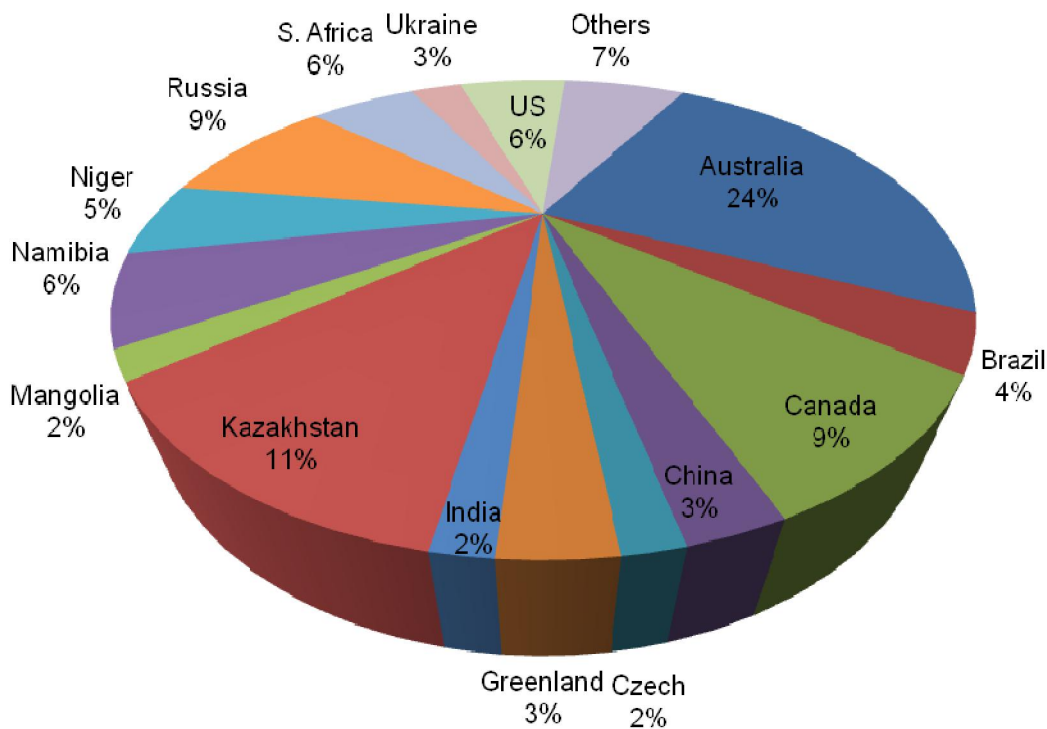


**Fig.1.3:** Distribution of global Uranium Resources [Red Book 2014].

**1.2 Overview of Indian Uranium Resources:** Most of the uranium deposits established in India, so far, falls under the category of low grade. At present, with the existing IAEA norms, India is poorly ranked in terms of its limited share to the global proven uranium resources. Nevertheless, with constant augmentation efforts, there has been gradual addition to the total uranium resources in the country including that of recent finding [8] in Cuduppa basin of Andhra Pradesh. Due to these augmentation efforts, proven uranium resources in the country has now gone up to 2.14 lakh tones [9] of uranium. Fig.1.4 presents state wise distribution of proven uranium resources in the country with three states namely Andhra Pradesh, Jharkhand and Meghalaya, as on date, contributes more than 80% of total resources in the county. Meghalaya based Mahadek basin, single largest sandstone hosted deposit in the country, ranked third in terms of its size by contributes 10% to the total 2.14 lakh tones of proven uranium resources in the country.

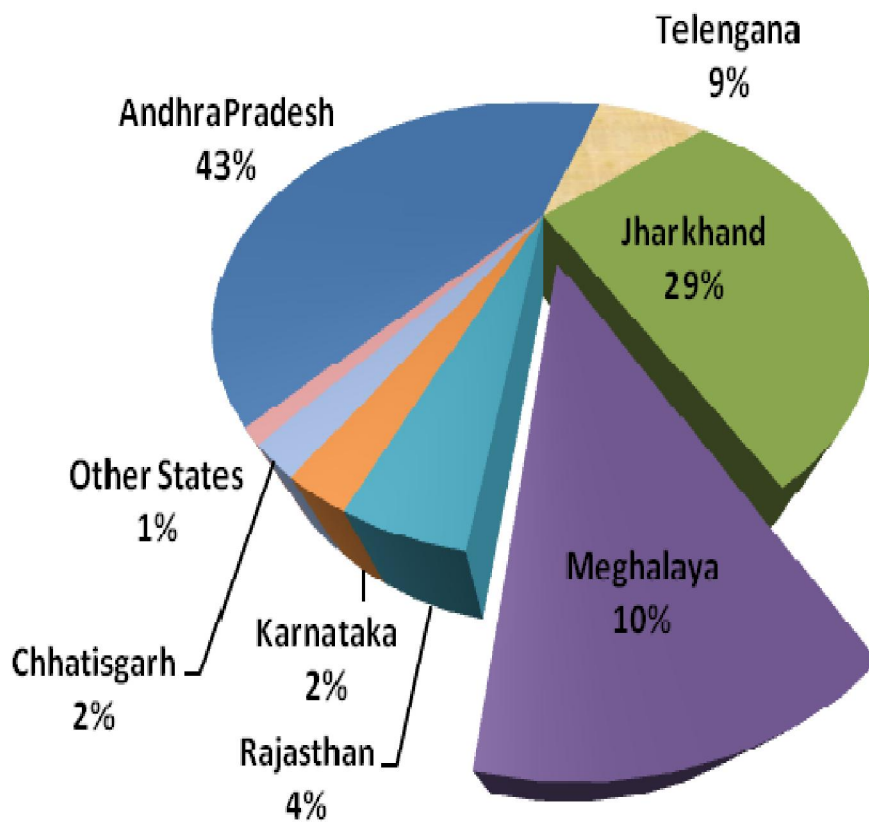


**Fig.1.4:** Distribution of uranium resources in India (As on October 2014).

Unlike some of the world's rich grade uranium deposits, ore grade found in the country (for most of the uranium deposits) are generally lean type [10] with typical average grade  $\leq 0.050\%$   $U_3O_8$ . Globally, Athabasca basin (Canada) with proven resources of more than 6 lakh te U and average grade 2%, contains more than two dozens of uranium deposits. Notably of them are super rich high grade uranium deposits of Cigar lake (1.39 lakh te U, average 18%) and McArthur River (1.89 lakh te U, average 21%). Similarly, Australia have significant uranium deposits in Jabiluka (67,000 te, average 0.49%) and Koongarra (14,500 te U, average 0.8%).

Other leading nations namely Kazakhstan, Namibia, Niger, Russia, South Africa and US also contains considerable tonnage of uranium deposits ranging from 0.055-0.10 % average grade. In global context, 0.10% is average uranium deposit grade with varying range 0.011% (Namibia -Trekopje ) to 21% (Canada-McArthur River).

In comparison to the global scenario, proven uranium resources in the country are low to medium tonnage with mostly poor grade. The only contributing uranium deposits from Mahadek basin (low to medium tonnage  $\sim 10,000$  te) of medium grade ( $\sim 0.10\%$ ) namely Domiasiat (now KPM: average grade 0.10% ) and Wahkyn (average grade 0.13%) [11,12,13] are comparable to that of global average grade. Fig. 1.5 presents status of leading uranium provinces in the country with Cuduppa basin, Singhbhum Shear zone, and Mahadek basin contributing to the tune of more than 80% of proven uranium resources. These leading contributors are being briefly being summarised with type of uranium occurrence.

**1.2.1 Bhima Basin:** This basin contains Vein type medium grade & low tonnage uranium deposit located at Gogi, in Karnataka state. Uranium ore grade found at Gogi is one of the richest (0.17% average  $U_3O_8$ ) in the country but of low tonnage ( $\approx 4300$  t).

**1.2.2 Cuduppa Basin:** There has been significant uranium findings in Cuduppa basin located in Andhra Pradesh. The basin readily added more than 40,000 te of low grades uranium resources to the existing one, in the country. To the Cuddapah basin, northern part host four major unconformity related low grade-low to medium tonnage U deposits namely Chitriyal, Lambapur, Peddagattu and Koppunuru. While southern part host dolostone based strata bound low grade-large tonnage uranium deposit especially at Tummalapalee, Rachakuntapalee and Kanampalee. Together with unconformity and strata bound uranium deposits type, this basin contributes highest 43% of proven uranium reserves in the country.

**1.2.3 Mahadek Basin:** This is one of the largest proven Sandstone-type uranium deposits in the country. This deposit is located under Mahadek basin of Meghalaya. Together with main deposit at Domiasiat (now KPM), Wahkyn and satellite deposits (Tyrnai, Gomaghat, Lostoin,

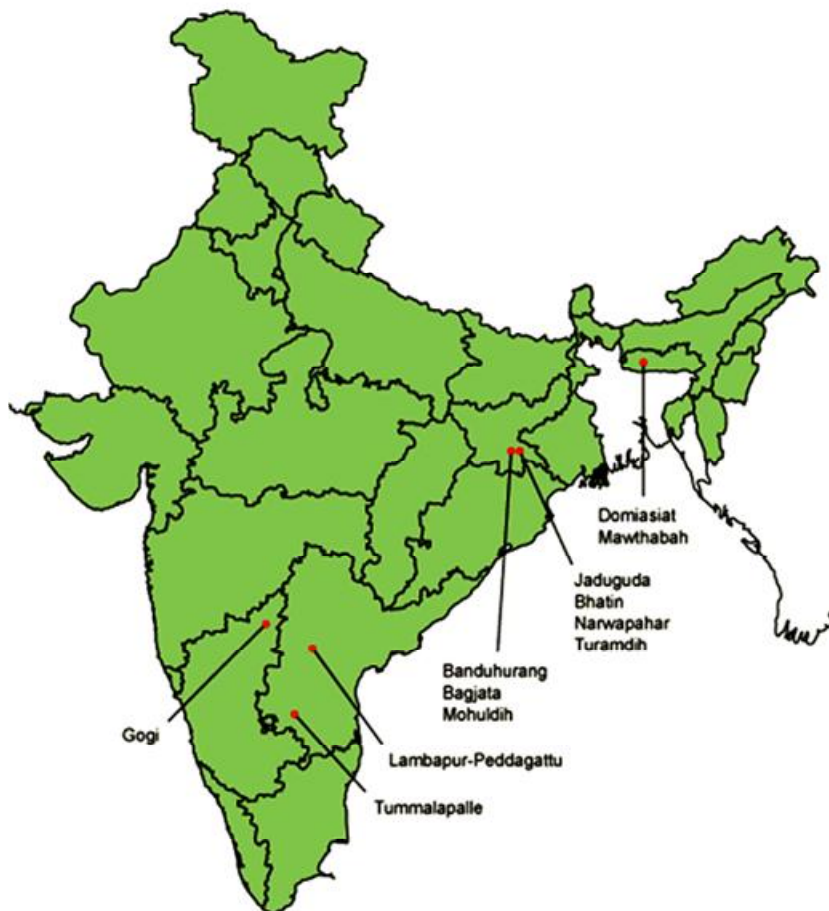


**Fig.1.5:** Major Uranium province in the country.

Wahkut and Umthongkut) basin, at present, contributes 10% of proven U resources of medium grade but low to medium tonnage.

**1.2.4 Singhbhum Shear Zone:** Located in Jharkhand state, this is one of the earliest finding of early fifties in the country. The first uranium deposit was discovered at Juduguda in Singhbhum Shear Zone (then part of Bihar). The Singhbhum Shear Zone (SSZ), hosts seventeen low grade-large tonnage Vein type uranium deposits, aggregating about 29% of proven uranium resources in the country. As on date, together with Jaduguda, Bhatin, Narwapahar, Turamdih, Bandhuhurng, Bagjata and Mohuldih findings, SSZ is one of the most important uranium province in the country contributing to the tune of 62,000 of proven uranium resources.

**1.3 About Mahadek Basin:** Departmental (AMD) exploration experience of four decades in Mahadek basin, shows challenging conditions of working environment. At present approximately 30% (aerial extent) of basin area have been explored with more than 21,000 tones of proven uranium resources, while the remaining promising part of the basin is masked by thick cover of younger non-mineralised rock and inaccessibility. The other operational challenges are typical prevailing tropical to subtropical climate (heavy rain falls), thick forest and poor logistics (roads and communication) etc. Further, oxidizing tendency of uranium with high uranium mobility in the sedimentary environment [4,5] such as Mahadek basin, makes measured  $\gamma$ - ray logs (in the exploratory blocks boreholes) vulnerable to the uranium migration conditions in the geological system.

**1.3.1 Geological Setting:** Meghalaya plateau, considered to be the north-eastern extension of the Precambrian peninsular shield, comprises rocks from the oldest Precambrian gneissic complex to the recent alluvium formations [14,15]. The Precambrian gneissic complex (para/ortho gneisses and migmatites) and Shillong Group of rocks (mainly quartzites) are exposed in the central, eastern and northern parts of Meghalaya plateau [16]. These are intruded by basic and ultrabasic intrusive and Neo Proterozoic granite plutons, such as South

Khasi batholith, Myllem granite, Kyrdem granite, Nongpoh granite [17]. The Lower Gondwana rocks (pebble bed, sandstone and carbonaceous shale) are observed in West Garo Hills. The Sylhet trap (mainly basalt, rhyolites and acid tuffs) of Middle Jurassic age is exposed in a narrow E-W strip along the southern border of Khasi Hills [18]. The Cretaceous Mahadek sandstones and Tertiary sediments occupy southern part of plateau and forms part of the Mahadek basin.

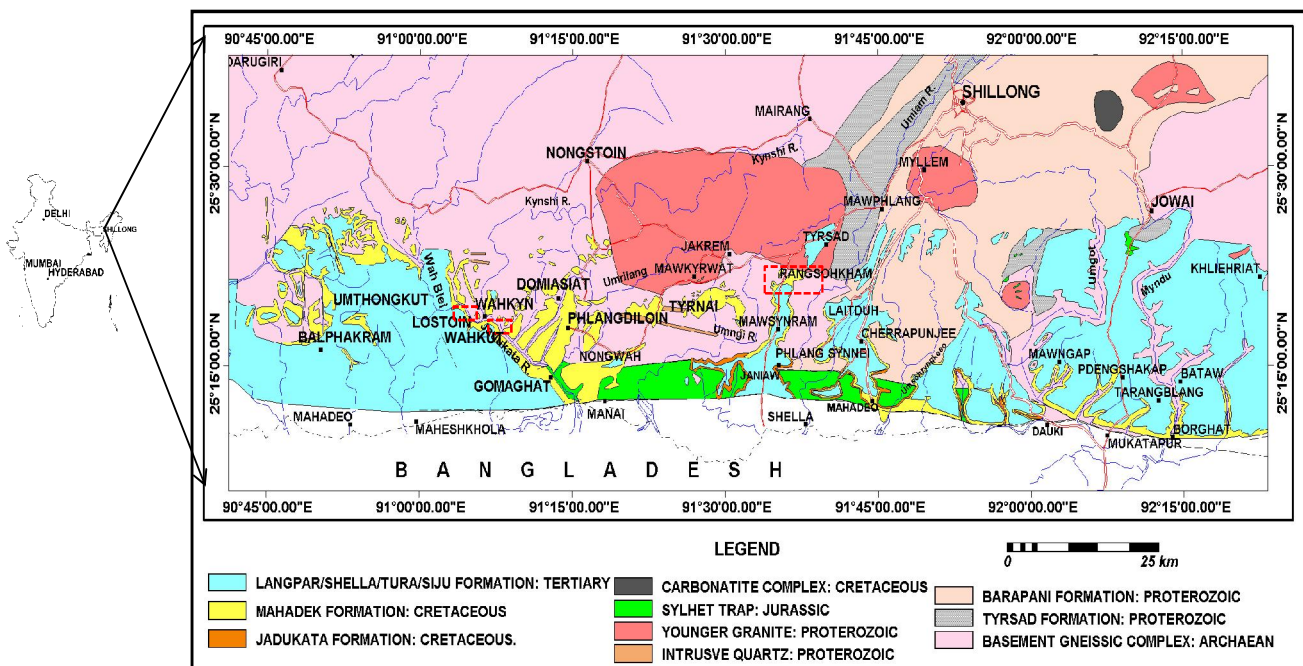


**Fig.1.6:** Mahadek basin with geological map.

Detail geological map of Mahadek basin containing study blocks is shown in Fig.1.6. This basin extends from the Jaintia Hills, in the east, to the Garo Hills in the west over nearly 180 km stretch and 7-18 km width from south to north in Jaintia, East Khasi, West Khasi and Garo Hills districts. Fluvial Lower Mahadek arkosic sandstone (thickness 30-70 m) and marine Upper Mahadek purple sandstone (thickness 50-300 m) are exposed over an area of 500 sq km. The remaining 1300 sq km area is overlain by younger Tertiary sediments viz Langpar formation- calcareous sandstone/shale, Sheila formation-alternations of sandstone and limestone, Baghmara formation-feldspathic sandstone, conglomerate and

clay etc.

The basin contains proven Sandstone type uranium deposits [11,12,13]. Uranium mineralization is hosted by the Lower Mahadek sandstone of upper Cretaceous age. Direct geological evidence in the basin [19] offers large uranium reserves potential of medium to small ore pocket size, grade  $<0.10\%$   $U_3O_8$ , disposed at shallow depth.

**1.3.2 Uranium Equilibrium Conditions:** Radiometric assay on drawn grab samples across a few exploratory blocks in the basin shows varying degree of disequilibrium in uranium series, measured from the  $45^\circ$  equilibrium line (shown dotted one) and plotted for analysed radiometric variables  $U_3O_8$  vs  $Ra_{(eq)}$  (radium expressed in terms of Ra equivalent or simply Ra). Quantitatively, regression fit between the two radiometric variables (U-group and Ra-group) gives estimation of disequilibrium factor ( $d = U_3O_8 / Ra$ ).

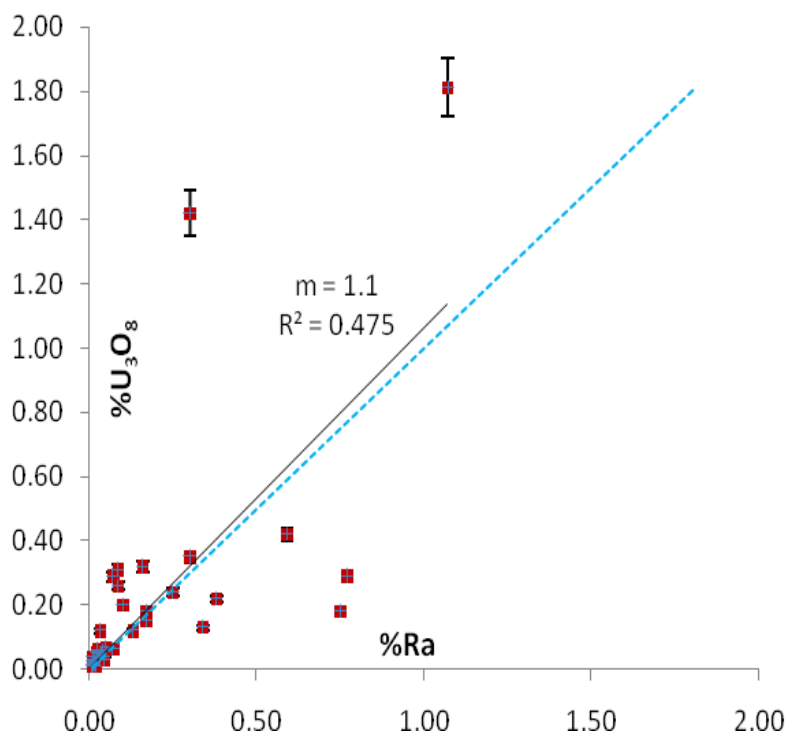


**Fig.1.7:** U disequilibrium status on Rangsohkham exploratory block grab samples (n=47). Dotted line shows equilibrium line (m:indicates disequilibrium factor).

Results analysed for the Rangsohkham exploratory block surface samples (n=47) indicates

mostly equilibrium condition ( $d=1.1$ ) as seen by the  $45^\circ$  equilibrium line (Fig 1.7).

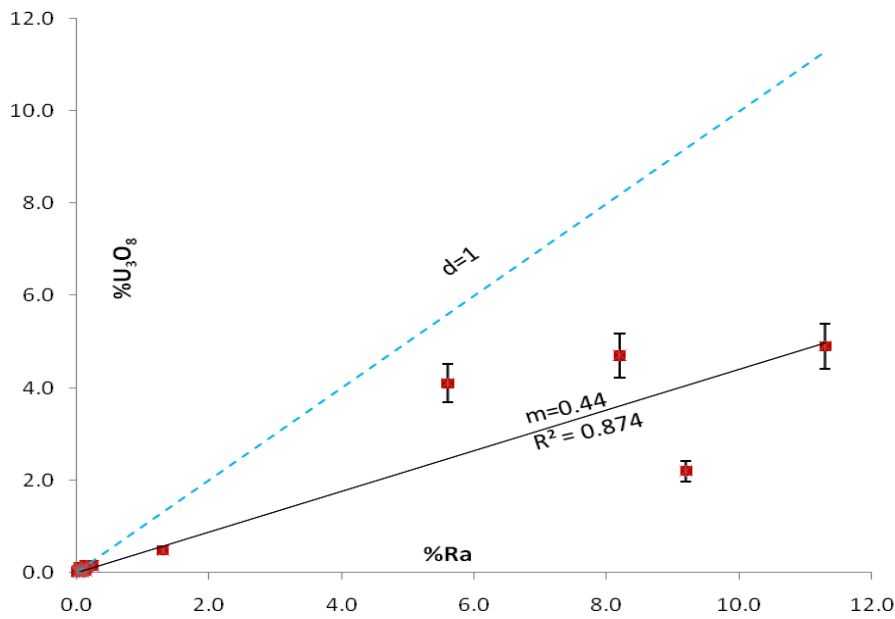


**Fig.1.8:** U disequilibrium status on Lostoin exploratory block grab samples (n=33). Dotted line shows equilibrium line (m:indicates disequilibrium factor).

Similarly, plotted disequilibrium status for Lostoin exploratory block grab samples (n=33) indicates severe departure ( $d<1$ ) in favor of Ra-group as seen by the  $45^\circ$  equilibrium line (Fig. 1.8).

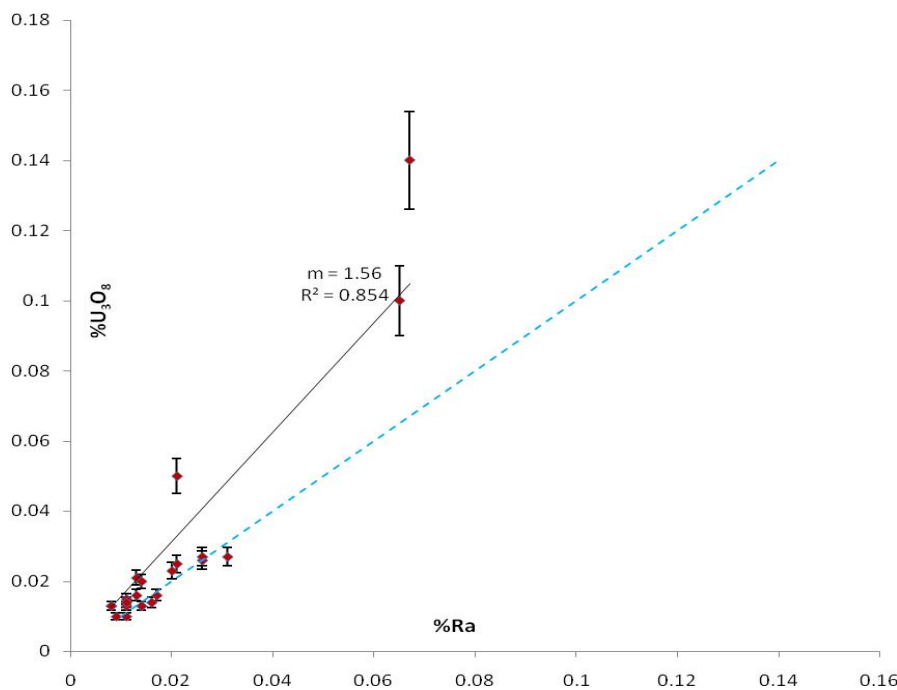


**Fig.1.9:** U disequilibrium status on Wahkut exploratory block grab samples (n=22). Dotted line shows equilibrium line (m:indicates disequilibrium factor).

On the other hand, plotted disequilibrium status for Wahkut exploratory block surface samples (n=22) shows disequilibrium ( $d > 1$ ) conditions in favor of U-group as seen by the  $^{45}\text{O}$  equilibrium line (Fig 1.9).

Prima facie, surface samples radiometrically analysed across the three exploratory blocks shows varying degree of uranium equilibrium conditions in Mahadek basin. This may affect bulk uranium ore tonnage across the exploratory blocks, being estimated by gross  $\gamma$ -ray logs [1,2] of reconnaissance boreholes.

During exploration phase in the basin, also seen is abrupt discontinuity between surface uranium mineralization and  $\gamma$ -ray logs in one of the exploratory block of Rangsohkhram [20]. Similarly, there are instances of  $\gamma$ -ray logs in reconnaissance boreholes, though showing good subsurface uranium mineralization but lacks good quality core recovery ( $\geq 90\%$ ) to affirm  $\gamma$ -ray logs with high confidence [21]. Thus one needs to have good understanding of uranium disequilibrium, for the most promising Mahadek basin, under challenging sedimentary environmental conditions.

**Deliberately left blank**

## **CHAPTER 2**

### **Analytical Setup and Measurements**

Identification of favourable radioactive zones and their interpretations to uranium exploration, is much dependent on the analytical inputs of representative samples drawn from the investigating area. Collected field/geological samples are usually analysed on analytical assemblies for their gross gamma activity, absolute uranium content and contributing primordial radio elemental (K,U,Th) concentration. The measuring analytical setups in the lab are optimised in such a manner that they provide good precision and accuracy for the analysed samples within the available time scale and resources. While optimising the analytical setup, one of the main considerations is the best possible detection limit, which in turn is governed primarily by a number of competing factors such as prevailing background, detector type/size, shielding requirements, sample geometry/size, and available counting duration etc.

Analytical techniques being used throughout this study work are non-destructive and passive in nature. And unlike chemical methods, radiometric analytical measurement offers several advantages such as sample repeatability, rapid measurement, process independent and inexpensive to use. With this background, this chapter briefly discusses all the relevant details in subsequent sections covering types of radiometric measurement setups with optimised parameters being used in the lab as well *in situ*  $\gamma$ -ray logging in the field.

**2.1 Natural Gamma Ray Spectrum:** Typical  $\gamma$ -ray spectrum on field/geological samples measured on NaI(Tl) detector setup is shown in Fig.2.1. Depending upon the type of application, a region of interest (ROI) is chosen to the natural  $\gamma$ -ray spectrum while setting up analytical measuring setup in the lab.

Gross gamma activity setups, measure gamma activity level using integral counting in the ROI of 0.3-3.0 MeV to that of natural  $\gamma$ -ray spectrum for field/geological samples. Whereas, spectral measures of primordial radio elemental (K,U,Th) concentration is done using differential counting of well defined photo peaks, in natural  $\gamma$ -ray spectrum,

contributed by the principle gamma emitters namely K-40 (1.46MeV) , U-238 (1.46 MeV, Bi-214) and Th-232 (2.62MeV, Tl-208).

During routine bulk sample analysis, only finite counting time is available per sample. There exist several constraints while optimising laboratory based setup. For a given detector type/size, shielding, prevailing background and finite counting time etc, sample geometry optimisation is the most suitable and cost effective method to achieve high quality analytical results.

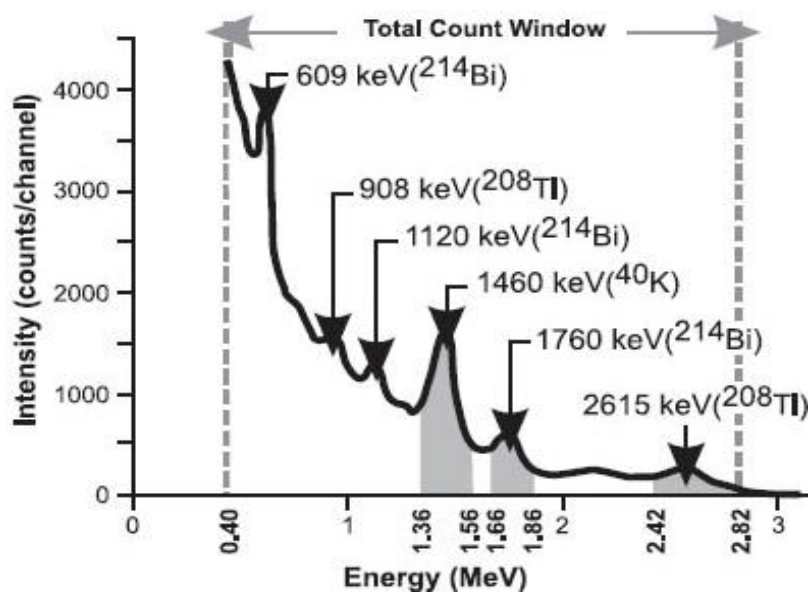


**Fig.2.1:** Typical natural gamma ray spectrum in geological sample.

**2.2 Gross Gamma Measurement:** Uranium prospecting work, typically begin with gross  $\gamma$ -activity measurement, commonly expressed in terms of equivalent uranium activity ( $eU_3O_8$ ), in field samples/drilled borehole core. Equivalent uranium activity is popular measures of gamma activity in uranium prospecting and mainly contributed by primordial radioelements (K,U,Th). The ROI for  $eU_3O_8$  measurements in natural gamma spectrum mainly consist 0.30-3.0 MeV and stands clear from the absolute  $U_3O_8$  content. Estimation of  $eU_3O_8$  in field/geological samples, while retaining similar counting interval to both standard and sample, is done by the following mathematical expression.

$$eU_3O_8 = \frac{A_{Std} N_S W_{Std}}{N_{Std} W_S} \dots\dots\dots(i)$$

Where  $A_{Std}$  : Denotes uranium standard activity expressed in-terms of ppm or %  $U_3O_8$

$N_{Std}$  and  $N_S$  : Denotes net standard and sample counts respectively,

$W_{Std}$  and  $W_S$  : Denotes standard and sample weight respectively.

The following gross gamma activity based setups are being used for the analytical inputs to the uranium prospecting work.

**2.2.1 Equivalent Assembly:** Sample brought to the lab are coarse grinded (minus 60 mesh size) to prepare representative sample in 100 gms geometry for gross radiometric measure on equivalent assembly. The assembly setup comprises a 3"x3" NaI(Tl) detector set up & processing electronics with counting system. Sample geometry include 3" dia container with 100 grams sample. Estimation of equivalent activity is done using equation (i).

After gross activity gamma measurements, active sample are sorted out based on the defined cutoff criteria of 100 ppm  $eU_3O_8$ . Field/geological samples meeting the cutoff grade, are only then processed for their absolute  $U_3O_8(\beta/\gamma)$  and percentage level spectrometric contents measurements, on other assembly setups. Optimised assembly parameters in the lab are listed on Table 2.1 having 10 ppm  $eU_3O_8$  detection limit.

Parameters.	$\gamma$ - Counting	Remark
Average background counts	1832 (n=5)	<ul style="list-style-type: none"> <li>• Detector type -NaI(Tl)</li> <li>• U Standard- 472 ppm</li> <li>• Std geometry -3" dia.</li> <li>• Std weight =100 gms</li> <li>• Counting time= 200 sec</li> <li>• Computed Sensitivity is for Std weight</li> </ul>
Gross Std counts	10805 (n=5)	
Sensitivity (Net counts/200 sec/ppm $U_3O_8$ )	19.01	

**Table 2.1:** Optimised equivalent assembly parameters on 3"x3" NaI(Tl) detector setup.

**2.2.2 Core Assay Assembly:** This assembly is mainly used to examine grade/thickness (GT) continuity index across mineralised ore zone (active zone) in reconnaissance boreholes to that of drilled borehole core. In the field, identification of active borehole core is done by means of active radiometric zone reported by *insitu*  $\gamma$ -ray logs of reconnaissance boreholes. Drilled core for the corresponding mineralised zone of boreholes is then transported to the lab for equivalent uranium activity measurements on core assay assembly.

The assembly comprises a circular array of 6 GM detectors (Fig.2.2) each 15 cm long (type 1015, ECIL make). Unlike equivalent assembly sample geometry,  $eU_3O_8$  measurement on this assembly is done using nearly  $2\pi$  cylindrical geometry for typical 15 cm average core length. In order to analyse varying drilled core sizes of dia 32 -62 mm, assembly (Fig.2.2) is equipped with provision for interchangeable circular guide.



**Fig.2.2:** Core assay assembly using circular array of GM detectors.

Typical optimised parameters on circular array core assay assembly for 52 mm core size are presented on Table 2.2 . With the existing detector setup, the assembly is easily capable to detect 100 ppm  $eU_3O_8$ .

Parameters	$\gamma$ - Counting	Remark
Background counts	592 (n=5)	<ul style="list-style-type: none"> <li>• Detector type- G.M tubes</li> <li>• Core Std dia =52 mm</li> <li>• U Standard =0.35%U3O8</li> <li>• Standard weight =544.5 gm</li> <li>• Counting time= 200 sec</li> <li>• Computed Sensitivity is for Std weight</li> </ul>
Gross Std counts	3282 (n=5)	
Sensitivity (Net counts/200 sec/ppm $U_3O_8$ )	0.77	

**Table 2.2** Optimised core assay assembly for typical 52 mm drilled borehole core.

**2.3 Beta Gamma Assembly:** Samples analysed for equivalent uranium activity and meeting the set cutoff criteria ( $\geq 100$  ppm  $eU_3O_8$ ) are then fine powder crushed (minus 120 mesh size) for absolute  $U_3O_8$  measurements using  $\beta/\gamma$  method described elsewhere [22]. The assembly setup measures simultaneous beta and gamma activities in field/geological samples. Estimation of radiometric  $U_3O_8$  is done by using the following equation,

$$U_3O_8 = C(U_\beta - U_\gamma) + U_\beta \quad \text{.....(ii)}$$

Where C is constant (=1.6, in this case) determined practically on  $\beta/\gamma$  assembly. It represents ratio of U-group to Ra-Group beta emitters in U-238 series.

$U_\gamma$  : Equivalent uranium activity measured by  $\gamma$ -counting and computed by (i)

$U_\beta$  : Equivalent uranium activity measured by  $\beta$ -counting and also computed similar to equation (i) except weight factor is replaced by rather density correction factor, as  $\beta$ -counting is surface phenomenon.

Beta gamma assembly essentially comprises a circular lead shield (Fig.2.3) housing  $1\frac{3}{4}$ " x 2" overlooking NaI(Tl) detector (7D8 type, Harshaw make) for  $\gamma$ -counting and under looking 2" dia pancake type end window  $\beta$  tube (LND 7314 type) for simultaneous  $\beta$ -counting. Sample geometry consist of circular 2" dia aluminum disk of 1" height able to hold 50 gms sample. During optimization of beta counting, an aluminum filter of 250 mg/cm<sup>2</sup>

thickness has been used to reduce the interference from pure beta emitters namely K-40 and Ra-E (Bi-214). Optimized assembly offers detection limit of 100 ppm  $U_3O_8(\beta/\gamma)$  for defined 50 gms sample geometry.



**Fig.2.3:** Beta/gamma ( $\beta/\gamma$ ) assembly.

Table 2.3 list details optimized parameters on the  $\beta/\gamma$  assembly.

Parameters	$\beta$ -Counting	$\gamma$ - Counting	Remark
Background counts	193(n=6)	3920	<ul style="list-style-type: none"> <li>• U Standard =50 gms</li> <li>• U Standard =0.11% <math>U_3O_8</math></li> <li>• Counting time= 500 sec</li> <li>• Computed Sensitivity is for Std weight</li> <li>• Al filter (beta) 250 mg/cm<sup>2</sup></li> </ul>
Gross Std counts	3937 (n=6)	22070	
Sensitivity (Net counts/500 sec/ppm $U_3O_8$ )	3.40	16.50	

**Table 2.3:**  $\beta/\gamma$  assembly setup with optimised parameters.

**2.3.1 Radiometric  $U_3O_8$  Benchmark Study:** Radiometrically analysed absolute uranium in field/geological samples, on  $\beta/\gamma$  assembly, is an important exploratory input to understand uraniumiferous nature of area under investigation. In order to ensure, high quality precision and accuracy being reported to the analysed samples, on optimized  $\beta/\gamma$  assembly, a quality check was performed. One set of test batch core samples (n=25), randomly selected for coring borehole WKT/ C-23 in Wahkut exploratory block, was analyzed for radiometric

$U_3O_8(\beta/\gamma)$  on  $\beta/\gamma$  assembly. This block was chosen, since it contains good database on coring borehole with high degree core recovery (>90%). Subsequently, radiometrically analysed samples were chemically analysed for  $U_3O_8$ . Fig.2.4 shows benchmark study of radiometrically analysed  $U_3O_8(\beta/\gamma)$  to that of chemically analysed  $U_3O_8$ . The test results show good consistency for the two set of independent measurements at high degree (>90%) confidence level.

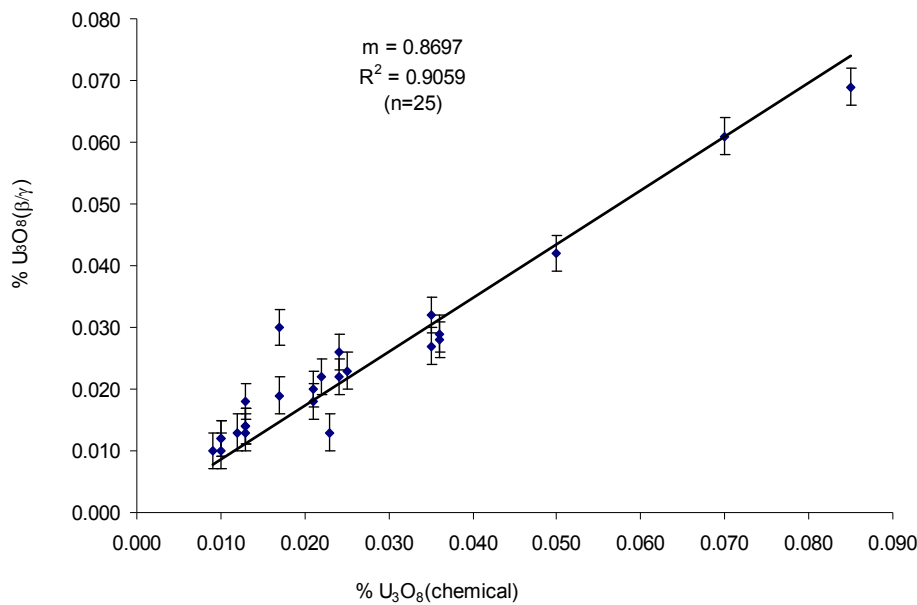


**Fig.2.4:** Radiometrically analysed  $U_3O_8(\beta/\gamma)$  vs chemically analysed  $U_3O_8$ .

**2.4 Gamma Ray Spectrometry:** Gamma ray spectrometric analysis of field/geological samples across the three chosen energy window (Fig 2.1) provides elemental concentration of contributing radio elements K,U and Th to the measured  $eU_3O_8$  on equivalent assembly. Uranium is rather being measured through Ra-group, since principle 1.76 MeV gamma contributor Bi-214, belongs to Ra-group. In view of possible geological disequilibrium consideration in Ra group, measured spectral activity through Bi-214 is expressed in terms of  $Ra_{(eq)}$ . However, for most of the ppm range analysis, one assumes equilibrium conditions of uranium series and  $Ra_{(eq)}$  is frequently exchanged to represent ppm level U concentration.

Long counting hours are needed for ppm range primordial radio elemental (K,U,Th) concentration measurements. On existing 5"x4" NaI(Tl) detector setup (Fig.2.5) and digital signal processing [23] based( dMCA) system with existing shielding, prevailing background and finite counting time, the required spectrometric parameters have been optimized (to meet better ppm range accuracy of primordial radio elements) by means of sample geometry optimisation.



**Fig.2.5:** dMCA based Gamma ray spectrometer using 5"x4" NaI(Tl) detector.

**2.4.1 Working Principle:** Gamma ray interaction with scintillation detector being statistical in nature, spectral measurements of primordial radio elemental concentration (K,U,Th) is done by selecting principle gamma contributor  $K^{40}$ (1.46MeV),  $U^{238}$ (1.76MeV),  $Th^{232}$ (2.62MeV) and related energy window also called channel width. The channel width is defined in terms of  $\pm 3\sigma$ , where  $\sigma$  is standard deviation of fluctuation of count rate around photo peak and determined experimentally by measuring detector resolution for known

gamma energy. Based on experimentally measured NaI(Tl) detector resolution ( $\approx 9\%$ ) for 662 KeV  $\text{Cs}^{137}$  photo peak, channel widths are assigned accordingly  $\pm 100\text{KeV}$  for K-channel and  $\pm 200\text{ KeV}$  for U & Th channels.

Further with a given sample geometry, standard weight, counting time (500 sec per observation) and identified spectral channel widths (K,U,Th), respective channel sensitivities are defined as,

$$S_K = \text{Net counts in K Channel} / \%K / 500 \text{ sec} \quad \dots\dots\dots(\text{iii})$$

$$S_U = \text{Net counts in U Channel} / \text{U ppm} / 500 \text{ sec} \quad \dots\dots\dots(\text{iv})$$

$$S_{Th} = \text{Net counts in Th Channel} / \text{Th ppm} / 500 \text{ sec} \quad \dots\dots\dots(\text{v})$$

On account of finite detector volume and Compton continuum contributed by the high energy gamma to lower channels, observed count one needs to be stripped off from the undesired Compton contribution shown on Fig.2.6.

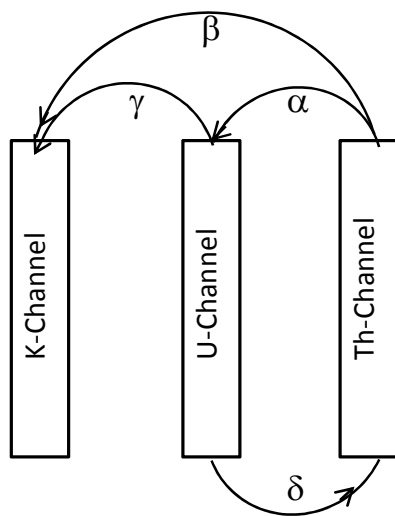


**Fig.2.6:** Compton contribution to  $\gamma$ - ray spectrometry.

This evaluates net channel sensitivities as defined by above equation (iii) to (v). In practice, this is achieved by defining Compton stripping constants  $\alpha$ ,  $\beta$ ,  $\gamma$  and  $\delta$  and then determining them practically on 5"x4" NaI(Tl) detector by means of measuring detector gamma response [3] for K , U, Th standards (of equal weights) across the three identified channels in

following manners,

$$\alpha = \text{Net counts in U Channel} / \text{Net counts in Th Channel} \dots\dots\dots(\text{vi})$$

$$\beta = \text{Net counts in K Channel} / \text{Net counts in Th Channel} \dots\dots\dots(\text{vii})$$

$$\gamma = \text{Net counts in K Channel} / \text{Net counts in U Channel} \dots\dots\dots(\text{viii})$$

$$\delta = \text{Net counts in Th Channel} / \text{Net counts in U Channel} \dots\dots\dots(\text{ix})$$

Where Net counts stands for background subtracted counts, denoted by  $N(\text{net})$  for the respective channel and calculate the net stripped counts  $N(\text{strip})$  in each channel, using following set of equations,

$$\text{Th Channel [2.62MeV]: } N^{Th}(\text{strip}) = N^{Th}(\text{net}) - \delta N^U(\text{net}) \dots\dots\dots(\text{x})$$

$$\text{U Channel [1.76MeV]: } N^U(\text{strip}) = N^U(\text{net}) - \alpha N^{Th}(\text{net}) \dots\dots\dots(\text{xi})$$

$$\text{K Channel [1.46 MeV]: } N^K(\text{strip}) = N^K(\text{net}) - \beta N^{Th}(\text{net}) - \gamma N^U(\text{net}) \dots\dots\dots(\text{xii})$$

Finally, for given standard weight and counting interval, stripped channel counts  $N(\text{strip})$  are converted to primordial radio elemental concentration (K,U,Th) using respective channel sensitivities, defined by equation (iii) to (v).

**2.4.2 Sample Thickness Optimization:** In view of statistical requirements, usually, long counting hours are needed for ppm range primordial radio elemental analysis of field samples. To achieve better system performance amid finite counting time and given resources namely 5"x4" NaI(Tl) detector setup and detector shielding, we looked upon to optimize existing 4"dia (200 gms) sample geometry (Fig.2.7). This was done in such a manner that there is minimal attenuation to the three photo peak of interest (Fig.2.1) for sample matrix of interest, namely K-1.46 MeV, U-1.76 MeV and Th-2.62 MeV respectively. The IAEA supplied standards have been used to determine linearity between sample thickness and count rate.



**Fig 2.7:** Old Sample geometry: 4" dia,200 gms.

Measured detector response to the standard set used vis-à-vis sample thickness for the three principle gamma photo peaks, in their defined channel window are plotted on Fig.2.8. Experimental plots (Fig.2.8) on determination of optimal sample thickness, expressed in terms of weight, gives 3.5cm as an optimal sample thickness for sample matrix of interest. Now using this optimal sample thickness, a new 5"dia 400 gms sample geometry was introduced (Fig.2.9) for the  $\gamma$ -ray spectrometry of PPM range sample analysis.

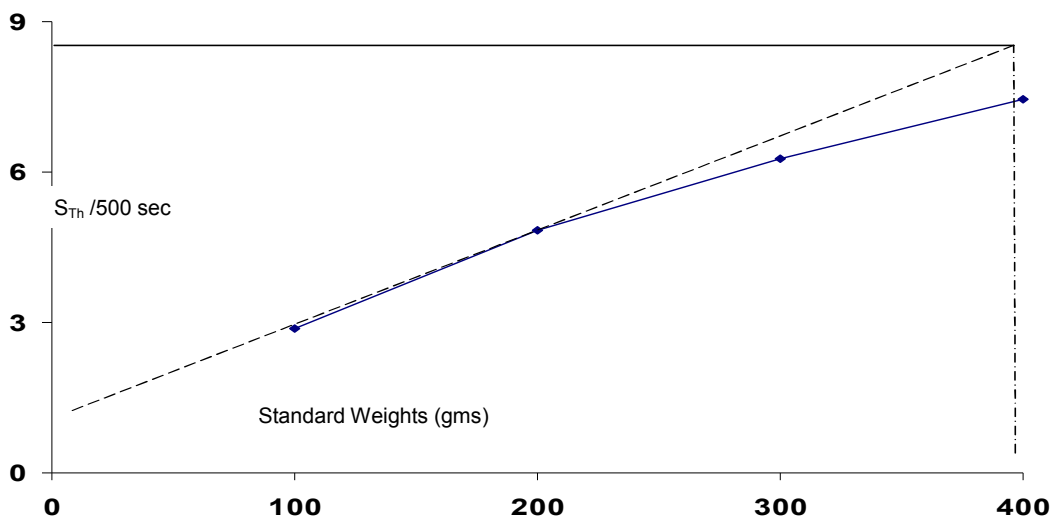
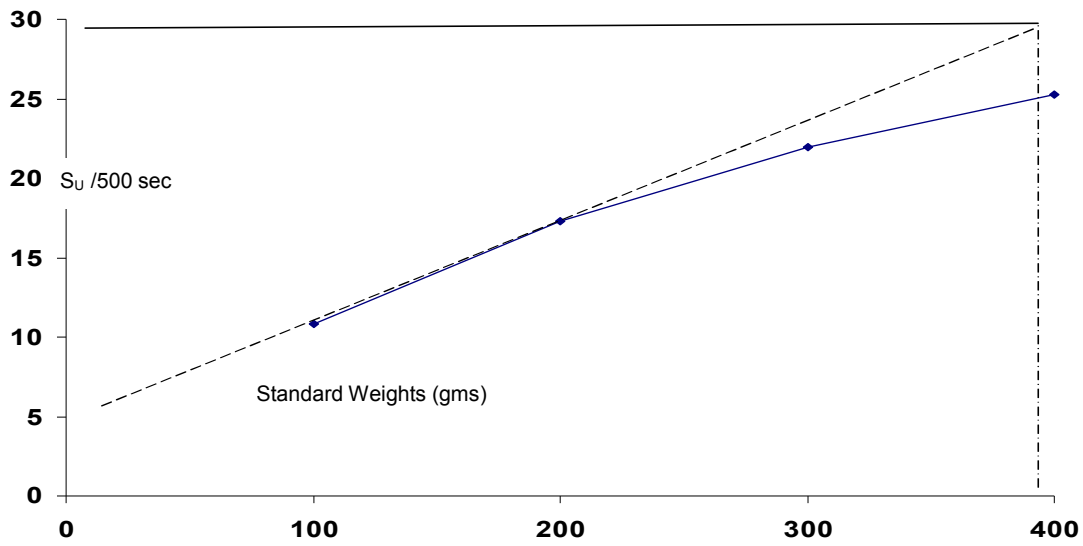
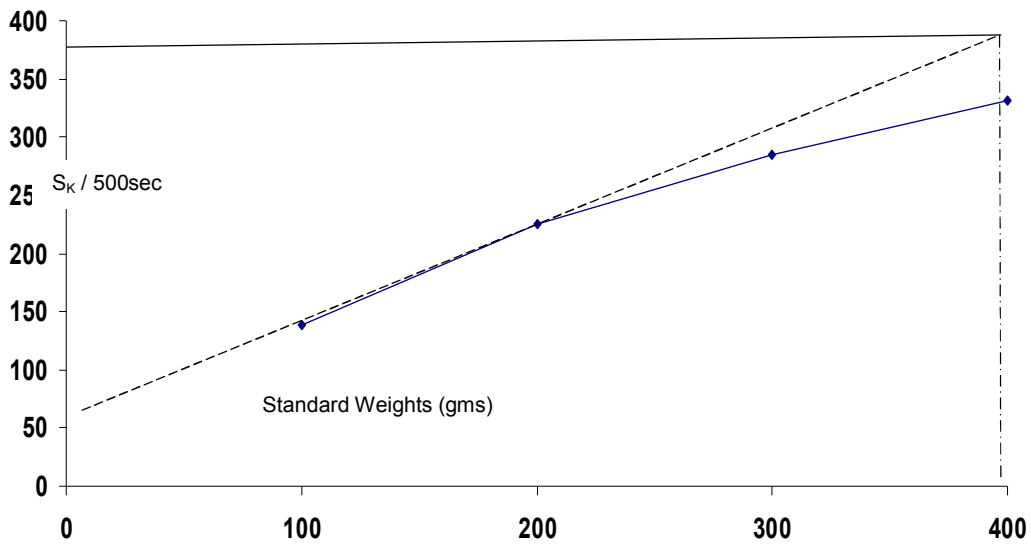


**Fig 2.8:** Channel Sensitivity vs Sample thickness (expressed in terms of weight).



**Fig 2.9:** New Sample geometry: 5" dia,400 gms.

Now using optimal sample thickness (expressed in weight) for the three energy channels, corresponding extrapolated sample sensitivity versus that measured experimentally are shown on Table 2.4. These experimental results shows good agreement between the two set of variables namely predicted and observed data values.

Counting Channels	Channel Sensitivities		Remark
	Extrapolated Value : 4" dia,400 gms geometry	Observed Value: 5" dia,400 gms geometry	
K- (1.46MeV)	385	375.8	Shows good match to the average measured value (n=39)
U- (1.76MeV)	29	29.1	
Th- (2.62MeV)	8.3	8.3	

**Table 2.4:** Channel sensitivities on optimised sample geometry: Predicted vs Measured.

Summary of optimized spectral parameters using 5"x4" NaI(Tl) detector and digital signal processing based MCA system, is presented on Table 2.5. This  $\gamma$ -ray spectrometer have been used for spectral contents measurements in field /geological samples.

Thus with the prevailing background conditions, there is an improvement to the three channel sensitivities for 5" dia 400 gms sample geometry (Fig.2.9) setup on 5"x4" NaI(Tl) detector based dMCA system ( $\gamma$ -ray spectrometer). This has significantly improved the required sensitivities and

minimum detection limits (MDL) for the three radio elements K , U and Th. Shown on Table 2.5, quantitatively optimized  $\gamma$ -ray spectrometer has resulted improved MDL of 40% in K channel, 36% in U channel and 27% in Th channel respectively.

Spectral parameters		Sample Geometry		Remark
		Existing:4"dia, 200gms	New : 5"dia, 400gms	
Stripping Constants		$\alpha=0.296, \beta=0.510,$ $\gamma=0.826, \delta=0.055$	$\alpha=0.360, \beta=0.615,$ $\gamma=0.843, \delta=0.041$	Detector resolution $\approx 9\%$ @662KeV [ $\text{Cs}^{137}$ ] Counting time:500 sec. Average background counts: K-Channel =396 U-Channel =187 Th- Channel =143
Sensitivity	K-Channel	$S_K=250.72$	$S_K=375.79$	
	U-Channel	$S_U=18.98$	$S_U=29.12$	
	Th-Channel	$S_{Th}=6.05$	$S_{Th}=8.25$	
MDL	K-Channel	0.5%	0.3%	
	U-Channel	2.2ppm	1.4 ppm	
	Th-Channel	6.0ppm	4.4 ppm	

**Table 2.5:** Optimised Spectral parameters on 5"x4" NaI(Tl) detector based dMCA system

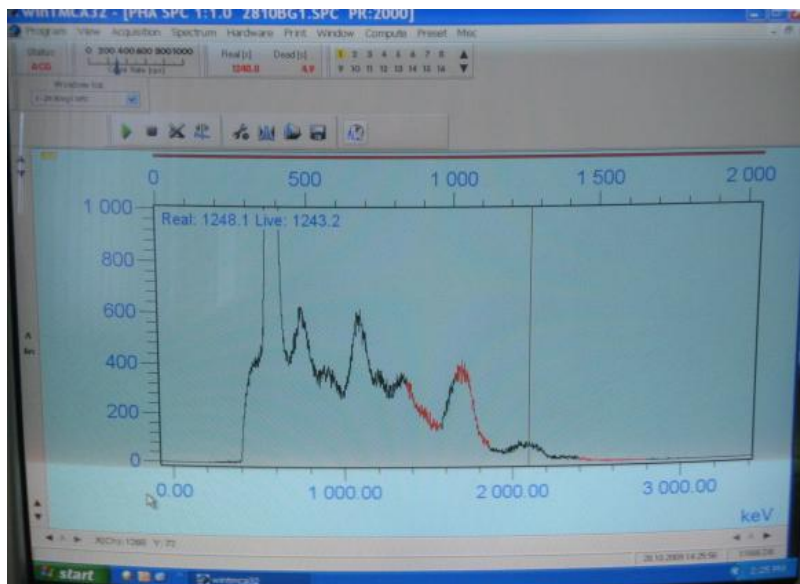


**Fig.2.10:** Acquired  $\gamma$ -ray spectrum on optimized dMCA system.

On the optimized  $\gamma$ -ray spectrometer in lab, typical acquired gamma spectrum for field/geological samples is shown on Fig.2.10.

**2.5 Gamma Ray Borehole Logging:** Measurement of subsurface uranium activity across the Mahadek basin exploratory blocks has been done, using natural  $\gamma$ -ray logging [1,2,3] of drilled boreholes. Gamma ray logging system essentially gives grade (G) and thickness (T) information on uranium mineralisation ore zone by measuring gamma intensity profile down along the boreholes, using 0.3-3.0MeV ROI of natural  $\gamma$ -ray spectrum (Fig.2.1). The system consists of logging probe, armoured cable, tripod, pulley, depth recorder and digital count rate meter (Fig.2.11).



**Fig.2.11:** Gamma Ray logging system for exploratory boreholes.

One of the main component of borehole logging system is G.M. detector (Type 1010, ECIL make) typically housed in 35 mm dia x 1.0 m long water tight brass housing. Logging probe is designed to withstand tens of bar water pressure in typical 600-1000 m deep boreholes. Probe has got built in electronics to support required detector power supply (+1000V), pulse shaping of detector signal and driver amplifier to transmit deep borehole  $\gamma$ -signal through armoured cable to count rate meter on surface. The logging probe is capable to provide 10 cm depth resolution with better than 100 ppm  $eU_3O_8$  detection limit for *insitu*  $\gamma$ -ray logs of exploratory boreholes. The gamma probe has got typical sensitivity of 120

counts per 100 ppm uranium standard. In view of logistic consideration in the basin, logging system has been designed to keep portability in mind with acceptable dead time to handle 1% uranium ore grade in the mineralised boreholes.

~~Deliberately left blank~~

## **CHAPTER 3**

# **Ambient Gamma Radiation Measurements**

Surrounding rock/soils medium in the earth crust, exhibits considerable spatial variation in ambient gamma levels owing to the different chemical and mineralogical composition of constituting rocks [24] that contains varying concentrations of  $K^{40}$ ,  $U^{238}$  and  $Th^{232}$  primordial radio elements. Thus, measurements on ambient gamma levels offer one of the basic and rapid tools (during initial course of radiometric field survey) to assess potential uranium occurrence in the area. Depending upon the regional geological features, suitable interpolation [25] on these acquired sample data points offers, quick assessment of gamma levels over the large area especially to the inaccessible location.

Literature review on kriging based interpolation techniques shows several field application including that of mineral exploration [26] to critical environmental studies [27, 28]. On irregularly spaced field sample data points, kriging algorithm offers several advantages in terms of providing good overview, easier to detect pattern to predicting data values over a large grid size.

In order to delineate the potential exploration targets over the greater and extended area of Mahadek basin, often characterized with inaccessibility/ remote location & poor infrastructure, study on ambient gamma level measurement is being taken up to understand the spatial continuity of sample data points in the area. The acquired sample data points will be used to develop an analytical model of sample variogram (with reasonably good confidence) and to interpolate sample data points over the known area in the basin.

With the view to carrying out uranium exploration work in targeted manner and in synergy to the ongoing exploration work in the basin, this Chapter discuss in subsequent section, study undertaken on ambient gamma radiation measurements in parts of Khasi Hills (18 sectors) to examine litho unit based spatial variation especially in relation to the hosting environment of Mahadek basin.

**3.1 Material:** Onsite measurements of ambient gamma levels in parts of Khasi Hills was done using battery operated high sensitivity environmental radiation monitor type ER-705M, designed to cover wide range of dose rates 8.7 nGy/h-87 $\mu$ Gy/h [29]. System utilizes 10" long G.M.detector (type LND-78017) with 2.5 mm thick cylindrical aluminium clad for energy compensation of low energy photons. Prior to field measurements, gamma response of monitoring system was checked in the lab using Cs<sup>137</sup> point source. GARMIN make GPS device (model GPS-V) was used to measure site coordinates in the field. Hand held dosimeters such as gamma survey meter ER-709 (Nucleonix) and AT6130 Radiation Monitor (Atomtex) were also used for cross checking on a few sample data points, in the field.

**3.2 Field Measurements:** Considering environmental and logistic constraints such as terrain difficulties, inclement/harsh weather and poor approach road network in the area, onsite measurement of ambient gamma levels in parts of Khasi Hills was undertaken in several phases. Fig.3.1 presents detail scheme of onsite measurements with 18 sectors of Khasi Hills and covering cumulative distance of 673 line km.

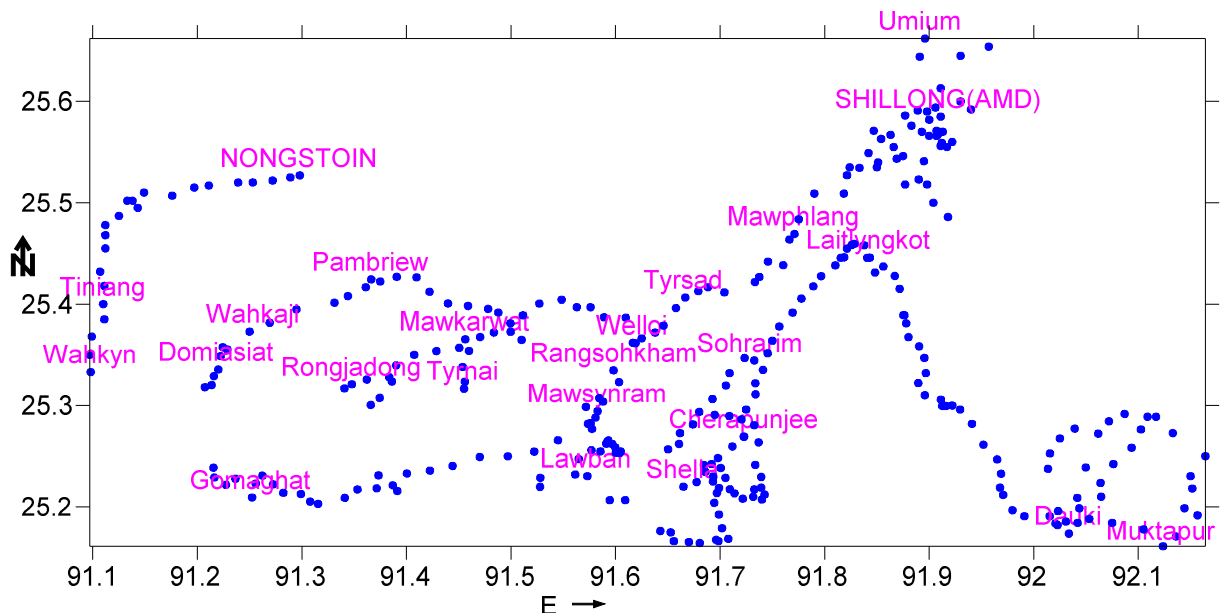


**Fig.3.1:** Georeference based ambient gamma measurements in part of Khasi Hills.

Field measurement begins en route generation of georeference points at about 2-3 km periodic interval, by means of vehicle borne milometer such that covering major land marks and lithological occurrences in the area. This generated 320 georeference points at an average interval of 2.1 km and total distance of 673 line km. On these georeference points, gamma field was measured at 1.0 m ground clearance with ~ 3 min counting time. Simultaneous measurement on site coordinates and type of lithological occurrence was recorded. To ascertain litho unit based reproducibility of measured ambient gamma dose (nGy/h) levels (within statistical limits) satisfactorily check measurements were also performed on few georeference points, en route.

A non terrestrial component of gamma field (mainly cosmic, atmospheric radon and scattered gamma) was measured over fresh water lake, with MSL 965 m, at Umium (Barapani) in the East Khasi Hills district. This lake is located ~ 17 km outskirts of state capital Shillong. Onsite measurement of gamma field was done over 150 deep thick water column of this water body. An average gamma field 63.3 nGy/h (n=10) was measured against the 83.2 nGy/h (n=4) that of river bed.

**3.3 Working Approach:** A generalised linear estimate [30] of quantity Z at unknown location  $x_0$  (say) can be mathematically expressed as

$$Z_0^* = Z^*(x_0) = \sum_{i=1}^n \lambda_i Z(x_i) \quad \dots\dots\dots (i)$$

Where  $Z_0^*$  is estimated value at location  $x_0$  using data value  $Z(x_i)$  measured at the sampling points  $i$  ( $=1,2,3\dots n$ ) each having weightage factor  $\lambda_i$  such that

$$\sum_{i=1}^n \lambda_i = 1 \quad \dots\dots\dots (ii)$$

Estimated value  $Z_0^*$  is differentiated from the true value  $Z_0$ . Determination of weightage factor  $\lambda_i$  is done experimentally by fitting variogram  $\gamma(h)$  on the measured data points

values  $Z(x_i)$  as a function of separation vector  $h$  (also called lag vector) using following equation.

$$\gamma(h) = \frac{1}{2N_h} \sum_{i=1}^{N_h} [Z(x_i + h) - Z(x_i)]^2 \quad \dots\dots\dots (iii)$$

Where  $N_h$  is the number of data pairs for the specified separation vector  $h$ . Denoted separation vector  $h$  is defined with certain direction and distance tolerance.

### 3.4 Data Analysis:

**3.4.1 Gamma Profiling of Litho Units:** Based on major prevailing lithological occurrence observed during field measurements, acquired data points were first clustered and represented by Box & Whisker plot for the six major litho units of Mahadek basin. Each box plot represents typical prevailing gamma levels with mean, median and range. Measured non-terrestrial component was also plotted on same scale to represent relative contribution. Fig.3.2 presents typical gamma profiling of major litho units of Mahadek basin with mean value represented by dot, within the box.

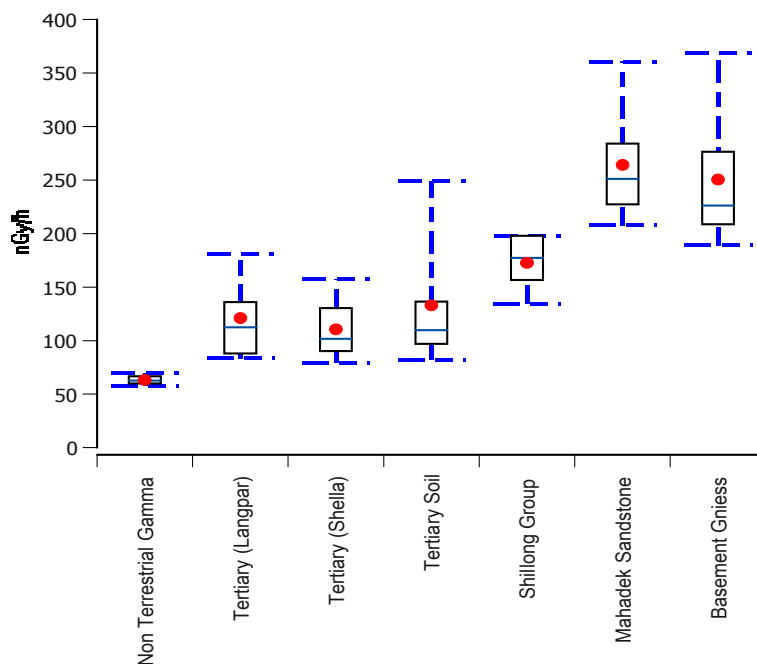


**Fig.3.2:**Gamma Profiling of major litho units of Mahadek basin.

**3.4.2 Analytical Model of Sample Variogram:** To begin with sample variogram on the acquired sample data points, we first defined variogram grid using geostatistical software Surfer™ (v 11.0). Presented in Fig.3.1, sample data (n=320) acquisition has been done over the 18 sectors of Khasi Hills amid environmental and logistic constraints. The acquired sample data (done under several phases) are generally irregularly spaced and sometime overlapped. This was partly resolved by means of filtering sample data points by defining a filtering criteria 1.1 km each on X and Y direction tolerances, in Surfer™. And replacing duplicate/overlapped data points to such locations by equivalent average data value. In this process, Surfer™ identified total 114 duplicate data points over 46 sample locations (on defined variogram grid) and replaced them with equivalent average value. Thus effectively giving n=252 active data points. Table 3.1 presents the complete statistical summary on two data sets.

Parameters	Sample data points		Remark
	Unfiltered (n=320)	Filtered (n=252)	
Average	136.2	133.9	<ul style="list-style-type: none"> <li>• Distribution of sample data points (either case) shows dominating contribution from gamma field &lt; 231 nGy/ h.</li> <li>• Data filtering is defined as X&amp;Y direction tolerance 1.1 km each and duplicate data points (said location) replaced with average one.</li> </ul>
Median	121.9	120.7	
Min	60	60.9	
Max	389.3	389.3	
Variance	2633	2533.4	
Std Dev	51.3	50.33	

**Table 3.1:** Acquired sample data points in parts of Khasi Hills: Statistical summary.

Post filtering, active data points (n=252) were further processed in Surfer™ for computation of sample variogram  $\gamma(h)$  defined by equation (iii), over all pair of observations  $N_h$  with specified lag vector ( $h$ ). Identification of lag vector ( $h$ ) was done by computing maximum lag distance (specifies the largest separation distance in the variogram grid) and any pair separated beyond this distance are excluded from the variogram grid.

Surfer™ identifies max lag distance as one third of diagonal extent of sample data points and computes as 43.41 km on radiometric survey undertaken with 25 lag points (default). This gave an average lag vector 1.74 km on the computed sample variogram. Table 3.2 presents detail parameters on sample variogram grid geometry.

NN Statistics		Lag parameters		Remark
Min	0.033 km	Max lag distance	43.41 km	• NN is Nearest Neighbour distance
Max	3.44 km			
Median	1.52 km	No's of lag points	25	• <i>h</i> is Lag Interval
Average	1.59 km			
Std dev	0.57 km	<i>h</i> : default	1.74 km	
		<i>h</i> : fitted	1.1 km	

**Table 3.2:** Sample variogram grid geometry parameters (n=252).

Above identified default lag vector is now used to model the computed variogram and fitting it to the theoretical mathematical function that best describe the spatial relationship of sample data points. After several iterations of variance optimisation on computed variogram, including varying lag vector 1.74 km (default) to 1.1 km, analytical model of sample variogram is best fitted to the following defined theoretical model [31] and shown in Fig.3.3.

$$\gamma(h) = c_0 + c \left[ \frac{3h}{2a} - \frac{h^3}{2a^3} \right] \quad \dots\dots\dots (iv)$$

Where  $c_0$ ,  $c$  and  $a$  refers to nugget, partial sill and range respectively.

In Fig.3.3, shown number indicates total number of observations pairs associated with each bin in the sample variogram. Table 3.3 presents the detail parameters on analytical model of fitted sample variogram.

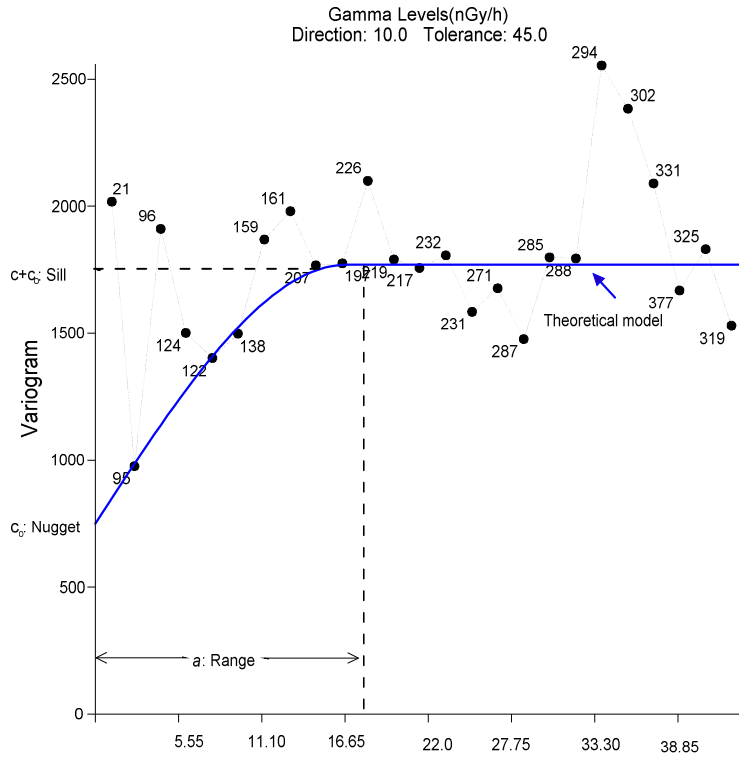


**Fig.3.3:** Sample variogram-Analytical model developed on sample data points. Numbers in the plot indicates total number of observations pairs associated with each bin.

Variogram Model		Remark
Spherical component	Scale :1020, Range: 18.82 km	<ul style="list-style-type: none"> <li>• Sill- Scale+Nugget</li> <li>• Sill=1770, Nugget/Sill = 0.42</li> <li>• Surfer™ refers 'Partial sil' as 'Scale' to the nested variogram model.</li> </ul>
	Anisotropy Ratio: 1.2	
	Anisotropy angle: 60 <sup>0</sup>	
	Direction:10 <sup>0</sup> , Tolerance:45 <sup>0</sup>	
Nugget component	750	

**Table 3.3:** Developed sample variogram model parameters (n=252).

**3.5 Sample Variogram Compatibility Check:** Estimation of data value over the new location is done using developed sample variogram model that then assigns appropriate weightage factor  $\lambda_i$  (for interpolation of data values) defined by equation (i). Accordingly, testing of fitted sample variogram (Fig.3.3) was done by firstly defining kriging interpolation (ordinary) on sample data points itself and then secondly take each data points in turn,

temporarily remove it from the sample data points, and use analytical model of sample variogram to predict it (missing data value) at its original location. This was practically done in Surfer™ by introducing interpolation grid and method (point kriging) on acquired sample data points (n=320). Like variogram analysis, acquired sample data points were filtered using readily defined filtering criteria in Table 3.1. Using advance option on kriging algorithm in Surfer™, defined analytical model of sample variogram (Fig.3.3) was selected together with default search parameters.

For interpolation grid, filtering criteria identified 155 duplicate data points at 65 locations of sample data points (n=320) and replaced them with equivalent average value. Table 3.4 list statistical summary on interpolation grid and filtered data points.

Interpolation Grid		Statistical summary: Sample data points			Remark
NN Statistics		Parameters	Measured Value	Predicated Value	<ul style="list-style-type: none"> <li>• n=230</li> <li>• Sample data points are filtered using pre-defined criteria in sample variogram analysis (Table 3.1).</li> <li>• Kriging technique minimises error (Std Dev &amp; RMD) while interpolating data points.</li> </ul>
Min	0.90 km	Average	134.38	134.13	
		Median	121	134.82	
Max	3.44 km	Min	66.80	84.60	
		Max	389.30	288.55	
Median	1.64 km	Variance	2468.32	965.62	
Average	1.76 km	Std Dev	49.68	31.07	
		RMD	0.384	0.264	
Std Dev	0.48 km	Skew	1.69	0.40	
		Kurto	4.56	-0.51	

**Table 3.4:** Developed sample variogram model: Compatibility check.

Now, filtered data points (n=230) together with defined kriging interpolation parameters in Surfer™ were then used to generate cross validation on sample data points (with default X,Y and data range). Statistical summary of predicted data values (using analytical model of sample variogram) together with active sample data points (n=230) are presented on Table 3.4 and comparative plots for the two data set is presented on Fig.3.4.

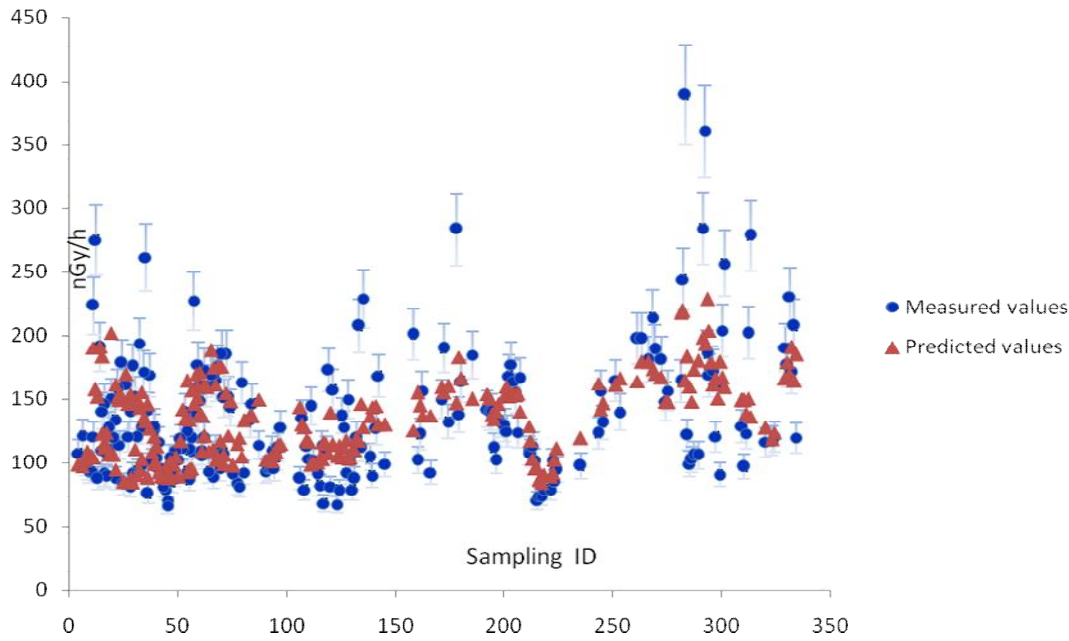


**Fig.3.4:** Ambient gamma levels-Predicted vs Measured (n=230).

To understand the relative variation seen on plotted Fig.3.4 between the two sets of data points, ANOVA test [32] has been performed. Table 3.5 presents the analysis results for the two data set.

ANOVA Test				
	Sum of Squares	df	Mean Square	F
Between Groups	6.96	1	6.96	0.004
Within Groups	786371.3	458	1716.97	
Total	786378.2	459		

**Table 3.5:** Variance analysis on predictability of sample data points.

**3.6 Interpolation of Sample Data Points:** After satisfactorily examining the compatibility of fitted sample variogram (Fig.3.3), readily defined interpolation grid and kriging interpolation parameters in Surfer™ were used to interpolate active sample data points (n=230) over the study area. As an additional measure on probabilistic kriging method, standard deviation was also defined in Surfer™ to estimate errors levels to the interpolated data values. While

generating interpolations grid values on active data points (n=230), default computed value on sample points grid interval namely 1.12 x 1.12 km and grid geometry 100 ( in X direction) x 47 (in Y direction) nodes, were retained. This generated 47000 node points for the range of coordinates covered by the present survey work in Mahadek basin. Interpolated data values and its corresponding standard deviation, generated over the grid

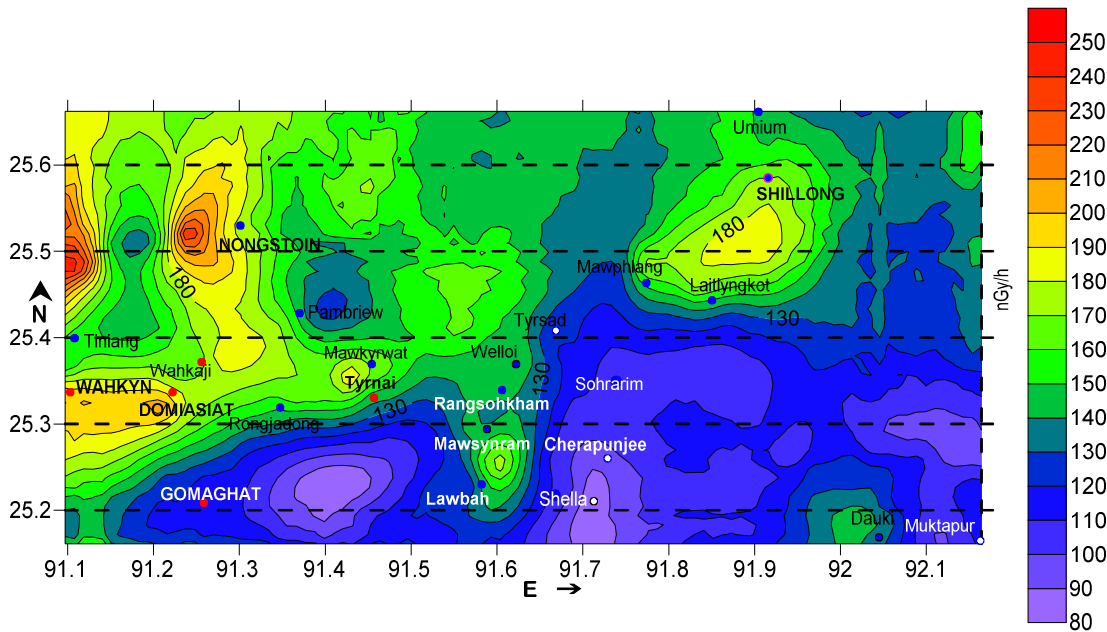


**Fig.3.5:** Interpolation of ambient gamma levels in Parts of Khasi Hills, showing delineated hot spots.

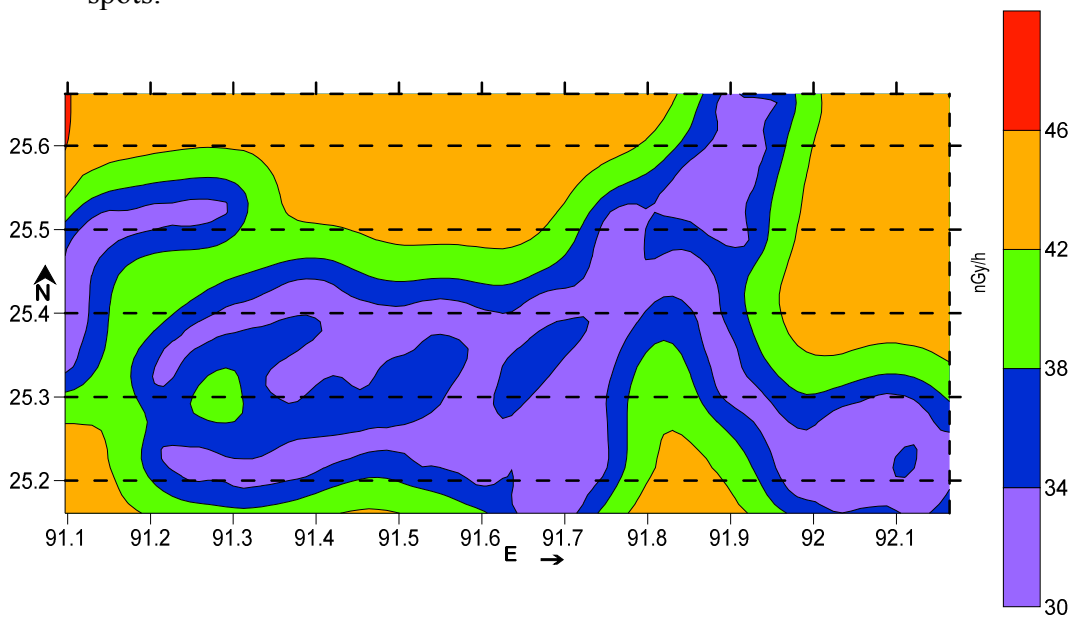


**Fig.3.6:** Standard error associated to the interpolated gamma levels in parts of Khasi Hills.

points were then plotted in Surfer™ to generate detail contour maps of interpolated gamma levels (Fig.3.5) and associated standard deviation (Fig.3.6) over the study area in the basin

### 3.7 Preliminary Findings

**3.7.1 Analytical Model of Sample Variogram:** Considering regional topography, during field work in Khasi Hills, it is unrealistic to assume linear sample variogram. Sensitivity analysis of computed sample variogram as a function of lag vector (Surfer™ call it lag interval) was done by varying lag vector ( $h$ ) from 1.74 km (default) to 1.2 km. It has been observed that both nugget effect and sill decreases substantially from 1100 to 750 and 2100 to 1770 respectively with better fit of computed sample variogram. Further varying lag vector ( $h$ ) below 1.2 km (up to 0.5 km) did not see major change in sample variance and critical parameters of sample variogram, identified and listed on Table 3.3. Accordingly, converged lag vector ( $h$ ) value 1.1 km giving reasonably good fit of computed sample variogram to that of theoretical model, was chosen.

Presented in Fig.3.3, sample variogram contains two major components namely Nugget and Spherical components. Nugget component ( $c_0$ ) is measure of random noise and corresponds to spatial variability of sample at very short distance. Spherical component with sill ( $c_0 + c$ ) represent sample variability from nugget effect to that levels off maximum over the range ( $a$ ) of 18.82 km. High nugget to sill ratio (0.42) and large fluctuation manifested by the data pairs on nested sample variogram (Fig.3.3) are physically observed during field measurements, in the form of high nugget presence.

Goodness of fit for the developed analytical model of sample variogram (Fig.3.3) is well supported by several alternate measures undertaken and presented in Table 3.5. Detail comparison of sample data points to that predicted one (Fig.3.4) shows good match-within experimental errors, except few high values ( $>231$  nGy/h) sample data points (mainly

basement granites in the area). The reported mismatch seen to the predicted data values are much within the statistical limits of distribution curve for the georeference sample data points (n=320) with 95% contribution coming from 231 nGy/h gamma levels. In addition to the listed statistical measures namely variance and RMD in Table 3.4, performed ANOVA test (Table 3.5) at high degree confidence (99%) gives F value (=0.004) lower than the critical value  $F_{critical}$  (= 6.90). It indicates that predicted data points are not significantly different from the measured one.

**3.7.2 Interpolation of Sample Data points:** Generated contours on interpolated gamma levels over the study area (Fig.3.5) gives good overview of ambient gamma levels with elevated gamma levels towards the parts of West Khasi Hills. And with the exception of Shillong and its extension, mostly lower gamma levels are observed over parts of East Khasi Hills. The lower gamma dose levels in parts of East Khasi Hills are much in relation to the major lithological occurrence of Mahadek basin (presented on Fig.1.6, Chapter-1) and well correlated to the predominate rock exposure of Tertiary formation (Shella sandstone and limestone) and Sylhet Trap, characterized with lower gamma levels (Fig.3.2). Elevated gamma levels to the Shillong and its surroundings are mainly attributed due to the Neo Proterozoic granites and quartzites of Shillong Group of rocks (Fig.3.2) having higher concentration of primordial radio elements. Elevated gamma dose levels in parts of West Khasi Hills are well correlated lithologically on ground, since major rock exposure is attributed due to the Mahadek sandstone (Upper and Lower Mahadek) and Precambrian basement granites both contributing high gamma levels (Fig.3.2).

As an overview to the interpolated gamma levels, presence of several high gamma anomalous zone (Fig.3.5) have been identified over the study area especially to the locations of known uranium occurrence in the basin viz Domiasiat [11,12], Wahkyn [13] and Tyrnai. Lithologically these delineated high gamma anomalous zone are well

correlated to the uranium mineralisation host rock (Lower Mahadek sandstone), in the basin. Elsewhere, high gamma anomalous zone namely around Nongstoin and to the North of Tiniang (Fig.3.5) are attributed to the basement Gneiss characterised with high gamma field (Fig.3.2) and not suitable to exploration work.

Estimated errors levels to the probabilistic Kriging method used in the present study is shown on Fig.3.6 (scale: standard deviation). Relative comparison of predicted values (Fig.3.5) and associated error levels (Fig.3.6) shows higher interpolation error to the furthest interpolated points vis à vis nearer one. Therefore as an assessment strategy and target based exploration approach in the area with good confidence (of interpolated data values) it is desirable to have sampling data points at closure (preferably ~1 km) sampling interval and limiting interpolated data values to the shorter distance, in the basin.

Thus, preliminary findings on ambient gamma radiation measurements in part of Khasi Hills, shows encouraging surface indicators in relations to the prevailing lithology. On experimental basis delineated gamma anomalous zones are lithologically well correlated to the existing uranium occurrences in the basin. With closure spatial resolution (~1km), the approach demonstrated under this study work holds promising application in locating the potential uranium occurrences over the inaccessible and similar geologically extended area, in the basin.

## **CHAPTER 4**

# **Uranium Hosting Environment Investigation**

Radiometric field survey undertaken for Rangsohkham exploratory block, in Mahadek basin, indicated significant surface uranium anomalies over a 1.5 km strike length, intermittently, in Lower Mahadek sandstone. To delineate *insitu* gamma radioactivity amid bulk mass effect presence, Shielded probe logging (surface logging) was done. Delineated surface activity on 62 channels, confirms continuity of observed gamma anomalies with average thickness 0.40-1.58 m and grade 0.015%-0.037%  $eU_3O_8$ . Further, radiometric analysis of drawn surface grab samples in the block, also indicates good surface uranium mineralization with average 0.170%  $U_3O_8$  (n=47) in the range of 0.10-1.81%  $U_3O_8$  (with negligible thorium content).

Uranium mineralization disequilibrium status examined on the grab sample, shows favourable equilibrium condition ( $d=1.1$ ) in the block. To trace subsurface continuity of observed surface uranium mineralization in the block, exploratory drilling was undertaken. However, despite favourable surface indicators, manifested by the surface radiometric measurements in the block,  $\gamma$ -ray logs did not intercept the expected uranium mineralization in the exploratory boreholes.

In absence of drilled borehole core, this Chapter examines the possible extreme disequilibrium scenario of subsurface uranium mineralisation in the block. In the subsequent sections, Chapter discuss about multivariate analysis of primordial radio elements using the concept of representative subsurface sampling on prevailing geological environments and determination of U-Th geo-coherence. These study findings on uranium exploratory behaviour in the system (in particular uranium hosting environment) have been benchmarked to the another exploratory block Lostoin, with proven uranium occurrence.

**4.1 About Rangsohkham Exploratory Block:** Located about 65 km southwest of state capital Shillong, East Khasi Hills district of Meghalaya (Fig.4.1), Rangsohkham exploratory block (Lat

25°19'35" E, Long. 91°35'10" N) lies about 30km east of proven uranium deposits in the basin [11,12,13] and have gross geological similarities to the Domiasiat and Wahkyn exploratory blocks.

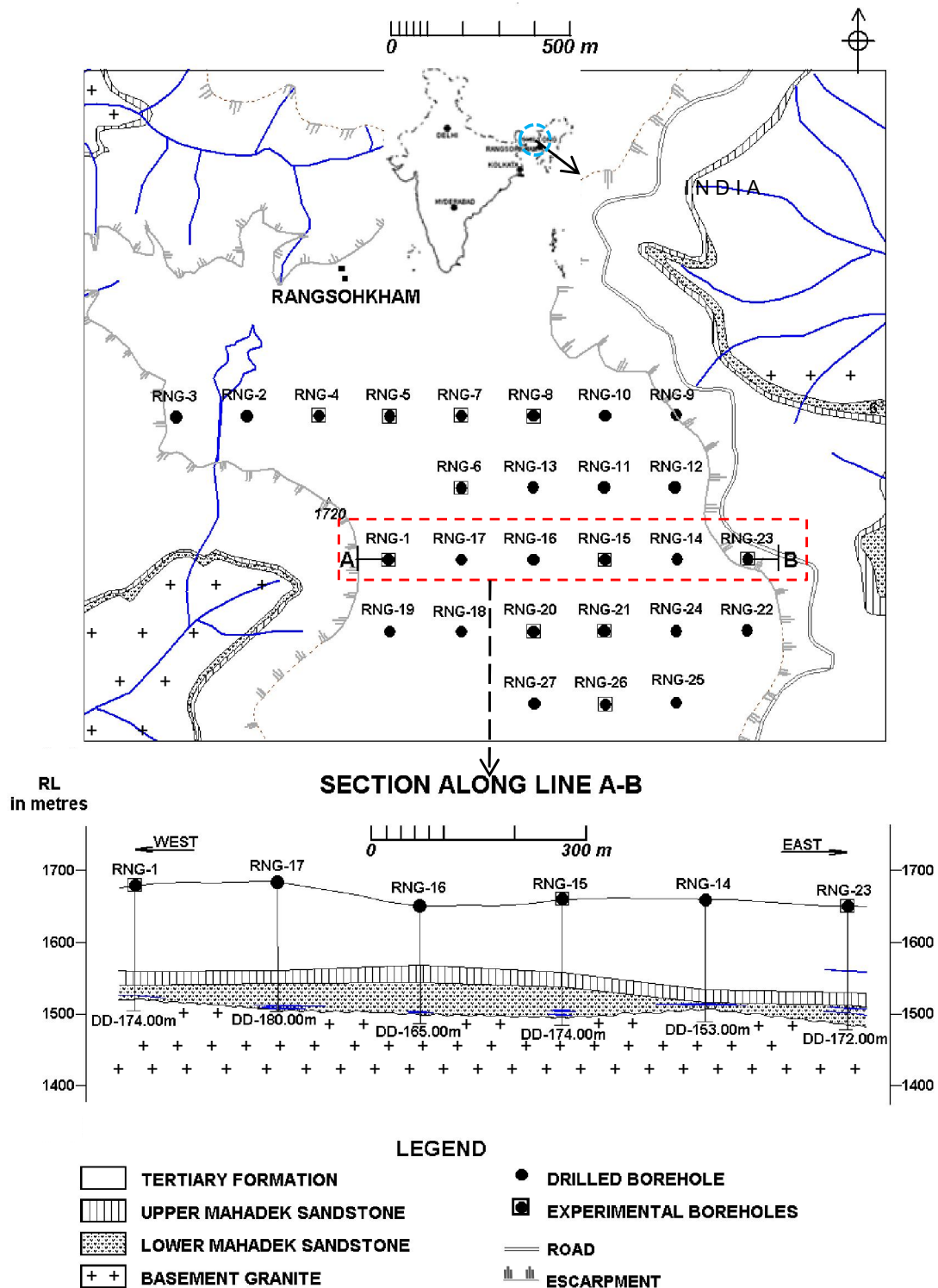


**Fig.4.1:** Rangsohkham exploratory block with drilled boreholes. Typical vertical cross section of borehole is shown by line section A-B.

Geologically, study block falls to the north of Raibah fault and exposes Tertiary (Shella/Langpar) and Mahadek sediments over granite gneiss Mahadek formation is the oldest sedimentary unit in the area, unconformably rests over basement granite, and classified in two sediments group namely Lower Mahadek (LM) and Upper Mahadek (UM) sediments. Lower Mahadek formation is the host rock for uranium mineralisation and characterized by the reduced facies rocks of grey coloured, compact, pebbly arkosic sandstone/feldspathic arkose with stringers of carbonaceous matter/pockets of resins and pyrite nodules at places.

Thickness of Lower Mahadek formation increases gradually towards the south and pitches out in the north. Upper Mahadek (UM) formation, purple coloured oxidized facies arkosic sandstone, lies above the Lower Mahadek formation, without any significant break in sedimentation, in the south. In the north, Upper Mahadek formation directly lies over the granite basement. In the block, general trend of sedimentary formations is E-W to ESE-WNW with 4-7° southerly dips.

**4.2 Borehole  $\gamma$ -ray Logging Status:** Total 29 exploratory boreholes with cumulative drilled depth of about 5000 m, were drilled in the block by means of DTH (non-core) drilling over an area of 2 sq km (Fig 4.1). Using G.M. logging system, drilled reconnoitry boreholes were  $\gamma$ - ray logged [1, 2] but most of them failed to intercept the expected uranium mineralisation [33,34] in the block vis à vis manifested and indicted by various surface measures undertaken, in the field.

**4.3 Uranium Mineralization Discontinuity Study:** In absence of active  $\gamma$ -ray logs and drilled borehole core, to understand uranium behaviour in the geological system, an alternate representative sampling based approach was introduced, in the exploratory block. Accordingly, 11 exploratory boreholes, were randomly selected to generate study samples especially across the three prevailing geological environments of this block.

**4.3.1 Sample Generation and Classification:** Lithological details of these experimental boreholes was recorded using physical examination of drilled borehole sludge. Presented on

Fig.4.1 line section, drilled borehole usually commences with Tertiary formation (thickness~ 87-151 m) followed by Upper Mahadek sediments (thickness~ 6-30 m ) then Lower Mahadek sediments (thickness~ 11-57 m) and finally Basement granite.

Selected boreholes (Table 4.1) were then sampled at 3m regular interval along the drilled borehole run. Representative sample, weighing about 1.0kg, was drawn to each 3.0 m non-core drill run, for radiometric analysis. In this process, a total of 179 numbers subsurface samples were generated. With the help of recorded borehole litholog, generated representative samples were then classified under the three main geological environments of Mahadek basin viz Upper Mahadek (UM), Lower Mahadek (LM) and Basement (BM). Thus having statistically significant numbers of samples in Upper Mahadek (n=44), Lower Mahadek (n=94) and Basement (n=41) respectively. Table 4.1 gives borehole wise summary of generated samples across the three geological environments of this block.

Borehole ID	Sample generated			Remark
	Upper Mahadek	Lower Mahadek	Basement	
RNG/1	2	8	5	<ul style="list-style-type: none"> <li>• 11 Non-coring boreholes were randomly chosen.</li> <li>• Sampling criteria includes each sample per 3 m drilled depth of respective geological formation.</li> <li>• Total 179 samples generated.</li> <li>• Distribution include: Upper Mahadek =44, Lower Mahadek=94 and Basement =41</li> </ul>
RNG/4	-	6	8	
RNG/5	-	5	4	
RNG/6	7	7	2	
RNG/7	1	7	3	
RNG/8	-	6	3	
RNG/15	5	14	4	
RNG/20	5	10	-	
RNG/21	-	11	3	
RNG/23	6	12	3	
RNG/26	18	8	6	

**Table 4.1:** Representative sampling of major Geological environments in Rangsohkham exploratory block.

**4.3.2 Radiometric Analysis:** Litho classified representative subsurface samples, were then radiometrically analysed for gross activity content ( $eU_3O_8$ ) followed by detail spectral gamma measurements. Optimised sample geometry (5" dia,400 gms) with 5"X4" NaI(Tl) detector setup coupled to DSP based 4K MCA system [35], has been used for ppm range primordial radio elemental measurements. Calibration source  $Cs^{137}$ ,  $Co^{60}$  and IAEA standards were used to

Geological Environments	Radio Elements	Mean (=n)	Range	Variance	Skewness	Kurtosis
UM	$eU_3O_8$	13.56 (=44)	7-31	17.55	1.52	5.75
	K	1.65 (=28)	1-2.7	0.19	0.27	-0.48
	U	3.35 (=43)	2-8	1.38	1.87	5.42
	Th	17.07 (=44)	7-48	44.72	2.25	9.82
LM	$eU_3O_8$	22.29 (=94)	6-79	199.73	1.49	2.57
	K	1.57 (=55)	1-3.9	0.39	2.04	5.12
	U	7.47 (=89)	2-59	83.46	3.96	17.94
	Th	28.36 (=94)	4-88	335.20	1.16	0.92
BM	$eU_3O_8$	27.14 (=41)	11-51	142.92	0.37	-1.13
	K	2.90 (=34)	1-4.3	0.933	-0.25	-0.98
	U	5.95 (=41)	2-11	4.85	0.58	-0.231
	Th	35.95 (=41)	4-81	422.25	0.33	-0.90
UM- Upper Mahadek, LM- Lower Mahadek, BM- Basement Except K (in %), other radio elemental concentration are in ppm. $Ra_{(eq)}$ - Measured by $\gamma$ - ray spectroscopy has been used to represent U. Th- has been used to represent $ThO_2$ .						

**Table 4.2:** Analytical summary on representative samples from major Geological environments.

calibrate  $\gamma$ -ray spectrometer and its K, U and Th channels. Natural  $\gamma$ -ray spectrum on each sample was acquired for 2000 sec counting time. These acquired spectral zones K (1.46MeV),U (1.76MeV) and Th (2.62MeV) were then analysed to estimate ppm range primordial radio elemental concentration [K,U,Th] in representative samples. Throughout the ppm range analysis of drawn representative samples,  $Ra_{(eq)}$  measured through  $\gamma$ - ray spectroscopy (also simply written as Ra) has been used to represent U concentration and vice versa. Table 4.2 presents analytical summary of analyzed samples across the three geological environments. Measured radio elemental concentration to the representative samples, is now being used to study major uranium index parameters across the three geological environments in the block. By simultaneous expression of U/K, U and Th/U uranium exploratory index has

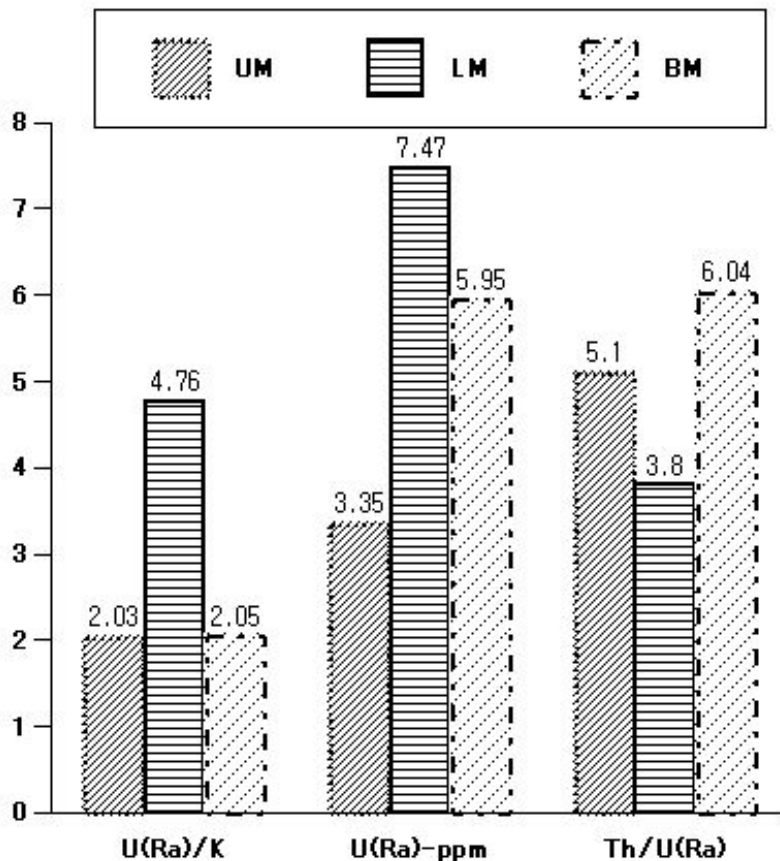


**Fig.4.2:** Uranium Index across the three Geological environments of Rangsohkham exploratory block.

been developed across the three geological environments, in the block and is shown in Fig. 4.2.

**4.3.3 Experimental Approach:** Prior to develop an experimental analysis on generated radiometric data (Table 4.2), we need to ascertain data integrity of drawn representative samples. That is they are not biased/contaminated and represent the three distinct geological environments, in the block. Variations in litho unit thickness across the study block have generated unequal number of samples to each geological environment. We also assume that the drawn samples across the three geological environments belong to normally distributed population.

**4.3.3.1 Hypothesis Building:** To validate the structure and strength of relationship between the three distinct groups (geological environments) and their mean, statistical test ANOVA [32] is used to test the null hypothesis [25]  $H_0$  for subsurface samples, stating that;

$H_0$ : Drawn representative samples are from single geological environments and biased (borehole sludge getting contaminated in the drilling process) i.e. there is no significant difference to the means of analysed radiometric data (K, U,Th) for the three geological environments.

Mathematically  $H_0 : \mu_{UM} = \mu_{LM} = \mu_{BM}$ , where  $\mu$  is mean of each radio element (K, U, Th) across the three distinct geological environments (UM,LM, BM).

Against the alternate hypothesis

$H_1$ : Stating that there is significant difference to the mean of analysed radiometric data (K, U,Th) for the three geological environments and sampling is not biased.

Mathematically  $H_1 : \mu_{UM} \neq \mu_{LM} \neq \mu_{BM}$  (at least one mean is different).

**4.3.3.2 Multivariate Analysis:** Gross  $\gamma$ -activity ( $eU_3O_8$ ) measured on representative borehole samples consists of contribution from primordial radio elements (K, U, Th) inherently present in the contributing geological environment. To understand dependent variable relationship, defined here  $eU_3O_8$ , to each independent contributor variable K, U and Th (across each geological

environments) a linear set of multivariate regression equation [25] is evaluated based on valid radio elemental data to each environment viz Upper Mahadek (UM), Lower Mahadek (LM) and Basement (BM).

**4.4 Data Analysis:** Analytical summary of representative samples, readily presented on Table 4.2, shows that there are occurrences of K & U concentration well below the detection limits particularly K (<1%) and U (< 2ppm). While performing data analysis on representative samples data, such non qualifying pair are defined as missing values and excluded from the respective equation set.

**4.4.1 Hypothesis Testing:** Having defined missing values of primordial radioelements in the data set, ANOVA test was performed to test null hypothesis on representative group samples from the three geological environments. Test summary of this analysis is presented on Table 4.3.

Radio Elements		Sum of Squares	df	Mean Square	F
<b>K</b>	Between Groups	40.87	2	20.434	40.72
	Within Groups	57.21	114	0.502	
	Total	98.08	116		
<b>U</b>	Between Groups	493.85	2	246.92	5.53
	Within Groups	7595.85	170	44.68	
	Total	8089.70	172		
<b>Th</b>	Between Groups	7780.81	2	3890.40	13.70
	Within Groups	49986.40	176	284.01	
	Total	57767.21	178		

**Table 4.3:** Rangsohkhram exploratory block, drawn representative samples: ANOVA Test.

Using available degree of freedom ( $\nu_1 = 2, \nu_2 = \infty$ ) in F- distribution, critical value of F-test at high degree of confidence (99%) is defined as  $F_c(2, \infty) = 4.63$  (from F-distribution Table). In Table 4.3, computed F-values for the all the three primordial radioelements (K,U,Th) are much

above than that of critical value  $F_c = 4.63$ . This concludes that  $H_0$  is rejected, which implies there is significant difference between the mean value of analysed radiometric data (K, U and Th) for the three groups of representative samples. It means that the representative sampling is not biased and they belong to three distinct geological environments, in the block.

**4.4.2 Uranium Equivalent Activity:** After validating the three distinct geological environments, in the block, multivariate regression analysis is performed on the distinct primordial radio elemental concentration from the three geological environments. Results of gross activity regression analysis ( $eU_3O_8$ ) performed at high degree of confidence (99%) across the three distinct geological environment is presented below in Table 4.4.

$eU_3O_8$	Regression Model	Goodness of fit ( $R^2$ )	Average $eU_3O_8$ activity	
			Predicted	Prevailing
UM (n=26)	2.39K+0.98Ra+0.45Th	99.3%	14.81	13.56
LM (n=53)	2.07K+1.00Ra+0.45Th	99.9%	23.49	22.29
BM (n=33)	2.39K+0.98Ra+0.43Th	99.8%	28.22	27.94
<ul style="list-style-type: none"> <li>• Regression coefficients are significant @1% level</li> <li>• Ra measured by <math>\gamma</math>- ray spectroscopy has been used to represent U.</li> </ul>				

**Table 4.4:**Analysed uranium equivalent activity-Regression model for Rangsohkham exploratory block.

Substituting prevailing mean K, U and Th values from Table 4.2, above regression equation gives good agreement between the prevailing and predicted  $eU_3O_8$  activities, across the three geological environments (Table 4.4).

**4.4.3 Radioelemental Correlation Matrix :** Geochemically, each of the primordial radioelements (K,U,Th) has got different properties to the surrounding geological environment. To understand inter elemental (K, U, Th) relationship on uranium behaviour in the system,

bivariate radioelement correlation index is generated using 3x3 matrix across the three distinct geological environments, in the block. Table 4.5 summarises the performed inter-elemental correlation index for the exploratory block, done at high degree of confidence (99%).

Radio Elements		K	U(Ra)	Th	Remark
K	UM=	1			<ul style="list-style-type: none"> <li>• Number in bracket indicates valid correlation pair of radioelements.</li> <li>• Radioelements pair having respective value &lt; detection limits, are excluded.</li> <li>• Matrix coefficients are significant @1% level</li> <li>• Ra measured by <math>\gamma</math>- ray spectroscopy has been used to represent U.</li> </ul>
	LM=				
	BM=				
U(Ra)	UM=	-0.561(n=27)	1		
	LM=	0			
	BM=	0			
Th	UM=	0	0.674(n=43)	1	
	LM=	0	0.268(n=89)		
	BM=	0.574((n=34)	0.581(n=41)		

**Table 4.5:** Radio elemental Correlation Matrix-Rangsohkham exploratory block.

**4.5 Rangsohkham Exploratory block Findings:** Plotted U index across the three distinctive geological environments (Fig.4.2) shows enhanced U concentration and lower  $Th/U$  ratio for Lower Mahadek geological environment. This is well supported by enhanced U coefficient in  $eU_3O_8$  regression equation (Table 4.4).

Interestingly  $eU_3O_8$  regression equations in Table 4.4, reflects constant Th coefficient for Mahadek sandstone (both Lower and Upper), indicating existence of single source rock. Relatively enhanced U concentration (Fig.4.2) in Lower Mahadek to depleted one in Upper Mahadek (Table 4.4), indicates U oxidation and its differential movement (Upper to Lower Mahadek) in the system. If no enrichment had taken place, then U and Th being geochemically coherent, should give high coefficient of correlation. But in Table 4.5, data especially reflect

poor correlation (0.268) between the two variables U and Th for Lower Mahadek. It means U enrichment has taken place in Lower Mahadek geological environments. This indicates preferential U mobilization to the hosting environment (Lower Mahadek). Relative enhanced U/K ratio for LM with respect to UM and BM (Fig. 4.2) also supports uranium enrichment to the hosting environment. All these tests have been performed at high degree (99%) confidence level.

**4.6 Validation of Experimental Findings:** After confirming the three geological environments, in the study block, validity of investigated U-Th geo-coherence for uranium hosting environment (Lower Mahadek) is further investigated over the Lostoin exploratory block, in West Khasi Hills district, having significant subsurface uranium mineralization (intercepted by the exploratory boreholes). Much similar to Rangsohkham, Lostoin exploratory block was also primarily identified based on extended geological favorability (Lower Mahadek) to the existing uranium resources in the basin [11,12, 13]. This new block is having limited coring boreholes amid poor core recovery [21] owing to prevailing environmental and geological conditions but have good subsurface uranium mineralisation in the reconnoitry boreholes.

**4.6.1 Lostoin Exploratory block:** Located about 140 km south west of the state capital Shillong, Lostoin exploratory block covers an area of about 2.5 sq km, under the West Khasi Hills district of Meghalaya. It also lies adjoining (north west) to the Wahkyn uranium deposit (Fig.4.3) [13], in the basin. A total 113 exploratory boreholes with cumulative drilled depth of 6919 m were drilled in the block (includes 7 coring boreholes of 723 m). Pitchblende, uraninite and coffinite are the primary uranium minerals in the block.

**4.6.1.1 Data Acquisition:** In view of limited coring boreholes (n=7) amid poor core recovery in this block, the concept of representative sampling introduced in Rangsohkham exploratory block reconnoitry boreholes is being extended to Lostoin exploratory block, to generate statistically significant number of representative samples. A total of 24 experimental boreholes (Table 4.6)

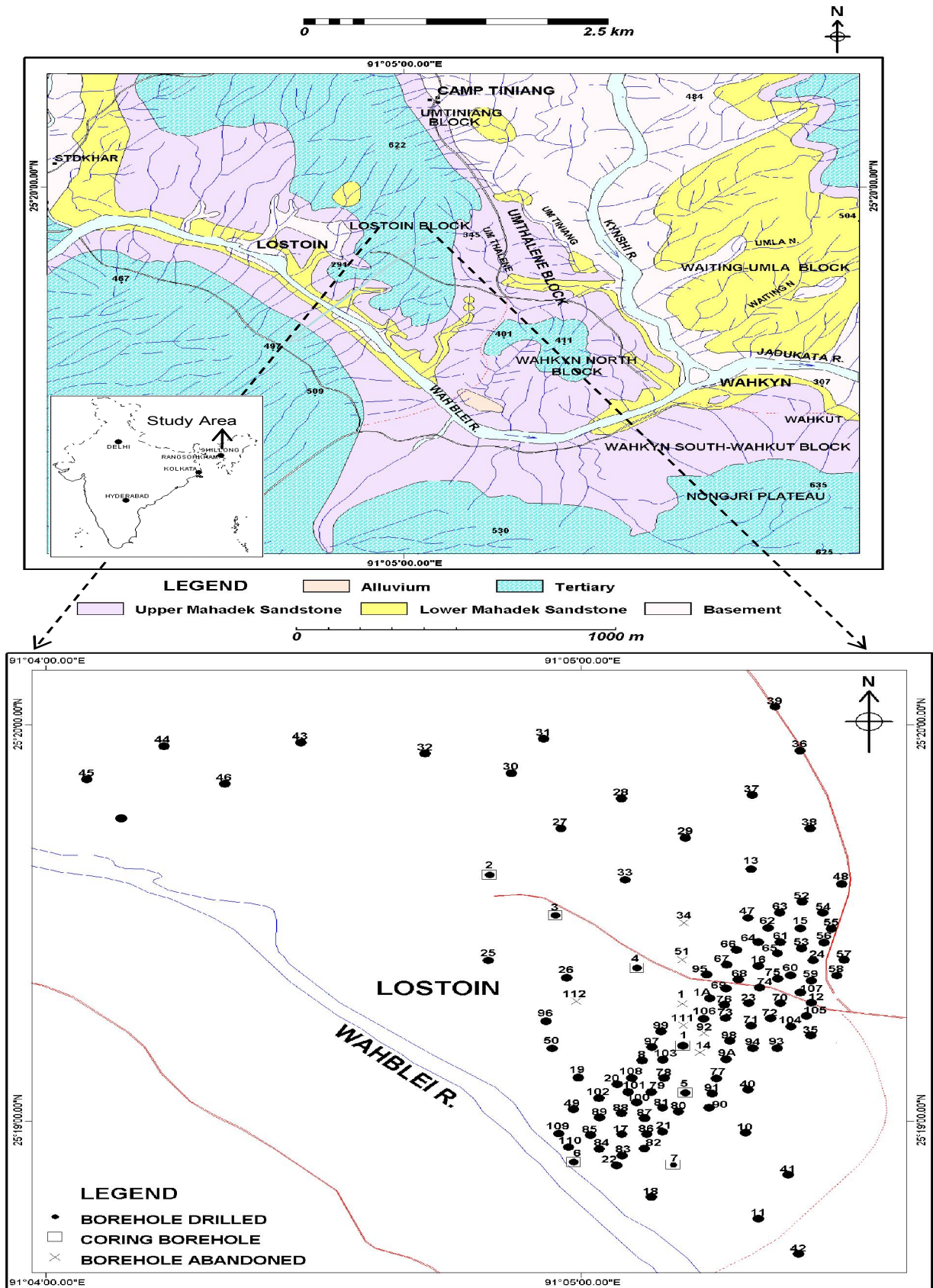


Fig.4.3: Loston exploratory block with drilled boreholes scheme.

were used to generate target group of samples, using defined qualifying criteria especially on the U hosting environment. Utilising  $\gamma$ - ray logging database, following qualifying criteria have been especially defined to the Lostoin exploratory block reconnaissance boreholes,

Borehole ID	Sample Generation		Remark
	Non-mineralised group	Mineralised group	
LST-15	02	03	<ul style="list-style-type: none"> <li>• Non coring process generate each sample per 3.0 m drill run</li> <li>• 24 Non coring borehole were chosen randomly in the block.</li> <li>• Non mineralised group sampling criteria includes Lower Mahadek thickness ~ 3 m in the borehole.</li> <li>• Only 16 Borehole qualified for non-mineralised zone, generating 24 samples.</li> <li>• Mineralised group sampling criteria includes Zone thickness &gt; 1.0 m and grade <math>\geq 0.010\%</math> <math>eU_3O_8</math>.</li> <li>• 22 Borehole qualified for mineralised zone, generating 40 samples.</li> </ul>
LST-54	01	01	
LST-61	01	01	
LST-62	01	01	
LST-65	01	01	
LST-66	01	03	
LST-74	-	01	
LST-75	-	01	
LST-76	01	01	
LST-78	-	02	
LST-79	-	02	
LST-80	-	01	
LST-81	-	04	
LST-83	01	02	
LST-84	02	01	
LST-85	03	-	
LST-86	01	04	
LST-87	04	02	
LST-88	01	-	
LST-89	-	02	
LST-90	-	02	
LST-98	01	02	
LST-100	01	02	
LST-101	02	01	

**Table 4.6:** Representative sampling of U hosting environment-Lostoin exploratory block.

a) Non-mineralised group: Hosting environment (Lower Mahadek) thickness ~3 m (in view of process driven 3.0 m drill run in reconnoitry borehole) and

b) Mineralised group: Zone thickness (T) ≥ 1.0 m with cut-off grade (G) 0.010%  $eU_3O_8$ .

Based on qualifying criteria, drawn representative samples were *insitu* dried to transport back to the lab for radiometric analysis and measurements. Whereas detail study on drawn mineralised group samples, exclusively used to study uranium series disequilibrium status in this block, is presented on Chapter-5. The non-mineralised group samples are being exclusively studied for uranium hosting environment behaviour with respect to the Rangsohkhram exploratory block finding.

The received samples in the lab were analysed for gross  $\gamma$ -activity ( $eU_3O_8$ ) and ppm range primordial radio elemental (K, U, Th) analysis using 5"x4" NaI(Tl) detector setup & MCA system [35]. Table 4.6 presents complete details of two groups of qualifying samples, generated in the block. Analytical summary of non-mineralised group samples from uranium hosting environment (Lower Mahadek) is presented in Table 4.7. The two distinct group of samples in Lostoin exploratory block are well supported by statistical measures and thus generating statistically significant number of representative samples.

Parameters	Mean	Range	Variance	Skewness	Kurtosis
$eU_3O_8$ (ppm)	60 (n=24)	24-87	273.39	-0.47	-0.48
K (%)	1.33 (n=20)	1.0-2.10	0.08	1.02	1.32
U (ppm)	36 (n=24)	07-76	342.55	0.14	-0.59
Th (ppm)	47 (n=24)	20-100	291.65	0.94	2.84

**Table 4.7:** Analytical summary -Lostoin exploratory block representative samples.

**4.6.1.2 Uranium Behaviour in the System:** Using non-mineralized group (Table 4.6) population (n=24), we investigated multivariate analysis of primordial radio elements (K,U,Th)

for the uranium hosting environment (Lower Mahadek) in Lostoin exploratory block. Experimental  $eU_3O_8$  regression model from Lostoin exploratory block vis à vis Rangsohkham exploratory block is presented on Table 4.8. Similarly examined U-Th geo-coherence for Lostoin exploratory block hosting environment (Lower Mahadek) vis à vis Rangsohkham exploratory block, using 3x3 inter elemental correlation matrix, is presented on Table 4.9. All these benchmark study have been performed at a high degree (99%) confidence level.

$eU_3O_8$ (Gross Activity)	Regression Model	Goodness of fit	Remark
Lostoin exploratory block (n=20), West Khasi Hills district	$2.05K+1.00Ra+0.45Th$	$R^2 =99.9\%$	<ul style="list-style-type: none"> <li>• Regression equation coefficient are significant @ 1%level</li> <li>• Ra measured by <math>\gamma</math>- ray spectroscopy has been used to represent U.</li> </ul>
Rangsohkham exploratory block (n=53), East Khasi Hills district.	$2.07K+1.00Ra+0.45Th$	$R^2 =99.9\%$	

**Table 4.8:** Uranium hosting environment- Benchmark study using multivariate analysis of study blocks

Radio Elements	K	U	Th	Remark
<b>K</b>	1			<ul style="list-style-type: none"> <li>• Matrix coefficient are significant @1% level</li> <li>• §: Lostoin exploratory block, West Khasi Hills district.</li> <li>• #: Rangsohkham exploratory block.</li> <li>• In U column, number in bracket indicates valid correlation pair.</li> </ul>
<b>U</b>	0	1		
<b>Th</b>	0	<sup>§</sup> 0.268 (n=24) <sup>#</sup> 0.268 (n=89)	1	

**Table 4.9:**Uranium hosting environment- Benchmark study on radio elemental correlation matrix of study blocks.

**4.6.2 Key Findings-Lostoin Exploratory block:** Geological continuity of Lostoin exploratory block in relation to the uranium hosting environment (Lower Mahadek) of Rangsohkham exploratory block, is well supported by the matching coefficients of gross activity regression analysis  $eU_3O_8$  (Table 4.8) followed by an inter primordial radioelements (K, U,Th) correlation matrix (Table 4.9), at a high degree of confidence (99%). These experimental measures on Lostoin exploratory block show similar disturbed U-Th geo-coherence (0.268) on uranium hosting environment and holds good to the large aerial extent ~60 km of Rangsohkham exploratory block, in Mahadek basin.

Thus radiometric study on representative samples of uranium hosting environment (Lower Mahadek) in Rangsohkham exploratory block confirms existence of good uranium bearing potential, similar to the proven uranium occurrence in Lostoin exploratory block. Factors that might have prevented this uranium in the system getting precipitated to form sizeable and rich ore zones in Rangsohkham exploratory block, are lean presence of carbonaceous matter and relatively less thickness of Lower Mahadek, seen in the block. Sporadically, wherever these essential conditions/criteria have met,  $\gamma$ -ray logs have given non co-relatable and thin uranium mineralization in few boreholes (poor grade and thickness) namely RNG/12 (0.061%  $eU_3O_8$  x 1.2 m) and RNG/14 (0.081%  $eU_3O_8$  x 2.0 m) both computed at 0.020% cut off grade.

**4.7 Uranium Disequilibrium Status:** In view of statistical requirements on active samples size and investigated lean uranium mineralization in Rangsohkham exploratory block, uranium disequilibrium status could not be estimated with good confidence. Although  $\gamma$ -ray logs in boreholes RNG/12 and RNG/14 did intercepted some uranium mineralization but representative sample could not be drawn due to geological limitations (borehole caving) in the field. Nevertheless, as a preliminary indicator of uranium disequilibrium in the block, representative

sample RNG/26/61 generated from RNG/26 borehole, gave  $U_3O_8 = 0.012\%$  with indicative parent favoring disequilibrium indicator 1.5 (measured by  $U_3O_8/Ra$  ratio).

# **CHAPTER 5**

## **Exploratory Block: Disequilibrium**

### **Investigation**

Oxidizing tendency of uranium in the sedimentary environment [36] creates disequilibrium in U series, which has implication on bulk ore tonnage measured by gross gamma measurements as well radon interference [37,38] to the measured  $\gamma$ -ray logs in borehole. Literature survey shows several studies on uranium disequilibrium aspect [4,5,39,40] that of dose rate measurements to uranium migration. This is pertinent to mention that bulk uranium ore tonnage estimated using mineralized zone grade (G) and thickness (T) information from  $\gamma$ -ray logs of exploratory boreholes [3] are primarily based on gross  $\gamma$  measurements. The logged borehole, then need to be validated by some independent process to confirm radon interference to the subsurface uranium mineralization and its equilibrium status.

As seen during the exploration phase, there are some of the critical aspect of uranium disequilibrium on exploration work being undertaken in the sedimentary environments of Mahadek namely observed discontinuity on subsurface uranium mineralization (Stated in Chapter-4), occasional radon presence in the borehole and poor core recovery in the boreholes.

Radiometric studies done on surface grab samples across a few exploratory block of Mahadek basin, readily indicates varying degree of uranium equilibrium conditions expressed in terms of disequilibrium factor (d). To understand these exploratory aspects, this Chapter investigate detailed uranium disequilibrium behavior and its distribution across the Mahadek basin study blocks especially to the Wahkut and Lostoin-having significant subsurface mineralization, located under the West Khasi Hills district of Meghalaya.

**5.1 About Wahkut Exploratory block:** Primarily indentified based on geological extension to the existing uranium resources [3], Wahkut exploratory block having an area of 2 sq km (Fig.5.1) is located ~ 150 km south west of state capital Shillong in the West Khasi Hills district, Meghalaya. Bound by the coordinates N ( $25^{\circ}18'-25^{\circ}18'45''$ ) and E ( $91^{\circ}05'-91^{\circ}07'30''$ ) exploratory

block has close proximity (~10 km) to the international border (Bangladesh) and to the confluence of two major rivers Wahblei and Kynshi-Jadukata flowing in the area. Uranium host

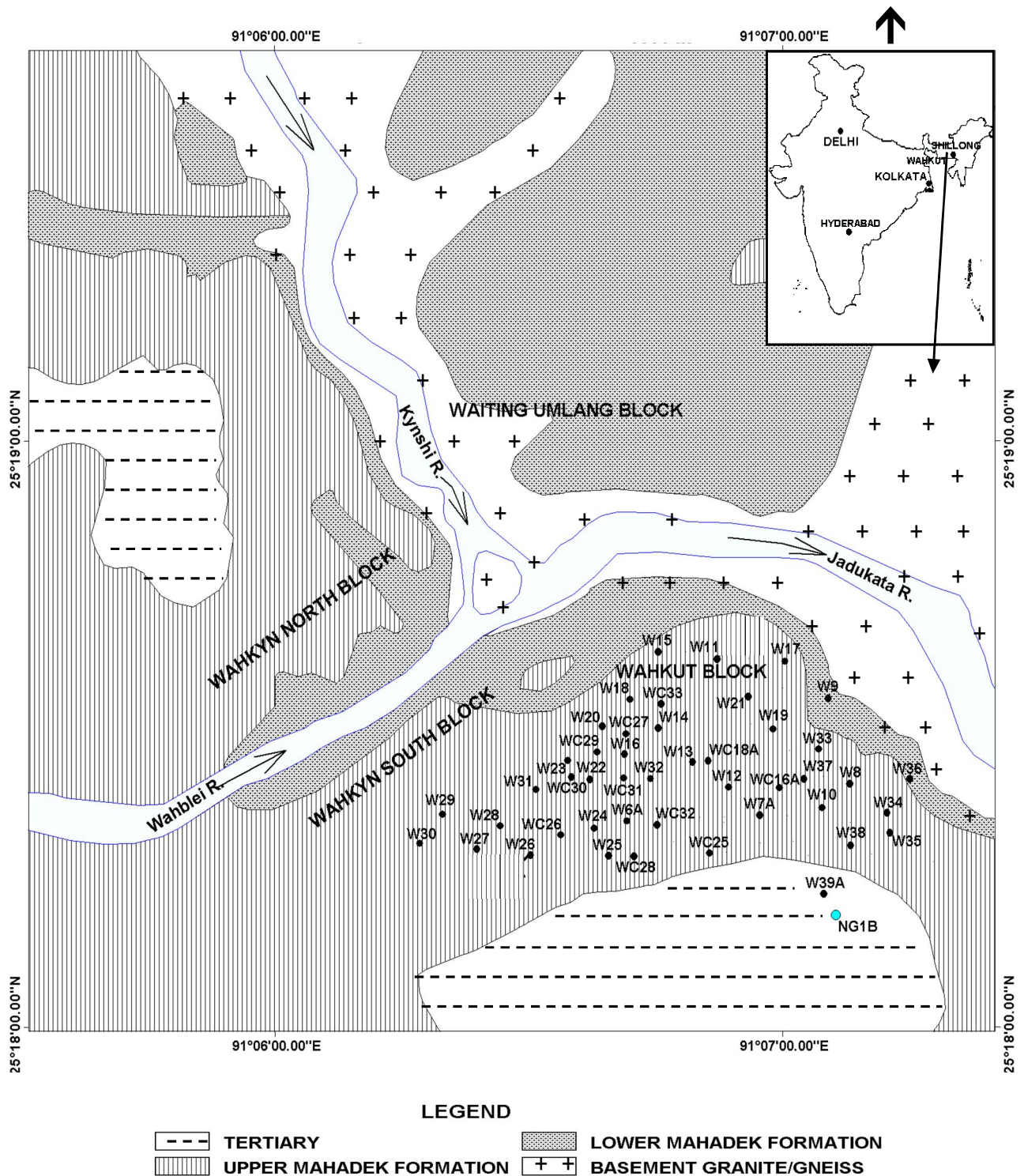


**Fig.5.1:** Wahkut exploratory block- Drilled borehole scheme with 'WC' as coring boreholes.

rock is arkose (feldspar rich sandstone) known as Lower Mahadek sandstone, of Upper Cretaceous age. Pitchblende and coffinite are the main uranium minerals, in the block.

**5.2 Uranium-Surface Equilibrium Condition:** Surface grab samples (n=22) radiometrically studied on Wahkut exploratory block, measures average  $U_3O_8 = 0.028\%$ , range 0.010-0.14% (thorium contents mostly < 0.010%). Plotted equilibrium condition on surface uranium mineralization in the block, readily presented under Chapter-1 (Fig.1.9), indicate parent (U) favoring disequilibrium condition  $d=1.56$ , measured by the  $45^\circ$  equilibrium line, with high degree of confidence ( $R^2=85.4\%$ ). In continuation to the Rangsohkhram exploratory block grab samples (Fig.1.7) with surface equilibrium status  $d=1.1$ , Wahkut exploratory block also indicate favorable uranium equilibrium condition on surface uranium mineralization. On the contrary, equilibrium condition manifested by Lostoin exploratory block grab samples (Fig.1.8), shows extreme condition for surface uranium mineralization ( $d<1$ ) deficient in uranium. Thus it become imperative to asses uranium mineralization equilibrium condition across the exploratory block in Mahadek basin.

**5.3 Boreholes  $\gamma$ -ray Logging Status:** To investigate subsurface continuity of uranium mineralization, non-coring (DTH) exploratory drilling was taken up in Wahkut exploratory block. Accordingly 39 reconnoitry boreholes were drilled in this study block (Fig.5.1) with 6000 m drilled depth. Reconnoitry boreholes  $\gamma$ -ray logs gave good subsurface mineralization. With the objective to study exploratory index parameters for uranium mineralization at high degree of confidence including disequilibrium status and confirmation of  $\gamma$ - ray logs in the block, 5000 m core drilling consisting 33 coring boreholes were taken up. The experimental coring borehole were planned to have high degree of core recovery (>90%). Thus, on cumulative 11,000 m drilling was taken up for the exploratory block, comprising 72 boreholes in total.

**5.4 Uranium Mineralization Exploratory Aspect:** Unlike for the Rangsohkhram exploratory block, good continuity of subsurface uranium mineralization, measured by  $\gamma$ -ray logging of reconnaissance boreholes, have been observed in Wahkut exploratory block. To ascertain logged boreholes free from radon interference and status of uranium equilibrium condition, Wahkut block coring boreholes database (n=33) was mapped to the set experimental qualifying criteria. Subsequently, coring boreholes meeting the defined qualifying criteria were only used to investigate uranium exploratory index parameters, in the block.

**5.4.1 Confirmation of  $\gamma$ -ray Logs:** To confirm apparent uranium ore zone grade (G) measured by gross  $\gamma$  measurements in boreholes (under sedimentary environment) with good confidence, a systematic radiometric study on coring borehole database has been taken up. This essentially maps U mineralized zone measured by *insitu*  $\gamma$ -ray logs-under field conditions, to that of the laboratory analysed radiometric core assay- under controlled condition. Prior to develop uranium mineralization correlation index on two set of measurement ( $\gamma$ -ray logs & radiometric core assay) following qualifying criteria has been especially defined on uranium mineralization grade (G) thickness (T) for coring borehole data base.

- a) Apparent cutoff grade (G) on  $\gamma$ -ray logs & Core assay  $\geq 0.010\% eU_3O_8$
- b) Mineralised zone thickness (T) on  $\gamma$ -ray logs & Core assay  $\geq 1.0$  m

Selection of qualifying criteria is based on the detection limit of G.M. detector being used for  $\gamma$ -ray logging of boreholes and the concept of sample volume [1] thickness in sedimentary environment such as Mahadek basin.

Now defined qualifying criteria on  $\gamma$ -ray log was used to identify corresponding active zone in drilled borehole core. The identified drilled borehole core was then arranged to lab transportation for detailed radiometric core assay under the controlled laboratory condition. In the lab, borehole core was analysed on core assay assembly (Chapter-2) at an average 15 cm

Sr No	BH ID	Borehole logging zone information			Core assay zone information			
		Logging depth(m)	Thickness(T)	Average grade (G)	Core zone depth (m)	Thickness (T)	Average grade (G)	Core recovery
1	WKT/C/1	125.30-127.40	2.20	0.032	126.10-127.93	1.83	0.044	95 %
2	WKT/C/2	137.00-141.50	4.60	0.041	137.61-141.39	3.78	0.044	94
3	WKT/C/12	157.70-158.90	1.30	0.053	158.56-159.66	1.10	0.058	95
4	WKT/C/19	59.00-61.10	2.20	0.016	59.42-61.14	1.72	0.020	98
		61.30-62.90	1.70	0.022	64.70-65.89	1.19	0.014	96
5	WKT/C/20	158.30-160.00	1.80	0.027	157.40-158.52	1.12	0.027	89
6	WKT/C/22	25.60-28.10	2.60	0.012	25.45-26.52	1.07	0.016	100
7	WKT/C/23	54.90-57.10	2.30	0.018	54.82-56.71	1.89	0.024	99
		70.90-72.20	1.40	0.050	71.00-72.15	1.15	0.068	93
8	WKT/C/26	169.10-171.50	2.50	0.035	168.60-169.61	1.01	0.029	73
9	WKT/C/27	59.30-61.10	1.90	0.075	58.84-60.65	1.81	0.063	100
10	WKT/C/28	193.80-195.10	1.40	0.017	194.14-195.21	1.07	0.015	100
		200.40-202.50	2.20	0.049	199.57-201.86	2.29	0.040	54
11	WKT/C/29	66.60-71.20	4.70	0.031	66.53-70.57	4.04	0.028	100
12	WKT/C/30	105.00-105.90	1.00	0.165	103.90-106.03	2.13	0.106	96
13	WKT/C/31	87.50-88.80	1.40	0.042	91.23-92.36	1.13	0.038	98
14	WKT/C/32	151.00-152.20	1.30	0.426	149.00-152.14	3.14	0.512	100
15	WKT/C/33	61.20-63.10	2.00	0.039	61.19-62.88	1.69	0.042	98
<ul style="list-style-type: none"> <li>• With defined experimental cut off criteria, 1.0 m zone thickness in <math>\gamma</math>-ray logs appears as &lt;1.0 m to the radiometric core assay for WKT/C/27 &amp; C/31 boreholes.</li> <li>• Radiometric core assay on WKT/C/30 &amp; C/32 borehole shows higher thickness than reported by <math>\gamma</math>-ray logs. Such extreme behavior of zone thickness is excluded while developing mineralised zone correlation index.</li> </ul>								

**Table 5.1:** Wahkut exploratory block qualifying boreholes:  $\gamma$ - ray logs and core assay.

core length for  $eU_3O_8$  measurement. During this process, 15 boreholes met the experimental qualifying criteria and generated a population of 18 mineralised zones on uranium mineralization presented in (Table 5.1) with an average core recovery  $\geq 90\%$ . On this simultaneous database ( $\gamma$ -ray log & core assay) mineralised zone grade/thickness (GT) continuity index was examined using linear regression [25] between the two set of variables namely laboratory analysed core assay and *insitu*  $\gamma$ - ray logs. Study findings are shown below in Fig.5.2.

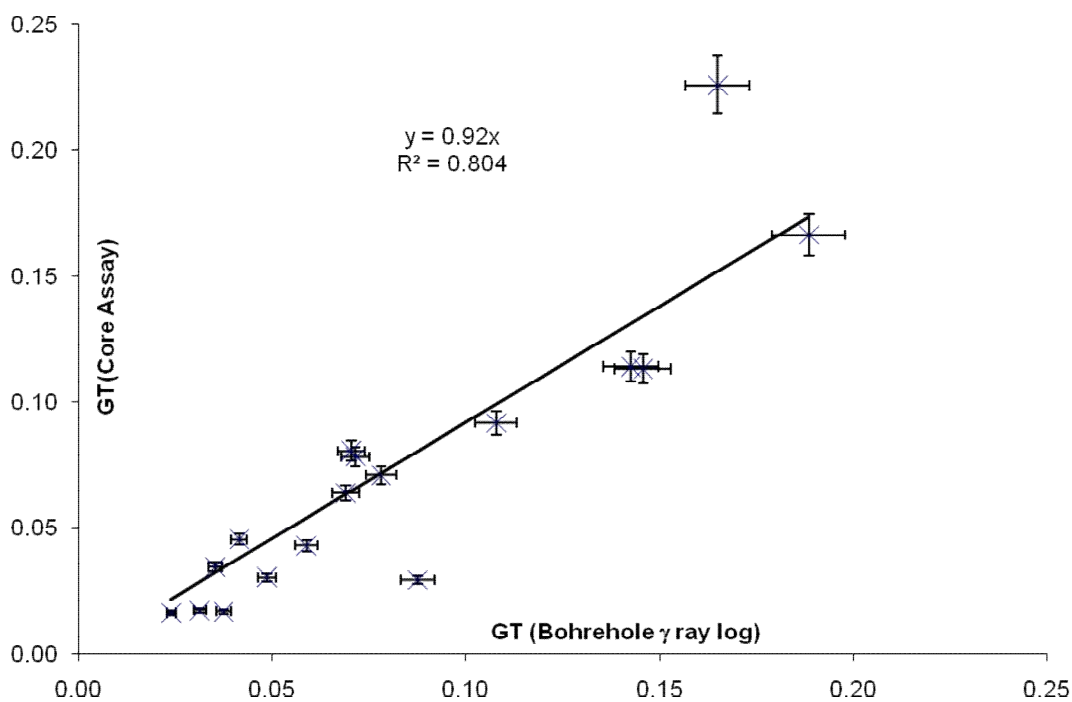


**Fig.5.2:** Wahkut exploratory block-Developed grade thickness (GT) continuity index on uranium mineralization.

**5.4.2 Uranium Disequilibrium Investigation:** In radiometric core assay, analyzed core length  $\sim 15$  cm, meeting the defined cutoff grade criteria  $\geq 0.010\% eU_3O_8$ , was then sorted out to generate borehole wise experimental database to study spatial variation of uranium disequilibrium in the exploratory block. The Qualified core sample was then split in two halves, one retained for geological study while the other half was crushed and powdered to -120 mesh size, for detail radiometric study  $eU_3O_8$ ,  $U_3O_8(\beta/\gamma)$  [22] and spectral

content determination. A laboratory based 5"x4" NaI(Tl) optimized detector setup [35] was used for  $\gamma$ -ray spectrometric content measurement.

Prior to investigate U mineralization equilibrium condition in Wahkut exploratory block, a benchmark study on reported radiometric uranium quality (Fig.2.4) has been done to ascertain quality control on  $\beta/\gamma$  assembly. Study findings are in agreement to the chemical analysis.

Sr No	BH ID	Disequilibrium factor (d)	Goodness of fit (%R <sup>2</sup> )	Remark
1	WKT/C-1 (n=24)	1.56	93.2	<ul style="list-style-type: none"> <li>• In the bracket n, indicates number of qualified samples to each qualifying borehole.</li> <li>• n<math>\geq</math> 8 is the minimum number of sample required database.</li> <li>• Thorium content mostly &lt;0.010%</li> </ul>
2	WKT/C-2 (n=38)	1.62	85.4	
3	WKT/C-3 (n=10)	1.40	93.4	
4	WKT/C-12 (n=11)	1.46	87.0	
5	WKT/C-13 (n=8)	1.56	87.4	
6	WKT/C-17 (n=15)	1.07	71.1	
7	WKT/C-19 (n=34)	1.57	83.8	
8	WKT/C-20 (n=15)	1.36	88.4	
9	WKT/C-21 (n=9)	1.51	95.5	
10	WKT/C-22 (n=23)	0.90	65.5	
11	WKT/C-23 (n=33)	1.58	94.3	
12	WKT/C-26 (n=15)	1.36	81.1	
13	WKT/C-27 (n=23)	1.24	88.1	
14	WKT/C-28 (n=42)	1.53	93.8	
15	WKT/C-29 (n=39)	1.45	94.3	
16	WKT/C-30 (n=19)	1.64	93.0	
17	WKT/C-31 (n=28)	1.98	92.8	
18	WKT/C-32 (n=15)	1.20	99.9	
19	WKT/C-33 (n=18)	1.76	90.5	
Average d=1.46				

**Table 5.2:** U disequilibrium status -Wahkut exploratory block qualifying boreholes.

In view of statistical requirements and high degree of confidence,  $n \geq 8$  core samples has been defined as minimum number of qualifying active samples on coring boreholes database. This has led 19 coring borehole, meeting the defined criteria. Subsequently, uranium disequilibrium status on the qualifying boreholes was studied using least square regression fit of  $U_3O_8$  and Ra variables. This regression slope gives best estimate of disequilibrium factor with minimal experimental error to each qualifying borehole. Table 5.2 present summary on uranium disequilibrium status, studied at high degree of confidence, across the 19 qualifying boreholes of Wahkut exploratory block.

**5.4.3 Uranium Disequilibrium-Vertical Distribution:** Exploratory borehole wise status on uranium disequilibrium presented on Table 5.2 gives average value 1.46 (range 0.90-1.98). These findings reveals parent favoring uranium disequilibrium status in Wahkut exploratory block. To study vertical nature of uranium disequilibrium condition in the block, 3 representative coring boreholes WKT/C-28, WKT/C-30 and WKT/C-32 ( having high degree core recovery and considerable active zone thickness) were chosen out of 19 qualifying boreholes. Appendix-A, presents detail status on distribution of vertical disequilibrium expressed by discrete  $U_3O_8 / Ra$  ratio at  $\sim 15$  cm depth resolution (micro level), on representative boreholes. To understand vertical distribution at rather macro level under the condition of some qualifying criteria, we examines vertical disequilibrium status (shown on Appendix-A) along  $\sim 3.0$  m core run, in the block. Study results and findings are presented overleaf in Table 5.3.

BH ID	Depth (m)	Disequilibrium status (d)		Remark	
		Macro Level	Overall		
WKT/C-28	193.00-195.72	1.49 (n=10)	1.48 (n=40)	<ul style="list-style-type: none"> <li>• Thorium contents mostly &lt;0.010%</li> <li>• Studied boreholes mostly contains average core run ~ 3 m.</li> <li>• Macro variation of U Disequilibrium is presented as an average for single core run.</li> <li>• Drilled core size 52 mm</li> <li>• Against each core run, average disequilibrium factor is quoted with no's of valid samples data.</li> <li>• Overall disequilibrium factor is stated by simple average.</li> <li>• For reasonably correlatable depth in boreholes, core run of recovery &lt; 50 % is excluded.</li> </ul>	
	195.72-199.00	1.54 (n=9)			
	199.00-202.00	1.45 (n=8)			
	202.00-203.14	1.42 (n=8)			
	203.14-205.00	1.48 (n=2)			
	205.00-207.00	-			
	207.00-210.00	1.48 (n=3)			
WKT/C-30	95.00-98.00	1.27 (n=2)	1.53 (n=19)	<ul style="list-style-type: none"> <li>• Against each core run, average disequilibrium factor is quoted with no's of valid samples data.</li> <li>• Overall disequilibrium factor is stated by simple average.</li> <li>• For reasonably correlatable depth in boreholes, core run of recovery &lt; 50 % is excluded.</li> </ul>	
	98.00-101.13	1.51 (n=7)			
	101.13-104.00	1.58 (n=5)			
	104.00-107.13	1.63 (n=5)			
WKT/C-32	146.00-149.00	1.68 (n=3)	1.29 (n=15)		<ul style="list-style-type: none"> <li>• Against each core run, average disequilibrium factor is quoted with no's of valid samples data.</li> <li>• Overall disequilibrium factor is stated by simple average.</li> <li>• For reasonably correlatable depth in boreholes, core run of recovery &lt; 50 % is excluded.</li> </ul>
	149.00-150.80	1.25 (n=6)			
	150.80-152.00	1.14 (n=5)			
	152.00-155.00	1.11 (n=1)			
	170.50-172.25	-			

**Table 5.3:** Vertical nature of U disequilibrium-Wahkut exploratory block.

**5.5 Wahkut Exploratory block Findings:** Detail radiometric studies undertaken for Wahkut exploratory block uranium mineralisation, in Mahadek basin, are being presented as follows.

**5.5.1 Confirmation of  $\gamma$ -ray Logs:** To mitigate radon presence in the borehole, *insitu*  $\gamma$ -ray logging of reconnoitory borehole is usually done after washing the borehole with fresh water for reasonable time (~1 hour). However, the experimental confirmation only

comes by mapping of mineralised zone grade thickness (GT) product using *insitu*  $\gamma$ -ray logs and laboratory analyzed radiometric core assay. In Fig.5.2, uranium mineralization correlation index 0.92 developed on radiometric core assay to  $\gamma$ -ray logs with good confidence, confirms measured  $\gamma$ -ray logs across the exploratory blocks are free from radon interference. Minor variation seen in Fig.5.2 for the two sets of variables, can be explained due to the differential sample volume of *insitu*  $\gamma$ -ray logs (typically 80 cm dia) and laboratory analysed core assay (52 mm dia).

During radiometric studies of uranium mineralized ore zone (Table 5.1), with the exception of boreholes WKT C/30 and WKT C/32, it has been observed, in general reported zone thickness (T) for core assay is mostly lower than that of corresponding  $\gamma$ -ray logs while both manifesting similar average grade (G). In view of this,  $\gamma$ -ray logs containing 1.0 m zone thickness are mostly reported as <1.0 m in core assay. Such observation could not be part of the current database. The only exceptional of simultaneous ore zone thickness (core assay and  $\gamma$ -ray logs) behavior seen for WKT C/30 and WKT C/32 boreholes, is mainly attributed to the presence of moderate to high uranium nuggets, as observed during radiometric core assay.

Thus, developed mineralised zone correlation index on Wahkut exploratory block not only confirms uranium mineralization free from radon influence but also holds promising application to the mineralised non- coring boreholes as well and to the mineralised coring boreholes having poor core recovery (due to various geological factors) under similar geological environment.

**5.5.2 Uranium Disequilibrium Pattern:** Lateral (Table 5.2) and vertical (Table 5.3) status of uranium disequilibrium for Wahkut exploratory block shows parent favoring disequilibrium with  $ThO_2$  values mostly < 0.010%. Using analysed status of uranium

disequilibrium on qualifying coring boreholes in Table 5.2, overall distribution status across the exploratory block is presented on Fig.5.3. Plotted uranium disequilibrium distribution (mean= 1.46, median=1.51,  $\sigma=0.25$ , skewness = -0.36, kurtosis=1.02 and range 0.90-1.98) shows uranium disequilibrium condition skewed towards higher side of mean 1.46. The plotted distribution of disequilibrium also indicates variation from near term equilibrium (0.90) to nearly twice of equilibrium condition in favor of parent uranium (1.98).

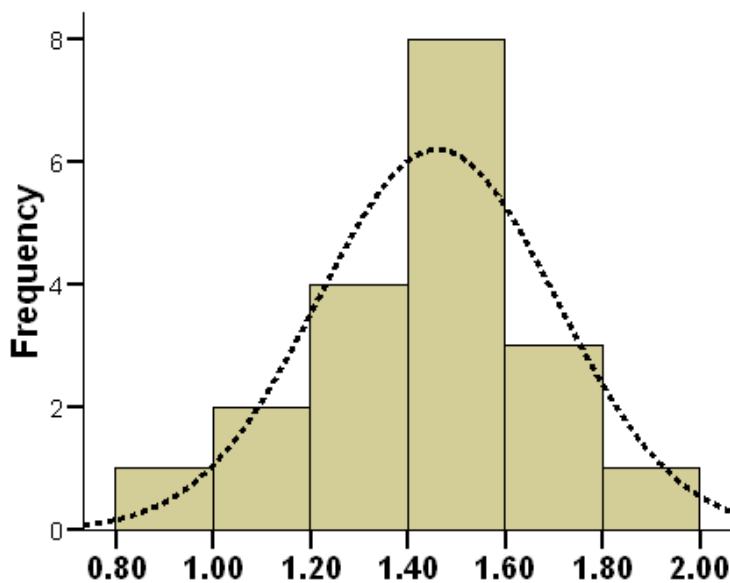


**Fig.5.3:** Uranium disequilibrium distribution-Wahkut exploratory block.

Presented in Table 5.3, periodical vertical nature of uranium disequilibrium (depth resolution ~3.0 m) in the boreholes also shows similar behavior to the reported variation of range and mean value, presented in Fig.5.3.

**5.6 Validation of Wahkut Exploratory block Findings:** Investigated findings on uranium mineralization equilibrium condition on Wahkut exploratory block, were examined over a practical case of Lostoin exploratory block, in Mahadek basin, having good subsurface uranium mineralization but with limited coring boreholes and restricted core recovery in drilled boreholes.

**5.6.1 About Lostoin Exploratory block:** As readily introduced in Chapter 4, Lostoin exploratory block was also identified primarily based on extended geological favorability to the existing uranium occurrences [13] in the basin. Radiometric assay on grab samples (n=33) show good uranium mineralization, average 0.54%  $U_3O_8$  (range 0.014-4.9% ) and thorium content mostly < 0.010%. However, equilibrium condition (stated in Chapter-1) on surface uranium mineralization (n=33) measured by  $45^\circ$  (d=1) equilibrium line, shows extreme disequilibrium condition (Fig.1.8).

Amid limited coring boreholes, poor core recovery and lean zone thickness, Lostoin exploratory block serves good opportunity to confirm reconnoitory boreholes  $\gamma$ - ray logs, free from Radon interference. Accordingly, Lostoin exploratory block findings on uranium mineralization disequilibrium status are being examined with respect to that of Wahkut exploratory block.

**5.6.1.1 Boreholes  $\gamma$ -ray Logging Status:** In total 106 non-coring boreholes with 6196 m cumulative depth were drilled over the 2.5 sq km area of Lostoin exploratory block (Fig.4.3). Gamma ray logs [1,2] of drilled boreholes indicate good subsurface uranium mineralization at relatively shallow depth. To confirm  $\gamma$ - ray logs free from radon interference and to ascertain uranium mineralization envelop continuity, 3000 m core drilling was proposed in the block. However, the task to be executed through an outsourced agency, could not be undertaken due to inherent environmental and administrative constraints. Therefore, as an alternate measure, limited core drilling was put in place using available in-house resources. Best efforts were put to achieve maximum exploratory progress with high quality core recovery. But prevailing geological conditions such as loose formations and repeated caving in the boreholes, led abandoning of several in-progress coring boreholes during the course of planned drilling work. Thus only 7 coring boreholes could reach the desired target depth in the block with about 723 m

cumulative depth. Table 5.4 presents uranium mineralization status on limited coring boreholes in the block together with core recovery.

**5.6.1.2 Confirmation of  $\gamma$ - ray Logs:** To examine status of Lostoin exploratory block subsurface uranium mineralization free from radon interference, pre-defined experimental qualifying criteria that of Wahkut exploratory block, was used. Accordingly, radiometric core assay on Lostoin exploratory block coring boreholes yielded a few mineralized zone (n=5). Now on Lostoin exploratory block  $\gamma$ - ray logs, mineralized zone grade thickness (GT) continuity of radiometric core was examined by means of using correlation index 0.92 (developed on Wahkut exploratory block), as predictor. The predicted core assay grade thickness (GT) that by  $\gamma$ - ray logs (Table 5.4) to that practically analysed on radiometric core assay (of drilled core) were plotted together as a function of Lostoin exploratory block  $\gamma$ - ray logs, on abscissa. Fig.5.4 presents the comparative status of uranium mineralisation zone (GT) continuity for Lostoin exploratory block, as predicted vs observed one.

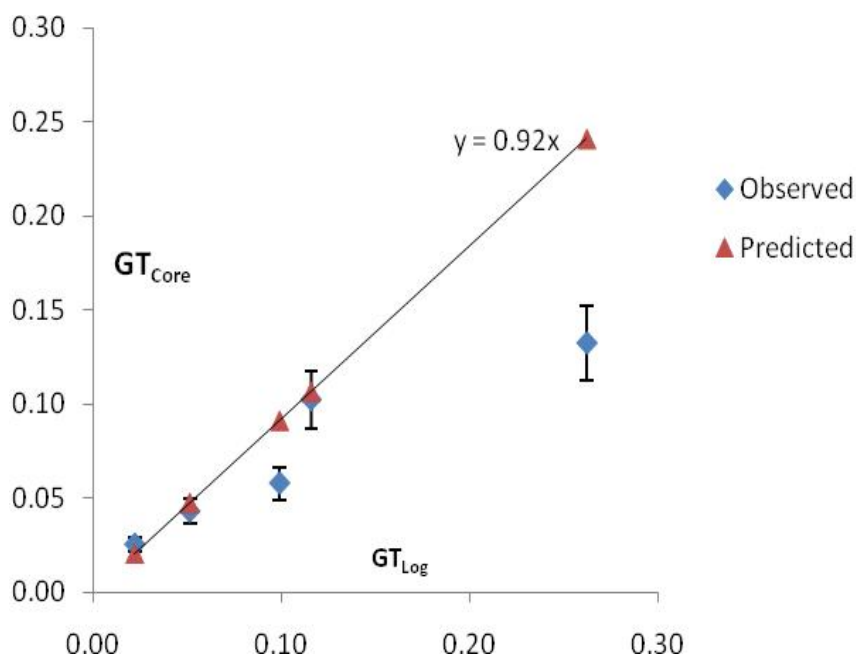


**Fig.5.4:** Lostoin exploratory block Grade Thickness (GT) behavior-Predicted vs Observed.

Sr No	BH ID	Borehole logging zone information				Radiometric Core assay zone information				
		Logging depth (m)	Thickness (T)	Average grade (G)	GT <sub>Log</sub>	Core zone depth (m)	Thickness (T)	Average grade (G)	Core recovery	GT <sub>Core</sub>
1	LST-C/1	71.60-77.20	5.70	0.046	0.2622	73.86-76.94	3.08	0.043	§80%	0.1325
		78.80-81.40	2.70	0.043	0.1159	78.87-80.87	2.01	0.051	§88%	0.1025
		81.80-83.40	1.70	0.014	0.0246	82.67-83.10	<1.00	0.011	89%	-
2	LST-C/2	65.30-67.30	2.10	0.047	0.0992	65.70-67.08	1.38	0.042	88%	0.058
3	LST-C/3	79.30-80.20	1.00	0.018	0.0176	79.00-79.85	<1.0	0.015	93%	-
4	LST-C/4	74.80-75.50	<1.00	0.039	-	74.70-75.20	<1.0	0.046	81%	-
5	LST-C/5	103.70-104.70	1.10	0.020	0.0224	104.00-104.50	1.0	0.026	90%	0.0254
6	LST-C/6	68.60-69.60	1.10	0.056	0.0614	67.73-68.50	<1.0	0.011	89%	-
		75.60-77.50	2.00	0.026	0.516	75.54-77.27	1.73	0.025	98%	0.043
7	LST-C/7	91.20-91.80	<1.00	0.021	-	91.06-91.65	<1.0	0.025	94%	-

Note-

- Mineralized zone having met grade thickness (GT) qualifying criteria of zone thickness (T) ≥ 1.0 m and cut off grade 0.010% eU<sub>3</sub>O<sub>8</sub> are only considered in the experimental analysis.
- Listed radiometric core assay zones contain 42 mm core size.
- § Physical examination on drilled borehole core shows mostly fractured to broken core pieces. First two γ- ray logging zone on LST-C/1 appears under two separate drill runs. For first logging zone, core run having 69% and 90% recovery (average 80%) while on second logging zone, have core run of 89% and 87% recovery (average 88%).

**Table 5.4:** Lostoin exploratory block coring boreholes:γ- ray logs vs core assay.

**5.6.1.3 Uranium Disequilibrium Status-Coring boreholes:** Using pre-defined qualifying criteria on minimal active sample requirements that of Wahkut exploratory block, Lostoin exploratory block coring boreholes were subjected to similar qualifying process. On qualifying coring borehole database, uranium disequilibrium status was than examined using least square regression fit between  $U_3O_8$  and Ra variables. Table 5.5 presents summary of investigated uranium disequilibrium status on Lostoin exploratory block coring borehole with average value  $d=1.57$ .

Sr No	BH ID	Disequilibrium factor (d)	Goodness of fit (%R <sup>2</sup> )	Remark
1	LST/C-1 (n=45)	1.64	95	<ul style="list-style-type: none"> <li>• Lostoin exploratory block had limited core drilling.</li> <li>• In bracket, n, indicates number of qualified samples</li> <li>• LST/C-6(n=3) do not meet set qualifying criteria on minimum sample required (n≥8) and hence excluded.</li> </ul>
2	LST/C-2 (n=26)	1.34	84.1	
3	LST/C-3 (n=12 )	1.50	71.3	
4	LST/C-4 (n=12)	1.82	93.4	
5	LST/C-5 (n=12 )	1.57	94.2	
Average d =1.57				

**Table 5.5:** Uranium disequilibrium status-Lostoin exploratory block coring boreholes.

**5.6.1.4 Uranium Disequilibrium Status-Non coring boreholes:** The qualified limited coring boreholes in Table 5.5, reveals parent favouring uranium disequilibrium in Lostoin exploratory block. However, radiometric studies on surface grab samples, indicate radium rich (uranium deficient i.e.  $d<1$ ) surface equilibrium condition. In view of reported lean zone thickness amid poor core recovery, seen on Lostoin exploratory block limited coring borehole (that may introduce distortion to the analysed uranium disequilibrium status) non- coring boreholes were examined to confirm overall uranium disequilibrium status in the block.

As stated in Chapter-4, representative sampling method [20] was used to validate uranium hosting environmental continuity over the Lostoin exploratory block. In order to

represent the similar geological condition on Lostoin exploratory block non-coring boreholes, representative samples drawn from uranium mineralised zone were also subjected to the pre-defined zone thickness (GT) consideration to that of Wahkut exploratory block i.e. mineralized zone thickness  $(T) \geq 1.0 \text{ m}$  and cut-off grade (G)  $0.010\% \text{ eU}_3\text{O}_8$ . During this process, out of 24 experimental boreholes (Table 4.6), 22 qualified on pre-defined cut-off criteria and yielded statistically significant representative sample data base (n= 40). Generated representative sample database, was then radiometrically analysed for  $e\text{U}_3\text{O}_8$ ,  $\text{U}_3\text{O}_8(\beta/\gamma)$  and  $\gamma$ -ray spectrometry. Table 5.6 presents analytical summary on representative samples across the non-coring mineralised boreholes of Lostoin exploratory block.

Parameters	Mean	Median	Range	Remark
$e\text{U}_3\text{O}_8$ (%)	0.031	0.018	0.010-0.26	<ul style="list-style-type: none"> <li>• Thorium values are mostly &lt; 0.010%</li> <li>• Out of 24 boreholes, 22 qualified on set criteria</li> <li>• n=40 representative samples were generated.</li> </ul>
$\text{U}_3\text{O}_8$ (%)	0.042	0.026	0.011-0.41	
Ra (%)	0.028	0.016	0.007-0.26	

**Table 5.6:** Analytical summary-Lostoin exploratory block mineralised group samples (n=40).

On drawn representative samples (Table 5.6) to minimize experimental error of measurement, least square regression fit have been used for  $\text{U}_3\text{O}_8$  and Ra variables. Resulting uranium disequilibrium status for the Lostoin exploratory block geological system, is presented on Fig 5.5, states parent favoring disequilibrium condition. This estimated value 1.58 on uranium disequilibrium, is in agreement to that studied on limited coring boreholes for Lostoin exploratory block.

During radiometric core assay, we have readily seen nugget presence in Wahkut exploratory block mineralised zone (Table 5.1) as well a few grab samples from Lostoin exploratory block (Fig.1.8). In order to investigate more realistic estimate of uranium

disequilibrium status in the block, nugget presence (Fig 5.5) seen to the non-coring boreholes was discounted, to have more conservative estimate of uranium disequilibrium status in the block.

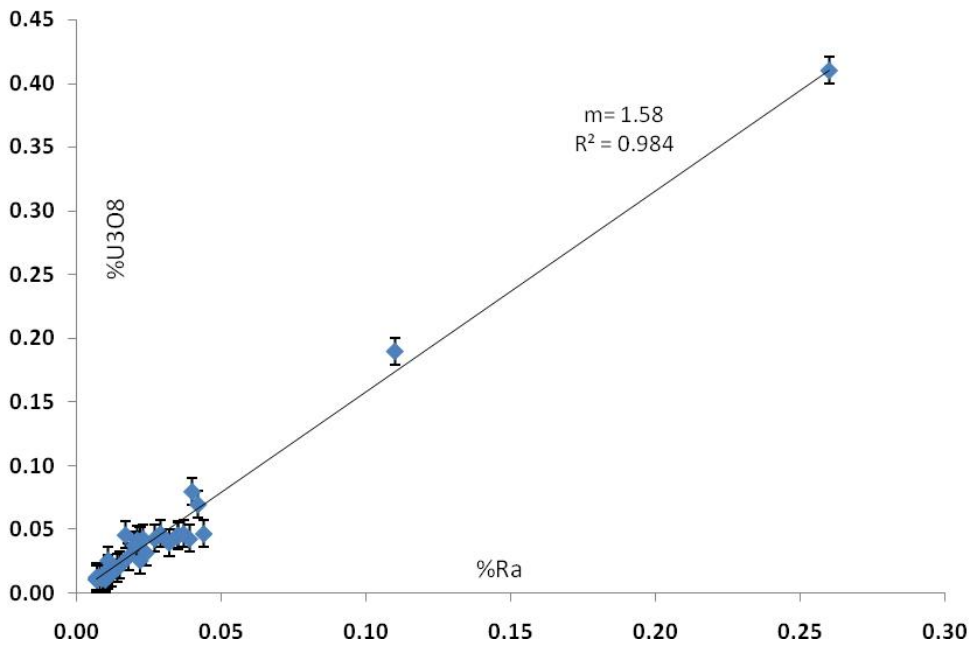


**Fig.5.5:** Lostoin exploratory block: U disequilibrium status using representative sampling (n=40).

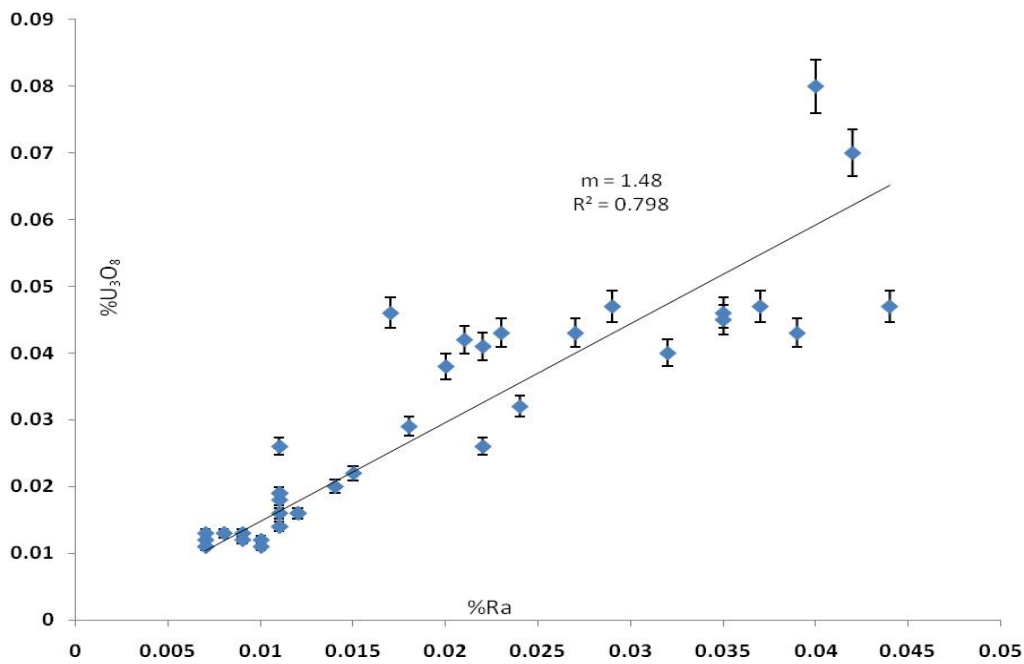


**Fig.5.6:** Lostoin exploratory block: Conservative estimates of U disequilibrium.

Fig 5.6 presents the conservative estimate 1.48 of uranium disequilibrium status with good confidence, in the block.

**5.6.1.5 Uranium Disequilibrium-Vertical distribution:** Spatial distribution of uranium disequilibrium in Lostoin exploratory block, examined on limited coring as well as non-coring boreholes shows similar parent favoring condition. In line to the Wahkut exploratory block

BH ID	Depth (m)	Disequilibrium status (d)		Remark
		Macro Level	Overall	
LST-C/1	64.00-65.10	-	1.46 (n=44)	<ul style="list-style-type: none"> <li>• Thorium contents mostly &lt;0.010%.</li> <li>• Studied boreholes mostly contains average core run ~ 3 m.</li> <li>• Macro variation of U Disequilibrium is presented as an average for single core run</li> <li>• Drilled core size 52 &amp;42 mm.</li> </ul>
	65.10-69.00	1.38 (n=4)		
	69.00-72.00	1.50 (n=1)		
	72.00-75.00	1.46 (n=14)		
	75.00-78.05	1.34 (n=11)		
	78.05-80.90	1.59 (n=10)		
	80.90-83.95	1.50 (n=4)		
	83.95-85.50	-		
LST-C/2	61.20-64.20	1.54 (n=3)	1.47 (n=22)	<ul style="list-style-type: none"> <li>• Against each core run, average disequilibrium factor is quoted with no's of valid samples data.</li> <li>• Overall disequilibrium factor is stated by simple average rather than regression method (Table 5.5).</li> <li>• For reasonably correlatable depth in the boreholes, core run of recovery &lt; 50 % is excluded.</li> </ul>
	64.20-65.70	-		
	65.70-67.55	1.15 (n=8)		
	67.55-70.65	1.77 (n=3)		
	70.65-74.65	1.54 (n=5)		
	74.65-76.75	1.83 (n=3)		
	76.75-78.35	-		

**Table 5.7:** Vertical nature of Uranium disequilibrium-Lostoin exploratory bock

study, vertical nature of uranium disequilibrium in Lostoin exploratory block was studied for the representative coring boreholes LST-C/1 and LST-C/2 (having reasonably good mineralised zone thickness). By using discrete  $U_3O_8 / Ra$  ratio at a depth resolution  $\sim 15$  cm, Appendix-B list micro detail for vertical distribution of uranium mineralization equilibrium condition to the representative boreholes. Subsequently, periodic macro behavior of uranium disequilibrium status was examined along  $\sim 3$  m core run for the representative boreholes. Table 5.7 summarizes typical variation of vertical uranium disequilibrium on the representative boreholes.

**5.7 Lostoin Exploratory block Findings:** After establishing similar geological continuity of Lostoin exploratory block (West Khasi Hills) hosting environment in Chapter-4, in relation to the Rangsohkhram exploratory block (East Khasi Hills), following are the key findings on Lostoin exploratory block uranium disequilibrium study.

**5.7.1 Confirmation of Subsurface Uranium Mineralization:** Uranium mineralization grade thickness (GT) correlation index 0.92 developed on Wahkut exploratory block, and used to predict core assay mineralised zone (grade thickness) in Lostoin exploratory block holds good (Fig.5.4) except one observation on LST-C/1 borehole. This experimentally confirms measured  $\gamma$ -ray logs free from radon interference. In Fig.5.4, sharp deviation observed between the predicted and observed mineralization value on LST-C/1, is mainly attributed to the poor core recovery (69%) on first drill core run vis à vis  $\gamma$ -ray log (Table 5.4). Further, radiometric core assay on LST-C/1 drilled core shows fractured to broken core pieces in this zone. Thus leading underestimation of mineralised zone thickness (T) and hence GT product, as seen in Fig.5.4.

In Table 5.4, close examination of Lostoin exploratory block qualifying mineralized zone, also reveals a similar behaviour on average grade (G) reported by both radiometric core assay and  $\gamma$ -ray borehole logs and relatively lower zone thickness (T) in core assay. This

observed behaviour in Lostoin exploratory block is much in agreement to that studied and observed on Wahkut exploratory block coring boreholes, in Mahadek basin.

**5.7.2 Uranium Disequilibrium Status:** Unlike surface grab samples, subsurface mineralized zone samples, shows parent favouring uranium mineralization in the block with disequilibrium factor of 1.57 (studied on limited coring boreholes-Table.5.4). This limiting case across the coring borehole is confirmed by non-coring borehole (Fig.5.5) in the block (at high degree confidence) with similar uranium disequilibrium factor of 1.58 .

Extreme deviation of uranium disequilibrium status manifested by surface uranium mineralization (Fig.1.8) indicates preferential leaching of uranium under the surface oxidising conditions seen over the sedimentary environments, in the basin. On representative samples (Fig.5.5), discounting the plotted nuggets (often seen during radiometric studies) in the block gives conservative status (1.48) of disequilibrium. Table 5.8 below presents summary of investigated equilibrium condition by various alternate method on Lostoin exploratory block.

<b>Exploratory Boreholes</b>	<b>Investigate Methods</b>	<b>Disequilibrium status (d)</b>	<b>Remark</b>
Coring (=5BH)	Least square fit	1.57	Table5.5, average
Non-coring (= 22BH)	Least square fit ( n=40)	1.58	R <sup>2</sup> =98.4%, Table 4.6,
	Least square Discounted Nugget (n=38)	1.48	R <sup>2</sup> =79.8 %, limiting case

**Table 5.8:** Investigated disequilibrium status-Lostoin exploratory bock.

Estimated conservative study on uranium disequilibrium factor for Lostoin exploratory block is much in agreement to that of comprehensive study on Wahkut exploratory block with mean value 1.46 (±0.25). Further Lostoin exploratory block conservative estimate on uranium disequilibrium factor 1.48 with discrete range 1.07-2.71 (manifested by discrete  $U_3O_8 / Ra$  ratio on representative sample) is in line to that observed for Wahkut exploratory block discrete

range (0.90- 2.98). A further, experimental finding on Lostoin exploratory block disequilibrium study also confirms a similar open system with parent favouring uranium migration.

In view of above similarities, for all practical purposes estimated uranium disequilibrium factor 1.46 in Wahkut exploratory block, also holds good for Lostoin exploratory block, in the basin.

## **CHAPTER 6**

### **Summary and Conclusion**

Radiometric studies undertaken by this thesis work across a few exploratory blocks of Mahadek basin, comprises the following measurements under the field and laboratory conditions.

- Ambient gamma radiation measurements in parts of Khasi Hills covering 673 line km, for litho profiling and identification of exploration targets.
- Analytical measurements on 108 grab samples, drawn from different exploratory blocks- to examine surface U mineralization equilibrium conditions.
- Gross-ray logging of 134 reconnoitory boreholes ( depth 11500 m) and confirmation of U mineralization continuity by using  $\gamma$ -ray logging of 40 coring boreholes (depth 5730 m).
- Radiometric core assay on selected boreholes ( 25 coring boreholes~ 375 m radiometric core)- to examine radon interference to the *insitu*  $\gamma$ -ray log.
- PPM range analytical measurements on 244 non-mineralised representative samples (drawn across 27 boreholes of two exploratory blocks)-to investigate uranium migration behavior in the system.
- Percentage level detailed analytical measurements on 530 active core samples (across 24 coring boreholes)- to examine U disequilibrium status for the exploratory blocks.
- Radiometric measurements on 41 mineralised zone representative samples (across 23 reconnoitory boreholes)-to confirm U disequilibrium status for the exploratory block having poor core recovery.

**Findings:** The key findings of this thesis work undertaken across the exploratory blocks, are as follows.

1. Preliminary findings on litho unit based ambient gamma measurement and its interpolation (with respect to the proven uranium occurrence) shows encouraging

- surface indicators to delineate potential uranium exploration targets in the basin.
2. Uranium deficient equilibrium status manifested by the surface grab samples of one of the study block, indicates highly oxidizing conditions in the basin.
  3. Uranium mineralization discontinuity, observed on Rangsohkhram exploratory block, is mainly attributed to the lean presence of reducing environment rather than of uranium disequilibrium conditions. U enrichment to the hosting environment is well supported by the enhanced U<sub>235</sub>/U<sub>238</sub> and Th/U ratio studied across the three prevailing geological environments. Further, disturbed U-Th geo-coherence (correlation index =0.268) to the hosting environment (LM) confirms uranium enrichment in the system and holds good over an aerial extent ~60 km, in the basin.
  4. Measured *insitu*  $\gamma$ -ray logs are free from the suspected radon interference (indicated by surface disequilibrium conditions) is confirmed by mineralized zone grade thickness (GT) continuity index 0.92 especially developed on laboratory analysed core assays and *insitu*  $\gamma$ -ray logs. This continuity index (0.92) as a predictor to the limited coring boreholes case of Lostoin exploratory block amid poor core recovery- holds good, in the basin.
  5. Uranium disequilibrium studies on exploratory blocks shows favorable disequilibrium condition of U mineralization. Lostoin exploratory block disequilibrium factor 1.48, shows gross similarity to that of Wahkut exploratory block disequilibrium factor (1.46±0.25). And although Rangsohkhram exploratory block have lean U mineralization in the system but the preliminary indicator on representative sample RNG/26/61 also suggest favorable disequilibrium indicator 1.5 (measured by  $U_3O_8$ /Ra ratio).
  6. Vertical distribution of uranium disequilibrium studied on few representative boreholes across the study block shows (on macro scale) good agreement to the lateral

disequilibrium status in the block-with mean value 1.46, and indicates open geological system with younger U mineralization.

7. Uranium disequilibrium factor 1.46 from present study, when benchmarked to the similar sandstone uranium deposit (grade ~0.050%  $U_3O_8$ ) of Goliad project, Texas (US) having 1.49 disequilibrium factor [41], shows good agreement between the two cases.

**Exploration Implication:** The confidence parameters generated by this study work have implications towards the extended exploration work, in the basin especially to the greater and inaccessible areas. Investigated geological continuity of uranium hosting environment, holds good over an aerial extent ~60 km, in the basin. Thus preliminary findings on litho unit based ambient gamma measurements and its interpolation holds promising application to delineate/locate new potential exploration targets especially to the extended land mass of basin.

Studied uranium disequilibrium status and core assays to *insitu*  $\gamma$ -ray logs correlation index (0.92) developed on mineralised ore zone continuity, across the exploratory blocks, holds good over a reasonable aerial extent (~16km), in the basin. Thus estimated disequilibrium factor 1.46, can be used to assess inferred uranium ore (often found in the basin) as well to convert apparent  $eU_3O_8$  grade in the exploratory block (measured by  $\gamma$ -ray logs) to actual  $U_3O_8$  tonnage.

**Further Scope:** Amid prevailing environmental and exploratory impediments, study findings on uranium exploratory index parameters can be utilized in setting up a comprehensive road map for the exploration of large uranium potential, occurring in the basin. Gamma ray logs of exploratory blocks, readily indicate shallow depth for U mineralisation in the basin, as compared to elsewhere in the country. And thus, are cost effective to mine.

Globally, sandstone type uranium deposits contributes nearly than one third [7] of proven resources vis à vis one tenths that in the country [9]. In analogy to this, baseline work undertaken by this study work is likely to augment exploratory work, in the basin, to uncover such potential in near future.

Deliberately left blank

## REFERENCES

1. Dodd Philip H., F. Drouillard Robert, P.Lathan Carl, 1967. Borehole logging methods for exploration and evaluation of uranium deposits. *Mining and Groundwater Geophysics*. 401-415.
2. Kileen, P.G.,1983. Borehole logging for uranium by measurement of natural  $\gamma$ -radiation. *Int J.Appl. Radiat.Isot.*34(1), 231-260.
3. IAEA technical Report Series No 212,1982. Borehole Logging for Uranium Exploration: A Manual.
4. Olley Jon M et al.,1997. Disequilibria in the Uranium Decay Series in Sedimentary Deposits at Allen's Cave, Nullarbor Plain, Australia : Implications for Dose Rate Determinations. *Radiation Measurements*. 27(2), 433-143
5. MaozhongMin, et.al., 2005. Uranium-series disequilibria as a means to study recent migration of uranium in a sandstone-hosted uranium deposit, NW China. *Appl. Radiat.Isot.* 63,115-125.
6. IAEA Technical Document No.1629, 2009. World Distribution of Uranium Deposits (UDEPO) with Uranium Deposit Classification.
7. Joint Report of Nuclear Energy Agency and the International Atomic Energy Agency, 2014. Uranium2014: Resources, Production and Demand.
8. Rai A.K. et al., 2002. Uranium Mineralisation in South-western part of Cuddapah Basin, Andhra Pradesh. *Expl. Res. for Atomic Minerals*.4, 79-94.
9. DAE Status Report on Indigenous Uranium resources (Dec'2014) to RajyaSabha, 2014.
10. Chaki Anjan, R.K. Purohit, R. Mamallan, 2011. Low grade uranium deposits of India-A bane or boon. *Energy Procedia*. 7,153–157.

11. Kaul Ravi, H. M. Varma, 1990. Geological evolution and genesis of the sandstone-type uranium deposit at Domiasiat, West Khasi Hills district, Meghalaya, India. *Expl. Res. for Atomic Minerals*.3,1-16.
12. Sunil Kumar, Rajendra Singh, R. Bahuguna, B. Sengupta, Ravi Kaul, 1990. Geological environment of sandstone-type uranium deposit, Domiasiat area, West Khasi Hills district, Meghalaya, India. *Expl. Res. for Atomic Minerals*. 3,17-26.
13. Sen D. B., A. S. Sachan, A. K. Padhi, S. K. Mathur, 2002. Uranium exploration in the Cretaceous Mahadek sediments of the Meghalava Plateau. *Expl. Res. for Atomic Minerals*.14,29–58.
14. Geological Survey of India (GSI),1974.*Geology and Mineral Resources of India*. Misc. Publ.30, Calcutta, p.77.
15. Nandi D.R.,1980. Tectonic Pattern in NE India. *Jour. Earth Sci.* 7(1),103-107.
16. Acharya S.K.,1976. A summary of the Precambrian Geology of the Khasi Hills, Meghalaya. *Geol. Surv. India. Misc. Publ.*23,Calcutta,p 311- 334.
17. Ghosh S., Chakraborty S., J.K. Bhalla, D.K.Paul, A.Sarkar, P.K. Bishu, S.N. Gupta, 1991. Geochronology and geochemistry of granite plutons from East Khasi Hills, Meghalaya. *Jour. Geol. Soc. of India*. 37, 331-342.
18. Baksi A.K., T.R. Barman, D.K.Paul, E.Farrar,1987. Widespread early cretaceous flood basalt volcanism in eastern India: Geochemical data from Rajmahal-Bengal-Sylhet Traps. *Chem. Geol.* 63,133-141.
19. Srivastava S.K., P.K. Kothari, Amit Majumdar, K.Umamaheswar, 2008. Occurrence of sandstone-type uranium mineralization in the Umthongkut area, Mahadek Basin, West Khasi Hills District, Meghalaya, India. *Current Science*. 94(12),17-26.

20. Kukreti B.M., Pradeep Pandey, R.V. Singh, 2012. Multivariate Analysis of Subsurface Radiometric Data in Rongsohkham area, East Khasi Hills district, Meghalaya (India) : Implication on Uranium Exploration. *Applied Radiation and Isotopes*.70,1644-1648.
21. Kukreti B.M., Pramod Kumar, G.K.Sharma, 2015. Development of experimental approach to examine U occurrence continuity over the extended area Reconnoitry Boreholes: Lostoin exploratory block, West Khasi Hills district, Meghalaya (India). *Applied Radiation and Isotopes*.104,167-174.
22. Eichholz G. C., J.W. Hilborn, C. McMahon, 1953. The determination of uranium and thorium in ores, *Canadian Journal of Physics*. 31(4),613-628.
23. Zeynalova O.V et.al., Application of Digital Signal Processing in Nuclear Spectroscopy. *Bulletin of the Russian Academy of Science: Physics*.73(4),506-511.
24. IAEA Technical Document No.566,1990. The use of gamma ray data to define the natural radiation environment.
25. Davis John C., 2002. *Statistical and Data Analysis in Geology (3e)*. John Willey & Sons, New York.
26. Matthew Kay and Roussos Dimitrakopoulos, 2000. *Integrated Interpolation Methods for Geophysical Data: Applications to Mineral Exploration*. *Natural Resources Research*. 9(1),53-63.
27. Wright S.M., D.C. Howard, J. Barry, J.T. Smith, 2002. Spatial variation of radio cesium deposition in Cumbria. *Geogr Environ Modeling*. 6,203-216.
28. Abraham J.S., A.C. Comrie, 2004. Real-time ozone mapping using a regression-interpolation hybrid approach, applied to Tucson, Arizona. *Journal of the Air & Waste Management Association*. 54 (8),914-925.
29. Nucleonix Manual, 2001. *Environmental Radiation Monitor type ER705M*, Nucleonix Systems (P) Ltd, Hyderabad (India).

30. Chilès J. Paul, P.Delfiner, 1999. *Geostatistics: Modeling Spatial Uncertainty (1e)*. John Willey & Sons, New York.
31. Pannatier Y,1996. *VarioWin-Software for spatial data analysis in 2D*, Springer-Verlag , New York.
32. Brown, M. B., B. Forsythe, 1974. Robust tests for the equality of variances; *Journal of the American Statistical Association*. 69,364-367.
33. Pandey Pradeep, 2008. *Shillong Basin Investigations-Annual Report:2008*. Unpublished Report, AMD Hyderabad.
34. Pandey Pradeep, 2009. *Shillong Basin Investigations-Annual Report:2009*. Unpublished Report, AMD Hyderabad.
35. Kukreti B.M., G.K. Sharma, 2012. Performance analysis of gamma ray spectrometric parameters on digital signal and analog signal processing based MCA systems using NaI(Tl) detector. *Appl. Radiat. Isot.* 70, 901–905.
36. Martinez, Aguirre, M. Garcia-Leon, M. Ivanovich, 1995. U and Th speciation in river sediments. *The Science of the Total Environment* 173/174, 203-209.
37. Strong K.P., D.M. Levins, 1982. Effect of moisture content on radon emanation from uranium ore and tailings. *Health Physics*. 42, 27-32.
38. Sakoda Akihiro, Yuichi Nishiyama, Katsumi Hanamoto , Yuu Ishimori , Yuki Yamamoto, Takahiro Kataoka, Atsushi Kawabe, Kiyonori Yamaoka, 2010. Differences of natural radioactivity and radon emanation fraction among constituent minerals of rock or soil. *Appl. Radiat. Isot.* 68, 1180-1184.
39. Smith K.J., L. Leon Vintro, P.I. Mitchell, P. Bally de Bois, D. Boust, 2004. Uranium–thorium disequilibrium in north-east Atlantic waters. *Journal of Environmental Radioactivity* 74, 199-210.
40. Gavshin V.M., M.S. Melgunov, F.V. Sukhorukov, V.A. Bobrov, I.A. Kalugin, J.

Klerkx, 2005. Disequilibrium between uranium and its progeny in the Lake Issyk-Kul system (Kyrgyzstan) under a combined effect of natural and manmade processes. *Journal of Environmental Radioactivity*. 83,61-74.

41. Goliad Project Technical Report NI 43-101, 2008. Uranium Energy Corp, Texas (US).

Deliberately left blank

## APPENDIX-A: Wahkut Exploratory block Status on Vertical U disequilibrium

1) Borehole : WKT/C-28, West Khasi Hills District.

Core Depth (m)		d	Drilled Core details		Remark
From	To		Recovery	Core Run (m)	
193.00	193.56	-	100%	193.00-195.72	<ul style="list-style-type: none"> <li>• Drilled Depth =221.00 m</li> <li>• Vertical resolution <math>\approx</math> 15 cm.</li> <li>• Core size 52 mm</li> <li>• Thorium contents &lt;0.010%</li> <li>• Discrete value on d is measured using core sample U/Ra ratio</li> <li>• For reasonably correlatable depth in the boreholes, core recovery &lt; 50 % excluded.</li> <li>• Core size &lt; 42 mm is not being considered due to poor sample volume.</li> <li>• Only active zone core (based on <math>\gamma</math>-ray logs) is being studied.</li> </ul>
	193.69	2.20			
	193.84	1.67			
	194.11	-			
	194.25	1.43			
	194.40	1.05			
	194.52	1.71			
	194.64	1.43			
	194.75	1.38			
	194.90	1.38			
	195.05	-			
	195.18	1.83			
	195.45	-			
195.72	0.82				
195.72	195.85	-	100%	195.72-199.00	
	196.00	2.13			
	196.72	-			
	196.86	1.50			
	197.33	-			
	197.48	1.67			
	197.63	1.82			
	197.78	1.59			
	198.06	-			
198.21	1.00				

	198.36	1.57	..continue	..continue	<ul style="list-style-type: none"> <li>• Core size 52 mm</li> </ul>
	198.51	-			
	198.65	1.33			
	198.88	-			
	199.00	1.22			
199.00	199.15	1.00	55%	199.00-202.00	<ul style="list-style-type: none"> <li>•Marked sample depth on 199.00-220.00 m, core run is indicative due to poor core recovery in the borehole</li> <li>• Core size 52 mm</li> </ul>
	199.30	-			
	199.44	1.55			
	199.75	-			
	199.89	1.80			
	200.04	1.50			
	200.16	2.00			
	200.30	-			
	200.41	1.15			
	200.54	1.79			
	200.60	0.82			
202.00	202.11	2.15	96%	202.00-203.14	<ul style="list-style-type: none"> <li>• Core size 52 mm</li> </ul>
	202.25	0.88			
	202.40	1.22			
	202.54	0.91			
	202.68	1.50			
	202.82	1.83			
	202.94	1.41			
	203.08	1.48			
203.14	203.23	1.58	99%	203.14-205.00	Core size 52 mm

	204.60	-	..continue	..continue	• Core size 52 mm
	204.94	-			
205.00	207.00	-	93%	205.00-207.00	• Core size 52 mm
207.00	207.28	-	86%	207.00-210.00	• Core run beyond 210.0-221.00 m contain recovery < 50% & reduced size of 32 mm. Hence do not qualify experimental criteria.
	207.41	1.37			
	207.56	1.79			
	207.69	1.27			
	209.41	-			

2) Borehole : WKT/C-30, West Khasi Hills District.

Core Depth (m)		d	Drilled Core details		Remark
From	To		Recovery	Core Run (m)	
95.00	97.30	-	96%	95.00-98.00	<ul style="list-style-type: none"> <li>• Drilled Depth =125.00 m</li> <li>• Vertical resolution <math>\approx</math> 15 cm.</li> <li>• Discrete value on d is measured using core sample U/Ra ratio</li> <li>• Core size 52 mm</li> <li>• Thorium contents <math>&lt;0.010\%</math></li> <li>• For reasonably correlatable depth in the boreholes, core recovery <math>&lt; 50\%</math> is excluded.</li> <li>• Only active zone core (based on <math>\gamma</math>-ray logs) is being studied.</li> </ul>
	97.44	1.20			
	97.73	-			
	97.88	1.33			
98.00	98.15	1.10	99%	98.00-101.13	
	98.70	-			
	98.85	1.57			
	98.99	-			
	99.14	2.00			
	99.57	-			
	99.72	1.75			
	99.99	-			
	100.12	1.33			
	100.26	-			
	100.41	1.59			
	100.55	-			
100.70	1.25				
101.11	-				
101.13	101.58	-	100%	101.13-104.00	
	101.73	1.22			
	101.88	1.00			
	102.01	2.56			
	102.13	1.89			
	103.90	-			
	104.00	1.25			
104.00	104.15	1.54	96%	104.00-107.13	
	105.44	-			

	105.59	1.11	..continue	..continue	<ul style="list-style-type: none"> <li>• Core size 52 mm</li> </ul>
	105.73	1.80			<ul style="list-style-type: none"> <li>• Core size 52 mm</li> </ul>
	105.88	2.20			
	106.03	1.52			
	107.02	-			

3) Borehole : WKT/C-32, West Khasi Hills District.

Core Depth (m)		d	Drilled Core details		Remark
From	To		Recovery	Core Run (m)	
146.00	147.27	-	99%	146.00-149.00	<ul style="list-style-type: none"> <li>• Drilled Depth =173.00 m</li> <li>• Vertical resolution <math>\approx</math> 15 cm.</li> <li>• Thorium contents &lt;0.010%</li> <li>• Core size 52 mm</li> <li>• Discrete value on d is measured using core sample U/Ra ratio</li> </ul>
	147.42	2..00			
	148.25	-			
	148.39	1.26			
	148.76	-			
	148.88	1.78			
	148.98	-			
149.00	149.68	-	100%	149.00-150.80	<ul style="list-style-type: none"> <li>• For reasonably corelatable depth in the boreholes, core recovery &lt; 50 % is excluded.</li> <li>• Only active zone core (based on <math>\gamma</math>-ray logs) is being studied.</li> </ul>
	149.83	1.23			
	149.97	1.44			
	150.11	1.45			
	150.25	0.73			
	150.40	1.00			
	150.52	1.62			
	150.80	-			
150.80	151.08	-	100%	150.80-152.00	<ul style="list-style-type: none"> <li>• Core size 52 mm</li> </ul>
	151.22	1.21			
	151.37	0.85			
	151.51	1.37			
	151.64	1.85			
	151.76	0.44			
	152.00	-			
152.00	152.14	1.11	94%	152.00-155.00	<ul style="list-style-type: none"> <li>• Core size 52 mm</li> </ul>
	154.83	-			
170.50	172.24	-	99%	170.50-172.25	<ul style="list-style-type: none"> <li>• Core size 52 mm</li> </ul>

**APPENDIX-B: Lostoin Exploratory block Status on Vertical U disequilibrium.**

1) Borehole : LST-C/1, West Khasi Hills District.

Core Depth (m)		d	Drilled Core details		Remark
From	To		Recovery	Core Run (m)	
64.00	65.05	-	95%	64.00-65.10	<ul style="list-style-type: none"> <li>• Drilled Depth =100.95 m</li> <li>• Vertical resolution ≈ 15 cm.</li> <li>• Thorium contents &lt;0.010%</li> <li>• Core size 52 mm (up to 69.00 m)</li> </ul>
	65.25	-	92%	65.10-69.00	
	65.38	1.09			
	65.48	1.88			
	65.59	1.36			
	65.74	1.18			
	68.66	-			
69.00	71.56	-	89%	69.00-72.00	<ul style="list-style-type: none"> <li>• Core size reduces to 42 mm.</li> </ul>
	71.68	1.50			
72.00	72.15	1.75	70%	72.00-75.00	<ul style="list-style-type: none"> <li>• Discrete value on d is measured using core sample U/Ra ratio</li> <li>• For reasonably correlatable depth in the boreholes, core recovery &lt; 50 % is excluded.</li> <li>• Only active zone core (based on <math>\gamma</math>-ray logs) is being studied.</li> </ul>
	72.29	1.50			
	72.42	2.54			
	72.95	-			
	73.02	1.53			
	73.17	1.44			
	73.28	1.13			
	73.39	1.22			
	73.49	1.63			
	73.58	1.56			
	73.69	1.86			
	73.80	1.71			
	73.90	1.36			
74.01	0.50				
74.10	0.77				
75.00	75.15	0.92	90%	75.00-78.05	<ul style="list-style-type: none"> <li>• Core size 42mm.</li> </ul>
	75.51	-			

	75.66	1.10	.continue	..continue	• Core size 42mm.
	75.81	1.13			
	75.96	1.55			
	76.11	1.25			
	76.25	1.17			
	76.39	1.21			
	76.53	1.30			
	76.68	1.60			
	76.82	1.86			
	76.95	1.67			
	77.77	-			
78.05	79.02	-			• Core size 42mm.
	79.17	1.35			
	79.32	1.87			
	79.47	1.61			
	79.62	1.87			
	79.77	1.13	90%	78.05-80.90	
	79.92	-			
	80.06	1.75			
	80.21	1.30			
	80.35	2.54			
	80.48	1.56			
	80.62	0.94			
80.90	81.03	0.77			• Core size 42mm.
	81.17	2.08			
	81.32	-			
	81.46	2.14	87%	80.90-83.95	
	82.16	-			
	82.27	1.00			
	83.58	-			
83.95	85.34	-	89%	83.95-85.50	• Core size 42mm.

2) Borehole : LST-C/2, West Khasi Hills District.

Core Depth (m)		d	Drilled Core details		Remark
From	To		Recovery	Core Run (m)	
61.20	62.28	-	82%	61.20-64.20	<ul style="list-style-type: none"> <li>• Drilled Depth =93.55 m</li> <li>• Vertical resolution ≈ 15 cm.</li> <li>• Thorium contents &lt;0.010%</li> </ul>
	62.40	1.56			
	62.52	1.57			
	62.65	1.50			
	63.67	-			
64.20	65.45	-	83%	64.20-65.70	<ul style="list-style-type: none"> <li>• Core size 52 mm (up to</li> </ul>
65.70	65.78	1.07	88%	65.70-67.55	<ul style="list-style-type: none"> <li>• Core size reduced to 42mm.</li> <li>• Discrete value on d is measured using core sample U/Ra ratio</li> <li>• For reasonably correlatable depth in the boreholes, core recovery &lt; 50 % is excluded</li> <li>• Only active zone core (based on <math>\gamma</math>-ray logs) is being studied.</li> </ul>
	65.93	0.53			
	66.07	1.26			
	66.22	1.75			
	66.37	1.08			
	66.52	1.22			
	66.67	1.50			
	66.95	-			
	67.09	0.76			
67.34	-				
67.55	69.21	-	90%	67.55-70.65	<ul style="list-style-type: none"> <li>• Core size 42mm.</li> </ul>
	69.36	1.88			
	69.50	1.73			
	69.64	1.71			
	70.35	-			
70.65	72.14	-	80%	70.65-74.65	<ul style="list-style-type: none"> <li>• Core size 42mm.</li> </ul>
	72.28	1.75			
	72.84	-			
	72.99	1.63			
	73.13	-			
	73.24	1.75			

	73.69	-	..continue	..continue	• Core size 42mm.
	73.82	1.45			
	73.91	1.14			
74.65	74.76	1.11	80%	74.65-76.75	• Core size 42mm.
	75.21	-			
76.75	78.03	-	80%	76.75-78.35	